4. OVERHEAD TRANSMISSION LINES

4.1 Line Parameters

The parameters R', L', and C' of overhead transmission lines are evenly distributed along the line[1], and can, in general, not be treated as lumped elements. Some of them are also functions of frequency; therefore, the term "line constants" is avoided in favor of "line parameters." For short-circuit and power flow studies, only positive and zero sequence parameters at power frequency are needed, which are readily available from tables in handbooks, or can easily be calculated from simple formulas. For the line models typically needed in EMTP studies, however, these simple formulas are not adequate enough. Usually, the line parameters must therefore be computed, with either one of the two supporting routines LINE CONSTANTS or CABLE CONSTANTS.

These supporting routines produce detailed line parameters for the following types of applications:

(a) Steady-state problems at power frequency with complicated coupling effects. An example is the calculation of induced voltages and currents in a de-energized three-phase line which runs parallel with an energized three-phase line. Both lines would be represented as six coupled phases in this case.

(b) Steady-state problems at higher frequencies. Examples are the analysis of harmonics, or the analysis of power line carrier communication, on untransposed lines.

(c) Transients problems. Typical examples are switching and lightning surge studies.

Line parameters could be measured after the line has been built; this is not easy, however, and has been done only occasionally. Also, lines must often be analyzed in the design stage, and calculations are the only means available for obtaining line parameters in that case.

The following explanations describe primarily the theory used in the supporting routines LINE CONSTANTS and CABLE CONSTANTS, though other methods are occasionally mentioned, especially if it appears that they might be used in EMTP studies some day. The supporting routine LINE CONSTANTS is heavily based on the work done by M.H. Hesse [27], though some extensions to it were added.

4.1.1 Line Parameters For Individual Conductors

The solution method is easier to understand for a specific example. Therefore, a double-circuit three-phase line with twin bundle conductors and one ground wire will be used for the explanations (Fig. 4.1). There are 13 conductors in this configuration. They will be called

[1]The "prime" in R', L' and C' is used to indicate distributed parameters in Ω/km, H/km and F/km.

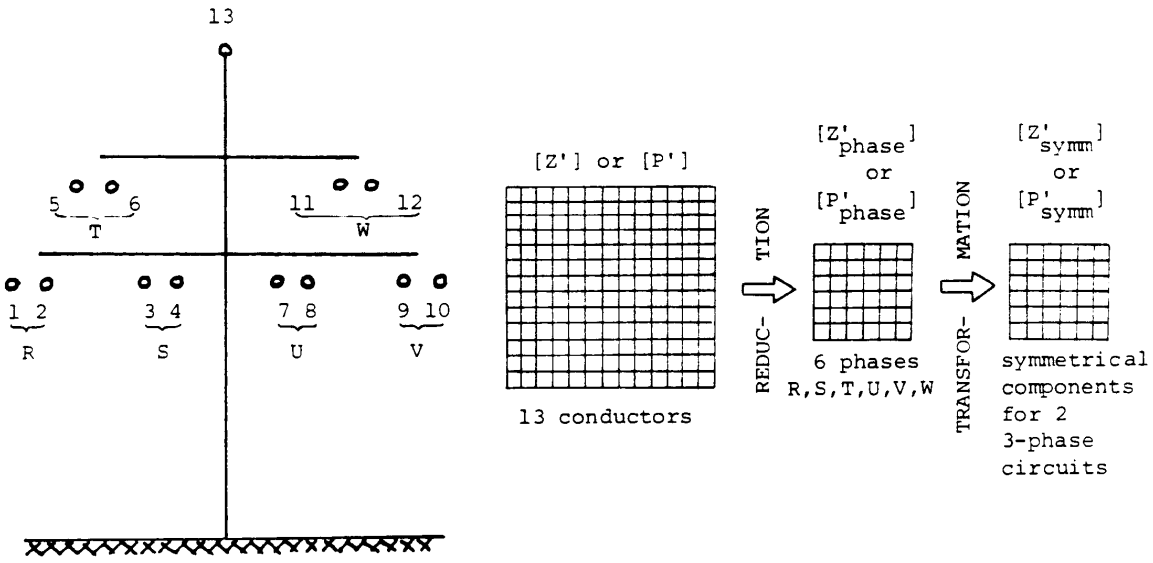

Fig. 4.1 - Line parameters

individual conductors[2], to distinguish them from the 6 equivalent phase conductors which are obtained after pairs have been bundled into phase conductors and after the ground wire has been eliminated.

4.1.1.1 Series Impedance Matrix

It is customary to describe the voltage drop along a transmission line in the form of partial differential equations, e.g., for a single-phase line as

$$-\frac{\partial v}{\partial x} = R'i + L'\frac{\partial i}{\partial t} \tag{4.1}$$

The parameters R' and L' of overhead lines are not constant, however, but functions of frequency. In that case it is improper to use Eq. (4.1); instead, the voltage drops must be expressed in the form of phasor equations for ac steady state conditions at a specific frequency. For the case of Fig. 4.1,

$$-\begin{bmatrix} \frac{dV_1}{dx} \\ \frac{dV_2}{dx} \\ . \\ . \\ . \\ \frac{dV_{13}}{dx} \end{bmatrix} = \begin{bmatrix} Z'_{11} & Z'_{12} & \cdots & Z'_{1,13} \\ Z'_{21} & Z'_{22} & \cdots & Z'_{2,13} \\ & & \cdots\cdots\cdots & \\ Z'_{13,1} & Z'_{13,2} & \cdots & Z'_{13,13} \end{bmatrix} \begin{bmatrix} I_1 \\ I_2 \\ . \\ . \\ . \\ I_{13} \end{bmatrix} \tag{4.2a}$$

[2]In the output of the supporting routine LINE CONSTANTS, they are called "physical conductors."

with V_i = voltage phasor, measured from conductor i to ground,

I_i = current phasor in conductor i,

or in general

$$-\left[\frac{dV}{dx}\right] = [Z'][I] \tag{4.2b}$$

with [V] = vector of phasor voltages (measured from conductor to ground), and

[I] = vector of phasor currents in the conductors.

Implied in Eq. (4.2) is the existence of ground as a return path, to which all voltages are referenced. The matrix $[Z'] = [R'(\omega)] + j\omega [L'(\omega)]$ is called the series impedance matrix; it is complex and symmetric. The diagonal element $Z'_{ii} = R'_{ii} + j\omega L'_{ii}$ is the series self impedance per unit length of the loop formed by conductor i and ground return. The off-diagonal element $Z'_{ik} = Z'_{ki} = R'_{ki} + j\omega L'_{ki}$ is the series mutual impedance per unit length between conductors i and k, and determines the longitudinally induced voltage in conductor k if a current flows in conductor i, or vice versa. The resistive terms in the mutual coupling are introduced by the presence of ground, as briefly explained in Section 3.1.

Formulas for calculating Z'_{ii} and Z'_{ik} were developed by Carson and Pollaczek in the 1920's for telephone circuits [28, 29]. These formulas can also be used for power lines. Both seem to give identical results for overhead lines, but Pollaczek's formula is more general inasmuch as it can also be used for buried (underground) conductors or pipes. Carson's formula is easier to program than Pollaczek's and is therefore used in both supporting routines LINE CONSTANTS and CABLE CONSTANTS, except that the latter includes an extension of Carson's formula for the case of multilayer stratified earth [30] as well. Carson's, Pollaczek's and other earth return formulas are compared in [31].

Two recent new approaches to the calculation of earth-return impedances are those of Hartenstein, Koglin and Rees [32], and of Gary, Deri, Tevan, Semlyen and Castanheira [33, 34]. Hartenstein, Koglin and Rees treat the ground as a system of conducting layers 1, 2, 3…n, with uniform current distribution in each layer (Fig. 4.2(a)). Their results come close to those obtained with Carson's formula. One advantage of their method is the fact that it is very easy to assume difference earth resistivities for each of the layers. Gary, Deri, et al. calculate self and mutual impedances with the simple formulas originally proposed by Dubanton,

$$Z'_{ii} = R'_{i-internal} + j\left\{\omega\frac{\mu_0}{2\pi}\ell n\frac{2(h_i+\bar{p})}{r_i} + X'_{i-internal}\right\} \tag{4.3}$$

and

$$Z'_{ik} = j\omega\frac{\mu_0}{2\pi}\ell n\frac{\sqrt{(h_i+h_k+2\bar{p})^2 + x^2_{ik}}}{d_{ik}} \tag{4.4}$$

in which p represents a complex depth,

$$\bar{p} = \sqrt{\frac{\rho}{j\omega\mu_0}} \qquad (4.5)$$

All other parameters are explained after Eq. (4.8), except for x_{ik} = horizontal distance between conductors i and k (Fig. 4.4), and ρ = earth resistivity. The results agree very closely with those obtained from Carson's formula, with the differences peaking at 9% in the frequency range between 100 Hz and 10 kHz and being lower elsewhere. This is a very good agreement, indeed, and Eq. (4.3) and (4.4) may therefore supplant Carson's formula some day. Fig. 4.2(b) shows a comparison of positive and zero sequence parameters for a typical 500 kV line.

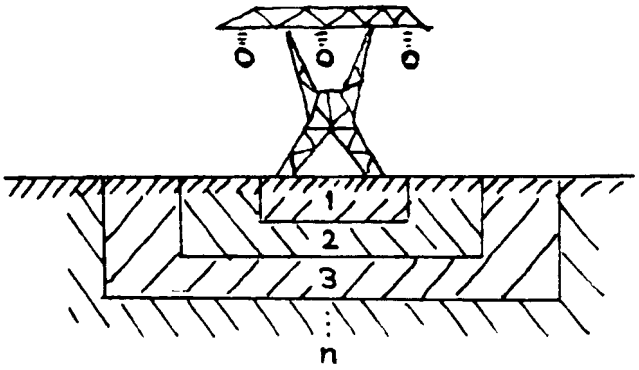

Fig. 4.2(a) - Alternative to Carson's formula: Ground represented as layers 1, 2,…n

Carson's formula

Carson's formula for homogeneous earth is normally accurate enough for power system studies, especially since the data for a more detailed multilayer earth return is seldom available. The supporting routine CABLE CONSTANTS does have an option for multilayer or stratified earth, however. Carson's formula is based on the following assumptions:

(a) The conductors are perfectly horizontal above ground, and are long enough so that three-dimensional end effects can be neglected (this makes the field problem two-dimensional). The sag is taken into account indirectly by using an average height above ground (Fig. 4.3).

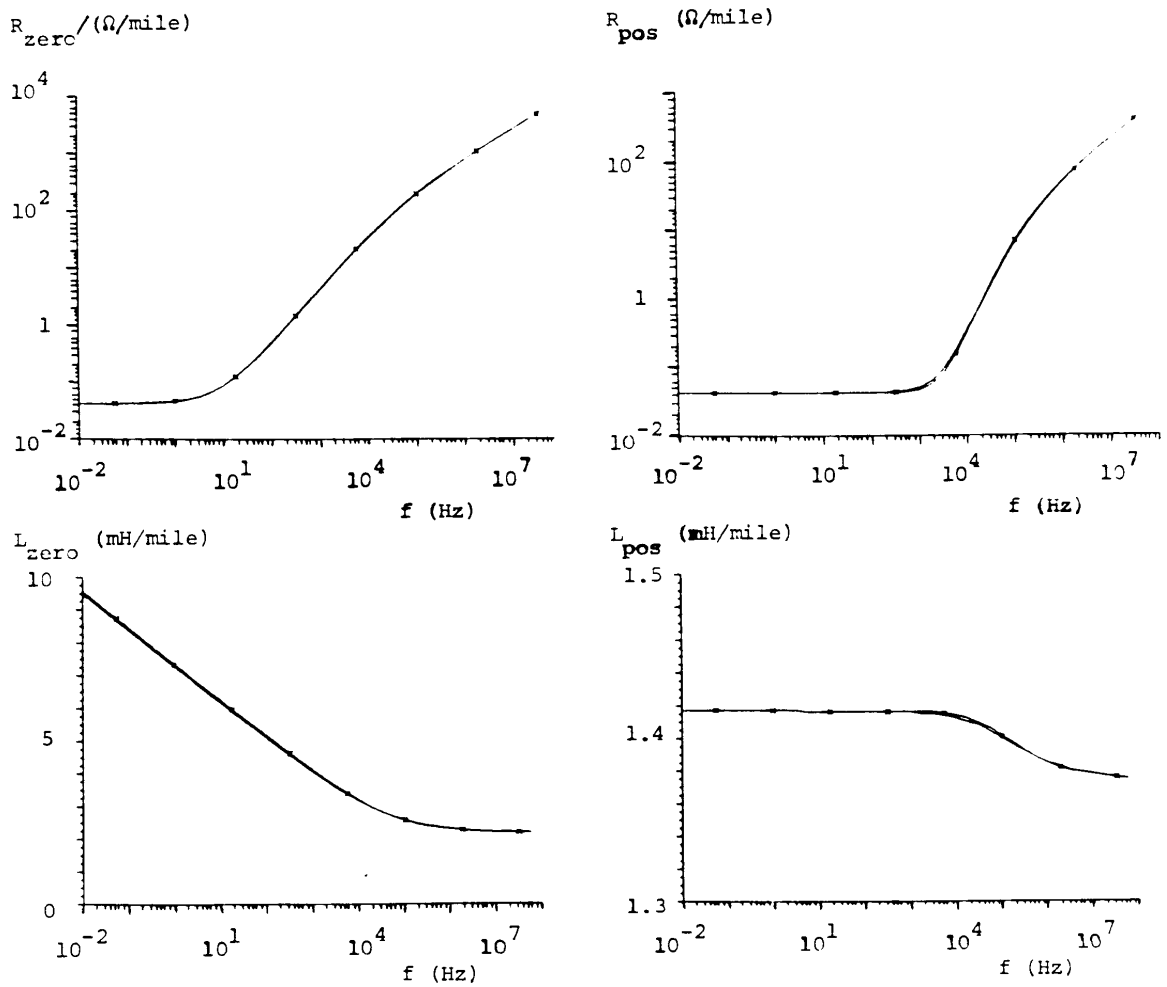

Fig. 4.2(b) - Alternative to Carson's formula: formula by Gary, Deri et al. (comparison with Carson's formula for a typical 500 kV line with bundle conductors; skin effect in conductors ignored)

(b) The aerial space is homogeneous without loss, with permeability μ_0 and permittivity ε_0.

(c) The earth is homogeneous with uniform resistivity ρ, permeability μ_0 and permittivity ε_0, and is bounded by a flat plane with infinite extent, to which the conductors are parallel. The earth behaves as a conductor, i.e., $1/\rho >> \omega\varepsilon_0$, and hence the displacement currents may be neglected. Above the critical frequency $f_{critical} = 1/(2\pi\varepsilon_0\rho)$, other formulas [35, 36] must be used (for ρ = 10,000 Ωm in rocky ground, $f_{critical}$ = 1.8 MHz, which is still on the high side for most EMTP line models).

(d) The spacing between conductors is at least one order of magnitude larger than the radius of the conductors, so that proximity effects (current distribution within one conductor influenced by current in an adjacent conductor) can be ignored.

The conductor profile between towers (Fig. 4.3) can be described

(a) as a parabola for spans ≤ 500 m,

(b) as a catenary for 500 ≤ spans ≤ 2000 m, and

(c) as an elastic line for spans > 2000 m.

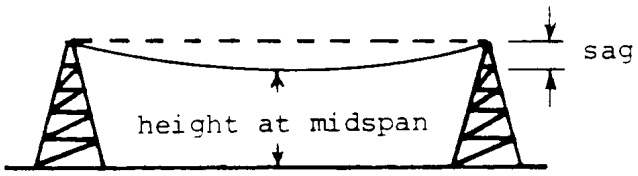

Fig. 4.3 - Conductor profile between towers

If the parabola is accurate enough, then the average height above ground is

$$h = height\ at\ midspan + \frac{1}{3} sag, \tag{4.6}$$

(4.6)

which is the formula used by both supporting routines LINE CONSTANTS and CABLE CONSTANTS. The elements of the series impedance matrix can then be calculated from the geometry of the tower configuration (Fig. 4.4) and from characteristics of the conductors. For the self impedance,

$$Z'_{ii} = (R'_{i-internal} + \Delta R'_{ii}) + j(\omega \frac{\mu_0}{2\pi} \ln \frac{2h_i}{r_i} + X'_{i-internal} + \Delta X'_{ii}) \tag{4.7}$$

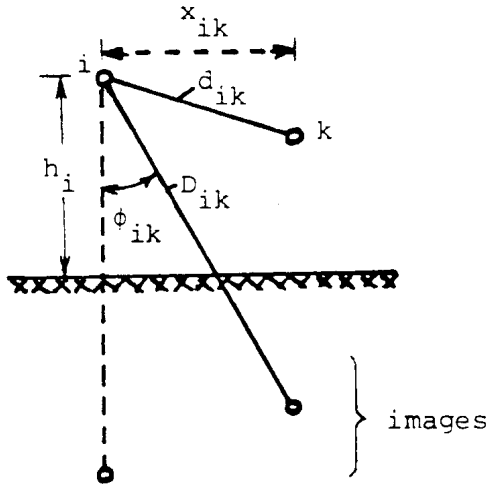

Fig. 4.4 - Tower geometry

and for the mutual impedance

$$Z'_{ik} = Z'_{ki} = \Delta R'_{ik} + j(\omega \frac{\mu_0}{2\pi} \ln \frac{D_{ik}}{d_{ik}} + \Delta X'_{ik}) \tag{4.8}$$

with μ_0 = permeability of free space. Using

$$\mu_0/2\pi = 2 \cdot 10^{-4} \; H/km \tag{4.9}$$

produces impedances in Ω/km. The parameters in Eq. (4.7) and (4.8) are

$R'_{i\text{-internal}}$ = ac resistance of conductor i in Ω/unit length,

h_i = average height above ground of conductor i,

D_{ik} = distance between conductor i and image of conductor k,

d_{ik} = distance between conductors i and k,

r_i = radius of conductor i,

$X_{i\text{-internal}}$ = internal reactance of conductor i,

ω = $2\pi f$ with f = frequency in Hz,

$\Delta R'$, $\Delta X'$ = Carson's correction terms for earth return effects.

Carson's correction terms $\Delta R'$ and $\Delta X'$ in Eq. (4.7) and (4.8) account for the earth return effect, and are functions of the angle ϕ ($\phi = 0$ for self impedance, $\phi = \phi_{ik}$ in Fig. 4.4 for mutual impedance), and of the parameter a:

$$a = 4\pi\sqrt{5} \cdot 10^{-4} \cdot D \cdot \sqrt{\frac{f}{\rho}} \tag{4.10}$$

with $D = 2h_i$ in m for self impedance,

D_{ik} in m for mutual impedance,

ρ = earth resistivity in Ωm.

$\Delta R'$ and $\Delta X'$ become zero for $a \rightarrow \infty$ (case of very low earth resistivity). Carson gives an infinite integral for $\Delta R'$ and $\Delta X'$, which he developed into the sum of four infinite series for $a \leq 5$. Rearranged for easier programming, it can be written as one series, and for impedances in Ω/km, becomes

$$\begin{aligned}
\Delta R' = \; & 4\omega \bullet 10^{-4}\{\pi/8 \\
& -b_1 a \bullet \cos\phi \\
& +b_2[(c_2 - 1na)a^2\cos 2\phi + a^2 \sin 2\phi] \\
& +b_3 a^3 \cos 3\phi \\
& -d_4 a^4 \cos 4\phi \\
& -b_5 a^5 \cos 5\phi
\end{aligned}$$

$$\begin{aligned}
\Delta X' = \; & 4\omega \bullet \{1/2(0.6159315 - 1na) \\
& +b_a a \bullet \cos\phi \\
& -d_2 a^2 \cos 2\phi \\
& +b_3 a^3 \cos 3\phi \\
& -b_4[(c_4 - 1na)a^4 \cos 4\phi + \phi a^4 \sin g 4\phi] \\
& +b_5 a^5 \cos 5\phi
\end{aligned}$$

$+b_6[(c_6\text{-}1na)a^6\cos 6\phi + \phi a^6 \sin 6\phi \quad -d_6 a^6 \cos 6\phi$

$+b_7 a^7 \cos 7\phi \quad +b_7 a^7 \cos 7\phi$

$-d_8 a^8 \cos 8\phi \quad -b_8[(c_8\text{-}1na)a^8 \cos 8\phi + \phi a^8 \sin 8\phi]$

$- \ldots\} \quad + \ldots\}$

in Ω/km (4.11)

Each 4 successive terms for a repetitive pattern. The coefficients b_i, c_i and d_i are constants, which can be precalculated and stored in lists. They are obtained from the recursive formulas:

$$\begin{gathered} b_1 = \frac{\sqrt{2}}{6} \text{ for odd subscripts}, \\ b_i = b_{1-2}\frac{sign}{i(i+2)} \text{ with the starting value} \\ b_2 = \frac{1}{16} \text{ for even subscripts}, \\ c_i = c_{1-2} + \frac{1}{i} + \frac{1}{i+2} \text{ with the starting value } c_2 = 1.3659315, \\ d_i = \frac{\pi}{4} \cdot b_i, \end{gathered} \tag{4.12}$$

with sign = ±1 changing after each 4 successive terms (sign = ±1 for i = 1, 2, 3, 4; sign = -1 for i = 5, 6, 7, 8 etc.).

The trigonometric functions are calculated directly from the geometry,

$$\cos\phi_{ik} = \frac{h_i + h_k}{D_{ik}} \quad \text{and} \quad \sin\phi_{ik} = \frac{x_{ik}}{D_{ik}}$$

and for higher-order terms in the series from the recursive formulas

$$a^i \cos i\phi = [a^{i-1}\cos(i-1)\phi \cdot \cos\phi - a^{i-1}\sin(i-1)\phi \cdot \sin\phi] \cdot a$$

$$a^i \sin i\phi = [a^{i-1}\cos(i-1)\phi \cdot \sin\phi + a^{i-1}\sin(i-1)\phi \cdot \cos\phi] \cdot a \tag{4.13}$$

For power circuits at power frequency only few terms are needed in the infinite series of Eq. 4.11. However, at frequencies and for wider spacings (e.g., in interference calculations) more and more terms must be taken into account as the parameter a becomes larger and larger [37, discussion by Dommel]. Once Carson's series starts to converge, it does so fairly rapidly. How misleading the results can be with too few terms in the series of Eq. 4.11 is illustrated for the case of a = 4 and ϕ = 0: If the series were truncated after the 1st, 2nd,…, 15th term, the percent error in $\text{Re}\{Z'_{ii}\}$ would be

+312, -748, -16, +798, -416, +365, -121, -93, +28, -15, +5.2,

+1.7, -0.35, +0.14, -0.04

For a > 5 the following finite series [38] is best used:

$$\Delta R' = \left(\frac{\cos\phi}{a} - \frac{\sqrt{2}\cos 2\phi}{a^2} + \frac{\cos 3\phi}{a^3} + \frac{3\cos 5\phi}{a^5} - \frac{45\cos 7\phi}{a^7} \right) \cdot \frac{4\omega \cdot 10^{-4}}{\sqrt{2}}$$

$$\Delta X' = \left(\frac{\cos\phi}{a} - \frac{\cos 3\phi}{a^3} + \frac{3\cos 5\phi}{a^5} + \frac{45\cos 7\phi}{a^7} \right) \cdot \frac{4\omega \cdot 10^{-4}}{\sqrt{2}} \quad in\ \Omega/km \tag{4.14}$$

Internal impedance and skin effect

In the old days of slide-rule calculations, the internal reactance $X'_{reactance}$ and external reactance $\omega\ \mu_0/2\pi$ ℒn 2h/r for lossless earth were often combined into one expression, by replacing radius r with the smaller "geometric mean radius" GMR to account for the internal magnetic field,

$$\omega \frac{\mu_0}{2\pi} \mathcal{L}n \frac{2h}{r} + X'_{internal} = \omega \frac{\mu_0}{2\pi} \mathcal{L}n \frac{2h}{GMR} \tag{4.15}$$

GMR was often included in conductor tables. Instead of or in addition to GMR, North American handbooks have also frequently given the "reactance at 1 foot spacing"[3] X'_A, which is related to GMR,

$$X'_A = \omega \frac{\mu_0}{2\pi} \mathcal{L}n \frac{1(foot)}{GMR(feet)} \tag{4.16}$$

with GMR in feet (or in m if X'_A is to be the reactance at 1 m spacing).

The concept of geometric mean radius was originally developed for nonmagnetic conductors at power frequency where uneven current distribution (skin effect) can be ignored. In that case, its meaning is indeed purely geometric, with GMR being equal to the geometric mean distance among all elements on the conductor cross section area if this area were divided into an infinite number of equal, infinitesimally small elements. For a solid, round, nonmagnetic conductor at low frequency,

$$GMR/r = e^{-1/4}$$

This formula changes to

$$GMR/r = e^{-\mu_r/4}$$

if the conductor is made of magnetic material with relative permeability μ_r; its geometric meaning is then lost. If skin effect is taken into account, its geometric meaning is lost as well. The name geometric mean radius is therefore

[3]The name comes form the positive sequence reactance formula $X'_{pos} = \omega\ \mu_0/2\pi$ ℒn GMD/GMR discussed in Eq. (4.56), for the case where the spacing among the three phases (expressed as geometric mean distance GMD) is 1 foot, with GMR given in feet as well.

misleading, and it is questionable whether it should be retained.

Eq. (4.15) gives the conversion formula between GMR and internal reactance,

$$GMR/r = e^{X'_{internal}/(\omega\frac{\mu_0}{2\pi})} \tag{4.17}$$

The internal reactance can be calculated for certain types of conducts [39, 40] as part of the internal impedance $R'_{internal} + jX'_{internal}$. Since $X'_{internal}$ is only a very small part of the total reactance for nonmagnetic conductors, its accurate determination is somewhat academic. More important is the calculation of $R'_{internal}$, because the increase of resistance with frequency due to skin effect can be considerable.

The internal impedance of solid, round wires can be calculated with well-known skin effect formulas, with $R'_{internal}$ being of more practical interest than $X'_{internal}$. Stranded conductors can usually be approximated as solid conductors of the same cross-sectional area[4] [41]. It has been claimed that steel-reinforced aluminum cables (ACSR) can usually be approximated as tubular conductors when the influence of the steel core is negligible, which is more likely to be the case with an even number of layers of aluminum strands, since the magnetization of the steel core caused by one layer spiralled in one direction is more or less cancelled by the next layer spiralled in the opposite direction. The supporting routine LINE CONSTANTS uses this approximation of an ACSR as a tubular conductor. If the magnetic material of the steel core is of influence, then calculations probably become unreliable, and current-dependent, measured values should be used instead. Since the solid conductor is a special case of the tubular conductor, the supporting routine LINE CONSTANTS uses only the formula for the latter, which is described as Eq. (5.7b) in Section 5.1.

Table 4.1 shows the increase in resistance and the decrease in internal inductance due to skin effect for a tubular conductor with $R'_{dc} = 0.0398$ Ω/mile, ratio inside radius/outside radius $q/r = 0.2258$ (Fig. 4.5), and $\mu_r = 1.0$. The internal inductance of a tube at dc is [48, p. 64]

$$L'_{dc} = 2 \cdot 10^{-4} \left\{ \frac{q^4}{(r^2-q^2)^2} \ln\frac{r}{q} - \frac{3q^2-r^2}{4(r^2-q^2)} \right\} \; H/km$$

or $0.454866 \cdot 10^{-4}$ H/km in this case. At high frequencies, $R'_{internal} = X'_{internal}$, with both components being proportional to $\sqrt{\omega}$. This is the region of pronounced skin effect. From Table 4.1 it can be seen that $R'_{internal}$ and $X'_{internal}$ are almost equal at 10 kHz (difference 2.2%), with the difference decreasing to 0.7% at 100 kHz, or 0.2% at 1 MHz.

[4]There are cases, however, where this approximation is not good enough. More accurate formulas are needed, for instance, for calculating the attenuation in power line carrier problems [39], as explained in Appendix VII.

Table 4.1 - Skin effect in a tubular conductor

f(Hz)	R'_{ac}/R'_{dc}	$L'_{internal\text{-}ac}/L'_{internal\text{-}dc}$
2	1.0002	0.99992
4	1.0007	0.99970
6	1.0015	0.99932
8	1.0026	0.99879
10	1.0041	0.99812
20	1.0164	0.99254
40	1.0632	0.97125
60	1.1347	0.93898
80	1.2233	0.89946
100	1.3213	0.85639
200	1.7983	0.66232
400	2.4554	0.47004
600	2.9421	0.38503
800	3.3559	0.33418
1000	3.7213	0.29924
2000	5.1561	0.21204
4000	7.1876	0.15008
6000	8.7471	0.12258
8000	10.0622	0.10617
10000	11.2209	0.09497
20000	15.7678	0.06717
40000	22.1988	0.04750
60000	27.1337	0.03879
80000	31.2942	0.03359
100000	34.9597	0.03004
200000	49.3413	0.02124
400000	69.6802	0.01502
600000	85.2870	0.01227
800000	98.4441	0.01062
1000000	110.0357	0.00950
2000000	155.5154	0.00672
4000000	219.8336	0.00475

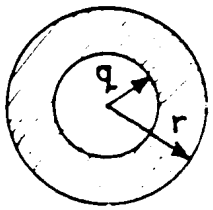

Fig. 4.5 - Tubular conductor

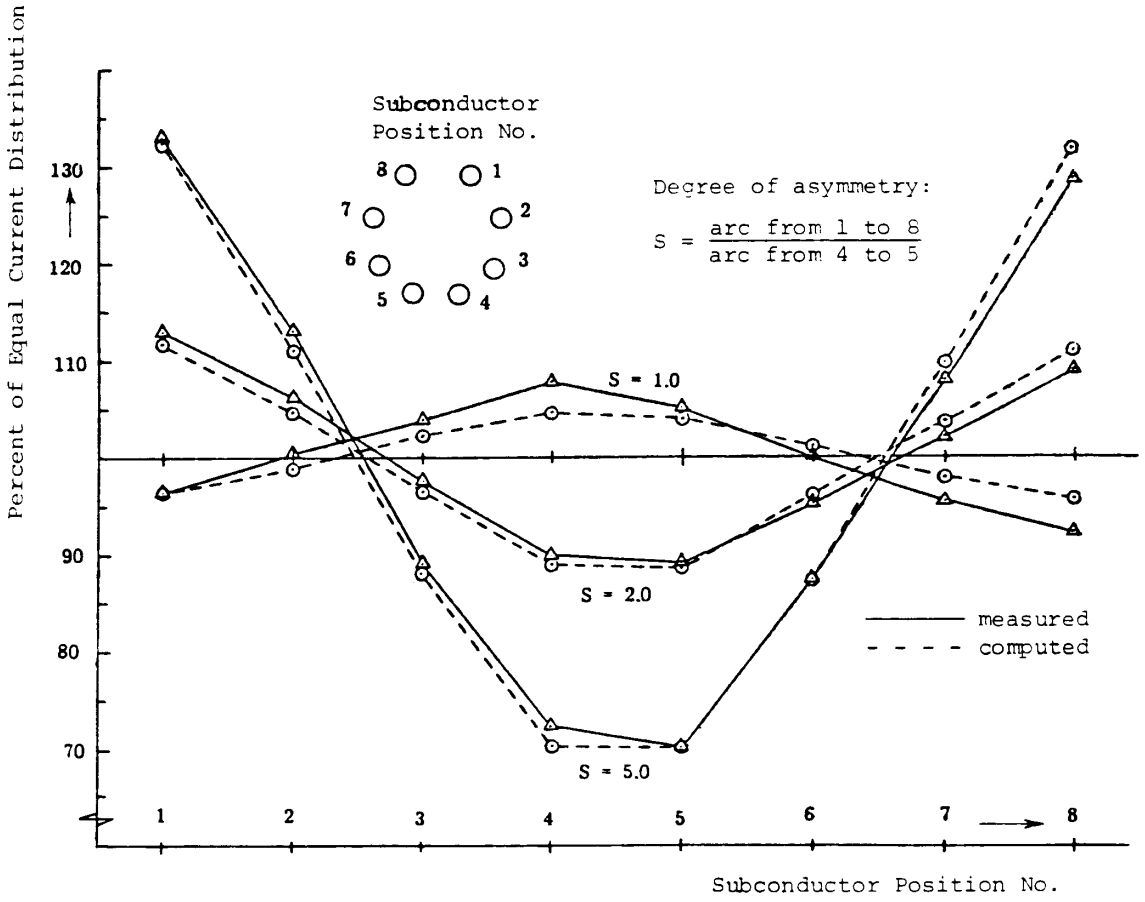

Fig. 4.6 - Current distribution within an 8-conductor bundle [42]. © 1976 IEEE

Example for using series impedance matrix of individual conductors

The matrix of Eq. (4.2) can be used to study the uneven current distribution within a bundle conductor. Fig. 4.6 shows measured and calculated values for the unequal current distribution in the 8 subconductors of an asymmetrical bundle for various degrees of asymmetry [42]. Asymmetrical bundling was proposed to reduce audible noise, but this advantage is offset by the unequal current distribution. The currents in this case were found from Eq. (4.2) with an 8 x 8 matrix, assuming equal voltage drops in the 8 conductors,

$$[I] = -[Z']^{-1}[dV/dx] \tag{4.18}$$

4.1.1.2 Shunt Capacitance Matrix

The voltages from the 13 conductors in Fig. 4.1 to ground are a function of the line charges:

$$\begin{bmatrix} v_1 \\ v_2 \\ \cdot \\ \cdot \\ \cdot \\ v_{13} \end{bmatrix} = \begin{bmatrix} P'_{11} & P'_{12} & \cdots & P'_{1,13} \\ P'_{21} & P'_{22} & \cdots & P'_{2,13} \\ \cdots & & & \\ \cdots & & & \\ \cdots & & & \\ P'_{13,1} & P'_{13,2} & \cdots & P'_{13,13} \end{bmatrix} \begin{bmatrix} q_1 \\ q_2 \\ \cdot \\ \cdot \\ \cdot \\ q_{13} \end{bmatrix} \tag{4.19a}$$

with q_i = charge per unit length on conductor i, or in the general case

$$[v] = [P'][q] \tag{4.19b}$$

Maxwell's potential coefficient matrix [P'] is real and symmetric. Its elements are easy to compute from the geometry of the tower configuration and from the conductor radii if the following two assumptions are made: (a) the air is lossless and the earth is uniformly at zero potential, (b) the radii are at least an order of magnitude smaller than the distances among the conductors. Both assumptions are reasonable for overhead lines. Then the diagonal element becomes

$$P'_{ii} = \frac{1}{2\pi\epsilon_0} \ln \frac{2h_i}{r_i} \tag{4.20}$$

and the off-diagonal element

$$P'_{ik} = P'_{ki} = \frac{1}{2\pi\epsilon_0} \ln \frac{D_{ik}}{d_{ik}} \tag{4.21}$$

with ε_0 = permittivity of free space. The factor $1/(2\pi\varepsilon_0)$ in these equations is $c^2 \cdot \mu_0/2\pi$, where c is the speed of light. With c = 299,792.5 km/s and $\mu_0/(2\pi) = 2 \cdot 10^{-4}$ H/km, it follows that

$$1/(2\pi\epsilon_0) = 17.975109 \cdot 10^6 \quad km/F \tag{4.22}$$

The inverse relationship of Eq. (4.19) yields the shunt capacitance matrix [C'],

$$[q] = [C'][v], \qquad with\ [C'] = [P']^{-1} \tag{4.23}$$

The supporting routine LINE CONSTANTS uses a version of the Gauss-Jordan process for this matrix inversion which takes advantage of symmetry [43]. This process was chosen because it can easily be modified to handle matrix reductions as well, which are needed for eliminating ground wires and for bundling conductors. Appendix III explains this Gauss-Jordan process in more detail.

The capacitance matrix [C'] is in nodal form. This means that the diagonal element C'_{ii} is the sum of the shunt capacitances per unit length between conductor i and all other conductors as well as ground, and the off-diagonal element $C'_{ik} = C'_{ki}$ is the negative shunt capacitance per unit length between conductors i and k. An example for a three-phase circuit from [44, p. 457] is shown in Fig. 4.7, with

$$[C'] = \begin{bmatrix} 12.161 & -2.625 & -2.625 \\ -2.625 & 11.729 & -1.349 \\ -2.625 & -1.349 & 11.729 \end{bmatrix} \; nF/mile$$

or $C'_{12\text{-mutual}} = 2.625$, $C'_{13\text{-mutual}} = 2.625$, $C'_{23\text{-mutual}} = 1.349$, $C_{2\text{-ground}} = 7.755$ nF/mile, etc.

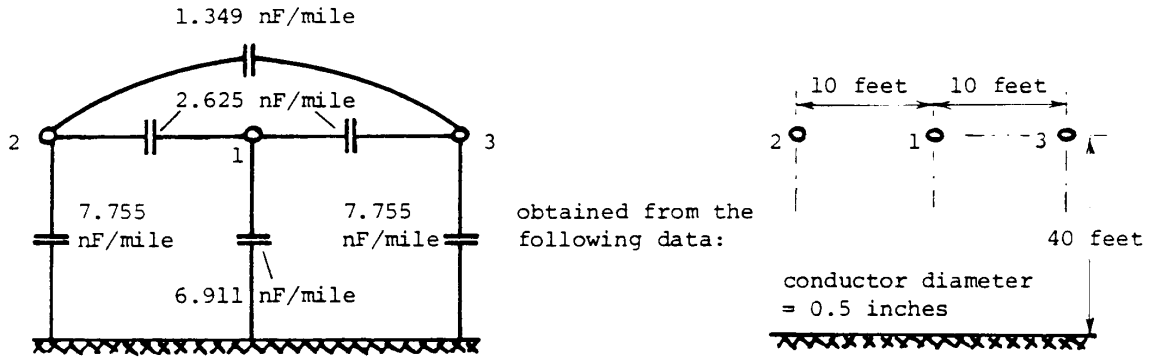

Fig. 4.7 - Mutual and shunt capacitances

For ac steady-state conditions, the vector of charges (as phasor values) is related to the vector of leakage currents [-dI/dx] by

$$[Q] = -\frac{1}{j\omega}\left[\frac{dI}{dx}\right] \tag{4.24}$$

Therefore, the second system of differential equations is

$$-\left[\frac{dI}{dx}\right] = j\omega\,[C']\,[V] \tag{4.25}$$

which, together with Eq. (4.2), completely describes the ac steady-state behavior of the multi-conductor line. Shunt conductances G' have been ignored in Eq. (4.25), because their influence is negligible on overhead lines, except at very low frequencies approaching dc, where the line behavior is determined by R' and G', with ωL' and ωC' becoming negligibly small. With G', the complete equation is

$$-\left[\frac{dI}{dx}\right] = [Y']\,[V] \tag{4.26a}$$

where

$$[Y'] = [G'] + j\omega\,[C'] \tag{4.26b}$$

At very high frequencies, the shunt capacitances are also influenced by earth conduction effects, and correction terms must then be added to Eq. (4.20) and (4.21). However, the earth conduction effect is normally

negligible below 100 kHz to 1 MHz [45]. In that case, the capacitances are constant, in contrast to series resistances and series inductances which are functions of frequency.

4.1.2 Line Parameters for Equivalent Phase Conductors

Equations (4.2) and (4.19) for all individual conductors contain more information than is usually needed. Generally, only the phase quantities are of interest. For the case of Fig. 4.1, the reduction from 13 equations to 6 equations for the phases R, S, T, I, V, W is accomplished by introducing the following conditions,

for grounding conductor 13: $dV_{13}/dx = 0$ in (4.2), $v_{13} = 0$ in (4.19),

for bundling conductors 1 and 2 into phase R:

$$I_1 + I_2 = I_R,\ dV_1/dx = dV_2/dx = dV_R/dx \text{ in (4.2)},$$

and

$$q_1 + q_2 = q_R,\ v_1 = v_2 = v_R \text{ in (4.19)}$$

and analogous for bundling the other phases. With these conditions, the matrices can be reduced to 6 x 6, as explained next. These reduced matrices will be called matrices for the equivalent phase conductors.

4.1.2.1 Elimination of Ground Wires

Normally, ground wires are continuous and grounded at every tower[5], which are typically 250 to 350 m apart. In that case it is permissible for frequencies up to approximately 250 kHz to assume that the ground wire potential is continuously zero [46]. This allows a reduction in the order of the [Z']- and [P']-matrices, with the reduction procedure being the same for both. Let the matrices and vectors in Eq. (4.2) be partitioned for the set "u" of ungrounded conductors, and for the set "g" of ground wires,

$$-\begin{bmatrix}[dV_u/dx]\\ [dV_g/dx]\end{bmatrix} = \begin{bmatrix}[Z'_{uu}] & [Z'_{ug}]\\ [Z'_{gu}] & [Z'_{g\,g}]\end{bmatrix}\begin{bmatrix}[I_u]\\ [I_g]\end{bmatrix} \tag{4.27}$$

Since $[V_g]$ and $[dV_g/dx]$ are zero, Eq. (4.27) can be reduced by eliminating $[I_g]$,

$$-\left[\frac{dV_u}{dx}\right] = [Z'_{reduced}]\ [I_u] \tag{4.28a}$$

where

$$[Z'_{reduced}] = [Z'_{uu}] - [Z'_{ug}]\,[Z'_{g\,g}]^{-1}\,[Z'_{gu}] \tag{4.28b}$$

Rather than using straightforward matrix inversion and matrix multiplications in Eq. (4.28b), the more efficient Gauss-Jordan reduction process of Appendix III is used in the supporting routine LINE CONSTANTS. [P'] is reduced in the same way, and $[C'_{reduced}]$ is found by inverting $[P'_{reduced}]$. At first sight it may appear as if less work

[5]Non-continuous "segmented" ground wires are discussed in Section 4.1.2.5.

were involved in reducing [C'], where the reduction simply consists of "scratching out" the rows and columns for ground wires "g." However, [C'] must first be found from the inversion of [P'], and it is faster to reduce a matrix than to invert it.

4.1.2.2 Bundling of Conductors

On high voltage power lines, bundle conductors are frequently used, where each "phase" or bundle conductor consists of two or more subconductors held together by spacers (typically 100 m apart). The bundle is usually symmetrical (S = 1.0 in Fig. 4.6), but unsymmetrical bundles have been proposed as well. Two methods can be used for calculating the line parameters of bundle conductors. With the first method, the parameters are originally calculated with each subconductor being represented as an individual conductor. Since the voltages are equal for the subconductors within a bundle, this voltage equality is then used to reduce the order of the matrices to the number of "equivalent phase conductors." With the second method, the concept of geometric mean distances is used to replace the bundle of subconductors by a single equivalent conductor. Both methods can be used with the supporting routine LINE CONSTANTS. The supporting routine CABLE CONSTANTS is limited to the second method.

Method 1 - Bundling of subconductors by matrix reduction

As in the elimination of ground wires, the matrix reduction process is the same for [Z'] and [P'], and will therefore only be explained for [Z']. Let us assume that the individual conductors i, k, l, m are to be bundled to make up phase R. Then the conditions

$$I_i + I_k + I_{\ell} + I_m = I_R$$

and

$$\frac{dV_i}{dx} = \frac{dV_k}{dx} = \frac{dV_{\ell}}{dx} = \frac{dV_m}{dx} = \frac{dV_R}{dx}$$

must be introduced into Eq. (4.2). The first step is to get I_R into the equations. This is done by writing I_R in place of I_i. By doing this, an error is of course made, which amounts to the addition of terms

$$Z'_{\mu i}(I_k + I_{\ell} + I_m)$$

in all rows μ; they must obviously be subtracted again to keep the equations correct. In effect, this means subtraction of column i from columns k, ℓ, m. These changes are shaded in Fig. 4.8.

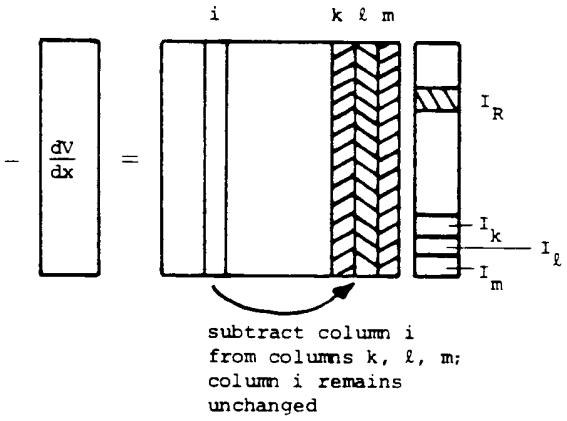

Fig. 4.8 - First step in bundling procedure

Columns k, ℓ, m are assumed to be the last ones in the matrix to make the explanation easier. The currents I_k, I_ℓ, I_m are still in the equations after execution of the first step of Fig. 4.8. To be able to eliminate them, there should be zeros in the left-hand side of the respective rows. This is easily accomplished by subtracting row i from rows k, ℓ, m, which produces zeros because $dV_i/dx = dV_k/dx$ etc. These changes are shaded in Fig. 4.9. The equations are now in a form which permits elimination of I_k, I_ℓ, I_m, in the same way as elimination of ground wires in Eq. (4.28). The four rows and columns for subconductors i, k, ℓ, m are thereby reduced to a single row and column for bundle conductor R.

Method 1 is more general than method 2 discussed next. For instance, it can easily handle the unequal current distribution in asymmetrical bundles described in Fig. 4.6.

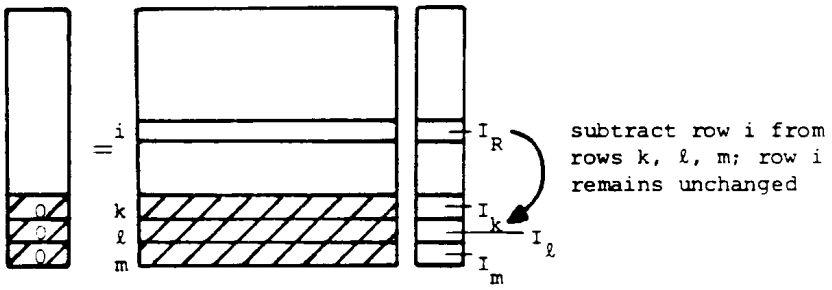

Fig. 4.9 - Second step in bundling procedure

Method 2 - Replacing bundled subconductors with equivalent single conductor

This method was developed for hand calculations [47], and while theoretically not limited to symmetrical bundles, formulas have usually only been derived for the more important case of symmetrical bundles. The following formulas are based on the assumption that

(a) the bundle is symmetrical (S = 1.0 in Fig. 4.6), and

(b) the current distribution among the individual subconductors within a bundle is uniform.

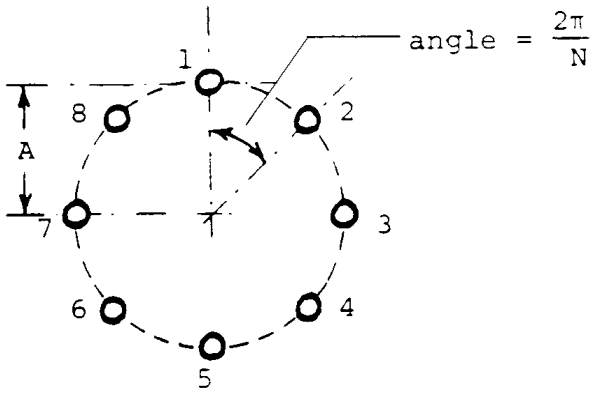

Fig. 4.10 - Symmetrical bundle with N individual subconductors

With these assumptions, the bundle can be treated as a single equivalent conductor in Eq. (4.15) by replacing GMR with the equivalent geometric mean radius of the bundle,

$$GMR_{equiv} = \sqrt[N]{N \cdot GMR \cdot A^{N-1}} \tag{4.29}$$

where

GMR = geometric mean radius of individual subconductor in bundle,

A = radius of bundle (Fig. 4.10).

Similarly, the radius r in Eq. (4.20) must be replaced with the equivalent radius

$$r_{equiv} = \sqrt[N]{N \cdot r \cdot A^{N-1}} \tag{4.30}$$

Comparison between methods 1 and 2

Both methods for bundling conductors give practically identical answers, at least in the example chosen for this comparison. The example was a 500 kV three-phase line with horizontal tower configuration, with phases 40 feet apart at an average height above ground of 50 feet. The symmetrical bundle consisted of 4 subconductors spaced 18 inches apart. Conductor diameter = 0.9 inches, dc resistance = 0.1686 Ω/mile, GMR = 0.3672 inches, r_{equiv} = 7.80524 inches from Eq. (4.30), and GMR_{equiv} = 7.41838 inches from Eq. (4.29). Table 4.2 compares the results in the form of positive and zero sequence parameters at 60 Hz. Obviously, the results are practically identical.

Table 4.2 - Comparison between methods 1 and 2 for bundling

Positive and zero sequence parameters at 60 Hz	Method 1 (Bundling by matrix reduction)	Method 2 (Equivalent conductors)

R'_{pos} (Ω/mile)	0.042223	0.042205
X'_{pos} (Ω/mile)	0.53394	0.53399
C'_{pos} (μF/mile)	0.021399	0.021397
R'_{zero} (Ω/mile)	0.31740	0.31738
X'_{zero} (Ω/mile)	2.0065	2.0065
C'_{zero} (μF/mile)	0.013456	0.013455

4.1.2.3 Reduced Matrices for Equivalent Phase Conductors

For the case of Fig. 4.1, elimination of ground wires and bundling of subconductors reduces the 13 x 13 matrices for the individual conductors to 6 x 6 matrices for the phases, e.g., for the series impedances,

$$-\frac{d}{dx}\begin{bmatrix} V_R \\ V_S \\ V_T \\ V_U \\ V_V \\ V_W \end{bmatrix} = \begin{bmatrix} Z'_{RR} & Z'_{RS} & Z'_{RT} & Z'_{RU} & Z'_{RV} & Z'_{RW} \\ Z'_{SR} & Z'_{SS} & Z'_{ST} & Z'_{SU} & Z'_{SV} & Z'_{SW} \\ Z'_{TR} & Z'_{TS} & Z'_{TT} & Z'_{TU} & Z'_{TV} & Z'_{TW} \\ Z'_{UR} & Z'_{US} & Z'_{UT} & Z'_{UU} & Z'_{UV} & Z'_{UW} \\ Z'_{VR} & Z'_{VS} & Z'_{VT} & Z'_{VU} & Z'_{VV} & Z'_{VW} \\ Z'_{WR} & Z'_{WS} & Z'_{WT} & Z'_{WU} & Z'_{WV} & Z'_{WW} \end{bmatrix} \begin{bmatrix} I_R \\ I_S \\ I_T \\ I_U \\ I_V \\ I_W \end{bmatrix}$$

or in general,

$$-\left[\frac{dV_{phase}}{dx}\right] = [Z'_{phase}]\,[I_{phase}] \tag{4.31}$$

and

$$-\left[\frac{dI_{phase}}{dx}\right] = j\omega[C'_{phase}]\,[V_{phase}] \tag{4.32}$$

For a three-phase single circuit with phases A, B, C, Eq. (4.31) would have the form

$$-\begin{bmatrix} \frac{dV_A}{dx} \\ \frac{dV_B}{dx} \\ \frac{dV_C}{dx} \end{bmatrix} = \begin{bmatrix} Z'_{AA} & Z'_{AB} & Z'_{AC} \\ Z'_{BA} & Z'_{BB} & Z'_{BC} \\ Z'_{CA} & Z'_{CB} & Z'_{CC} \end{bmatrix} \begin{bmatrix} I_A \\ I_B \\ I_C \end{bmatrix} \tag{4.33}$$

The diagonal element Z'_{kk} in Eq. (4.33) is the series self impedance of phase k for the loop formed by phase k with return through ground and ground wires, and the off-diagonal element Z'_{ik} is the series mutual impedance between phases i and k. The self impedance of phase k <u>is not</u> the positive sequence impedance. To obtain impedances which

come close to the positive sequence values, we would have to assume symmetrical currents in Eq. (4.33),

$$I_B = a^2 I_A \quad and \quad I_C = a I_A , \quad with \quad a = e^{j120^\circ}$$

and then express the voltage drop in phase A as a function of I_A only,

$$-\frac{dV_A}{dx} = Z'_{A-symm} I_A, \quad with \; Z'_{A-symm} = (Z'_{AA} + a^2 Z'_{AB} + a Z'_{AC}) \tag{4.34a}$$

and similarly for phases B and C,

$$-\frac{dV_B}{dx} = Z'_{B-symm} I_B, \quad with \; Z'_{B-symm} = (Z'_{BB} + a Z'_{AB} + a^2 Z'_{BC}) \tag{4.34b}$$

$$-\frac{dV_C}{dx} = Z'_{C-symm} I_C, \quad with \; Z'_{C-symm} = (Z'_{CC} + a^2 Z'_{AC} + a Z'_{BC}) \tag{4.34c}$$

The values of the three impedances $Z'_{A\text{-}symm}$, $Z'_{B\text{-}symm}$, $Z'_{C\text{-}symm}$ in Eq. (4.34) are not exactly equal, but their average value is the positive sequence impedance. Because of slight differences in the three values, the voltage drops are slightly unsymmetrical (or the currents become slightly unsymmetrical for given symmetrical voltage drops). As discussed in Section 4.1.3, transposing a line eliminates or reduces these unsymmetries at power frequency, though not necessarily at higher frequencies.

In the capacitance matrix of a three-phase line, C'_{AA} would be the sum of the coupling capacitances to phases B and C and of the capacitance to ground, and C_{AB} would be the negative value of the coupling capacitance between phases A and B. Assuming symmetrical voltages, Eq. (4.32) would show slight unsymmetry in $[dI_{phase}/dx]$, analogous to that of Eq. (4.34).

4.1.2.4 Nominal π-Circuit for Equivalent Phase Conductors

The matrices in Eq. (4.31) and (4.32) are the basis for practically all EMTP line models. Even in studies where ground wires must be retained, it is still these matrices which are used, with phase numbers assigned to the ground wires as well. A three-phase line with one ground wire is conceptually a four-phase line, with phase no. 1, 2, 3 for phase conductors A, B, C and phase no. 4 for the ground wire.

One type of line representation uses cascade connections of nominal π-circuits, as discussed in Sections 4.2.1.1 and 4.2.2.1. This polyphase nominal π-circuit with a series impedance matrix and equal shunt capacitance matrices at both ends, as shown in Fig. 3.10, is directly obtained from the matrices in Eq. (4.31) and (4.32),

$$[R] + j\omega[L] = \ell \cdot [Z'_{phase}] \tag{4.35}$$

and

$$\frac{1}{2} j\omega [C] = \frac{1}{2} j\omega \ell\, [C'_{phase}] \tag{4.36}$$

where ℓ is the length of the line.

The cascade connection of nominal π-circuits approximates the even distribution of the line parameters reasonably well up to a certain frequency. It does ignore the frequency dependence of the resistances and inductances per unit length, however, and is therefore reasonably accurate only within a certain frequency range.

Strictly speaking, it may not be quite correct to treat the real part of $[Z'_{phase}]$ as a resistance, and the imaginary part as a reactance, as done in Eq. (4.35), especially for lines with ground wires. For a three-phase line with phases A, B, C and ground wire g, the original 4 x 4-matrix is reduced to a 3 x 3-matrix with elements

$$Z'_{ik-reduced} = Z'_{ik-original} - \frac{Z'_{ig-original} Z'_{kg-original}}{Z'_{g\,g-original}} \tag{4.37}$$

Even if $Z'_{ik\text{-}original}$ could be separated into resistance and reactance without any doubt, the real part of the second term in Eq. (4.37) depends on the imaginary parts of the three impedances as well, unless the R/X-ratios of all three impedances were equal. There is also some doubt about separating $Z'_{ik\text{-}original}$ into resistance and reactance because of the earth as an implied return conductor, as mentioned in Section 3.1. Nonetheless, experience has shown that nominal π-circuits do give reasonable answers in many cases, and they are at least correct at the frequency at which the matrices were calculated (and probably reasonably accurate in a frequency range around that specific frequency).

Example for using nominal π-circuits

Electrostatic and magnetic coupling effects from energized power lines to parallel objects, such as fences or de-energized power lines, are important safety issues, and have been well described in two IEEE Committee Reports [37, 49]. A case of a fence running parallel to a power line (Fig. 4.11) is discussed here, as an application example for nominal π-circuits.[6] By simply treating the fence as a fourth phase conductor, the following series impedance and shunt capacitance matrices are obtained:

$$[Z'_{phase}] = \begin{bmatrix} 0.4054 + j0.9859 & symmetric! & & \\ 0.0574 + j0.4265 & 0.4054 + j0.9859 & & \\ 0.0574 + j0.4265 & 0.0574 + j0.3742 & 0.4054 + j0.9859 & \\ 0.0581 + j0.3168 & 0.0581 + j0.3291 & 0.0581 + j0.3044 & 1.8607 + j0.9953 \end{bmatrix} \Omega/km$$

and

[6]For electrically short lines, as in this example, electrostatic coupling effects can be solved by themselves with $[C'_{phase}]$, and magnetic coupling effects by themselves with $[Z'_{phase}]$. For solving such cases with the EMTP, it is usually easier to use nominal π-circuits which combine both effects. With that approach, electrically long lines can be studied as well, provided an appropriate number of π-circuits are connected in cascade.

$$[C'_{phase}] = \begin{bmatrix} 7.5709 & symmetric & & \\ -1.6266 & 7.3088 & & \\ -1.6304 & -0.8349 & 7.2999 & \\ -0.1688 & -0.2758 & -0.1189 & 6.9727 \end{bmatrix} nF/km$$

From these matrices, the nominal π-circuit matrices are calculated with Eq. (4.35) and (4.36).

Power line conductors:
$R'_{internal}$ = 0.348 Ω/km
X'_A = 0.4755 Ω/km (60 Hz)
(reactance at 1 m spacing)
diameter = 12.7 mm
frequency = 60 Hz
Fence:
$R'_{internal}$ = 1.802 Ω/km
solid conductor (nonmagnetic)
diameter = 4.064 mm
length = 2 km

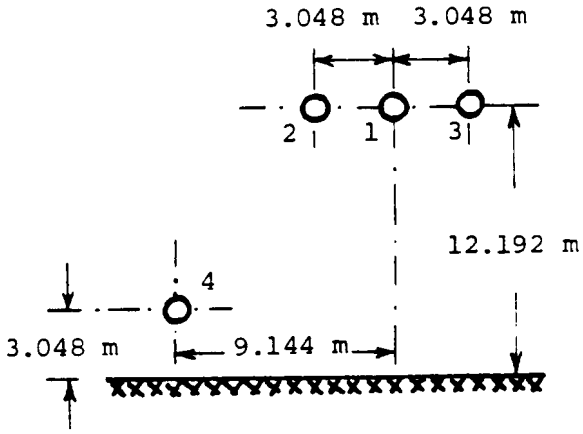

Fig. 4.11 - Fence 4 running parallel with power line phase conductors 1, 2, 3

Assume that the fence is insulated from the posts and nowhere grounded. To find the voltage on the fence due to capacitive coupling, simply connect voltage sources to phases 1, 2, 3 at the sending end, and leave 1, 2, 3 at the receiving end as well as 4 at both ends open-ended. Assuming V = 345 kV RMS, line-to-line, the fence voltage becomes V_4 = 3.97 kV. If phase 1 were at zero potential because of a phase-to-ground fault, with phases 2 and 3 still at rated voltage 345/√3 kV, then the fence voltage would increase to V_4 = 6.84 kV. These answers are practically independent of fence length.

Now assume that the 2 km long fence is grounded at the sending end and open-ended at the receiving end. To find the voltage in the fence for a load current of 1 kA RMS, simply add current sources to phases 1, 2, 3 at the receiving end, with symmetrical voltage sources at the sending end. Phase 4 is connected to ground at the sending end and open-ended at the receiving end. The answer will be $V_{4\text{-receiving end}}$ = 0.043 kV, which increases dramatically to 6.442 kV if the currents are changed to I_1 = 10 kA, $I_2 = I_3 = 0$ to simulate a phase-to-ground fault. For this last case, the fence current would be 1.526 kA if the fence were grounded at both ends. These answers are practically independent of the voltage on phases 1, 2, 3, which can easily be verified by setting them zero.

4.1.2.5 Continuous and Segmented Ground Wires

(a) Circulating Currents in Continuous Ground Wires

Assume that ground wire no. 13 of Fig. 4.1 is grounded at each tower. If the ground wire is not eliminated,

then the series impedance matrix for equivalent phase conductors will be a 7 x 7 matrix. Its elements can then be used to calculate the longitudinally induced voltage in the ground wire,

$$-\frac{dV_g}{dx} = Z'_{gR}\, I_R + Z'_{gS}\, I_s + \ldots Z'_{gW}\, I_W + Z'_{gg}\, I_g \tag{4.38}$$

If tower and tower footing resistances are ignored, then $V_g = 1$ at all towers as long as span $<<$ wavelength, or

$$I_g = -\frac{Z'_{gR}\, I_R + Z'_{gS}\, I_S + \ldots Z'_{gW}\, I_W}{Z'_{gg}} \tag{4.39}$$

Since the mutual impedances from the phase conductors to the ground wire are never exactly equal, the numerator in Eq. (4.39) does not add up to zero even if the phase currents are symmetrical. Therefore, there is a nonzero ground wire current I_g, produced by positive sequence currents, which circulates through ground wire, towers and ground (Fig. 4.12). This circulating current produces additional losses, which show up as an increase in the value of the positive sequence resistance, compared with the resistance of the phase conductors. Handbook formulas would not contain this increase, but the elimination of the ground wires discussed in Section 4.1.2.1 will produce it automatically. In one particular case of a single-circuit 500 kV line, this increase was 6.5%.

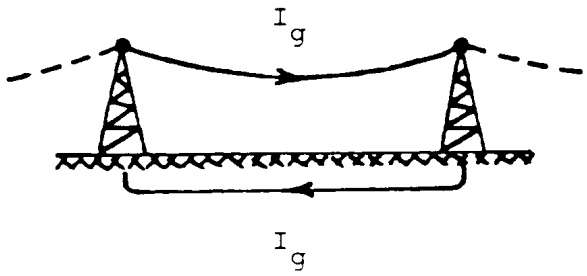

Fig. 4.12 - Circulating current in ground wire

The inclusion of tower and tower footing resistances may change the results of Eq. (4.39) somewhat. If we assume equal resistance at all towers, then it appears that the voltage drop produced by the current in the left loop (Fig. 4.13) is canceled by the voltage drop produced by the current in the middle loop, and Eq. (4.39) should therefore still be correct, except in the very first and very last span of the line. This assumes that the phase currents do not change from one span to the next, which is reasonable up to a certain frequency.

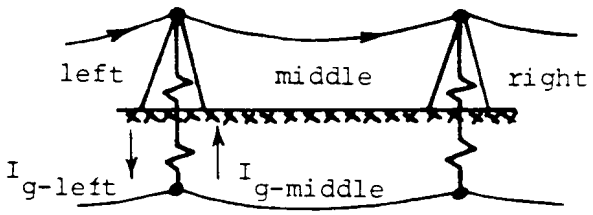

Fig. 4.13 - Cascade connection of loops

(b) Segmented Ground Wires

To avoid the losses associated with these circulating currents, some utility companies use segmented ground wires which are grounded at one tower, and insulated at adjacent towers to both ends of the segmentation interval, where they are interrupted as well (Fig. 4.14).

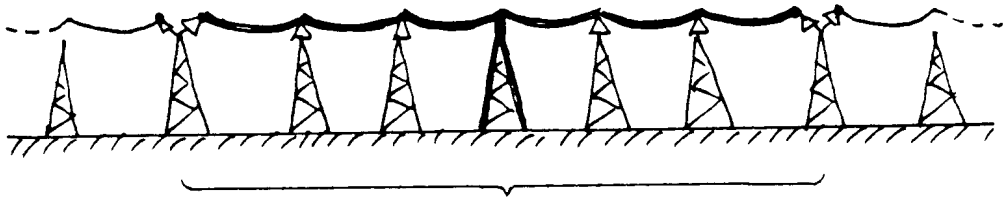

"T-configuration"
in segmentation interval
Δ = insulator

Fig. 4.14 - Segmented ground wires

They still act as electrostatic shields for lightning protection, but when struck by lightning, the segmentation gaps and the small insulators will flash over, thereby making the ground wire continuous again. The supporting routine LINE CONSTANTS has an option for segmented ground wires, which ignores[7] them in the calculation of the series impedance matrix since they have no influence on the voltage drops in the phase conductors, but takes them into account in the calculation of the capacitance matrix because the electrostatic field is not influenced by segmentation.

(c) Reduction Effect of Continuous Ground Wires on Interference

Interference from power lines in parallel telephone lines becomes a problem if there are high zero-sequence currents in the power line, e.g., in case of a single-phase-to-ground fault. Assume a three-phase line with one ground wire g and a parallel telephone line P as shown in Fig. 4.15. For zero sequence currents, which implies equal currents in phases A, B, C, the voltages in P induced by currents in A, B, C will add up in the same direction (Fig. 4.16). The voltage induced by the ground wire current I_g will have opposite polarity, however, since this

[7]An exception are studies where it can be assumed that the gaps and insulators have flashed over. For such studies, ground wires must be treated as continuous, as suggested by W.A. Lewis. Switching and lightning surge studies may fall into this category.

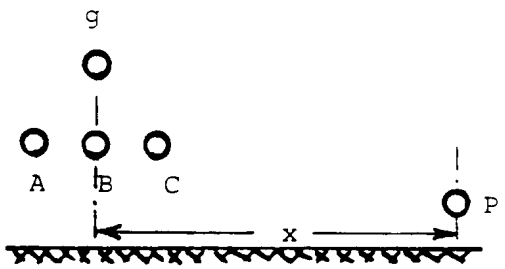

Fig. 4.15 - Parallel telephone line P close to a power line with phases A, B, C and ground wire g

current flows in opposite direction, thereby reducing the total induced voltage - dV_p/dx. Part of this beneficial reduction may be offset by an increase in the zero sequence currents because ground wires also reduce the zero sequence impedance of lines (typically by 5 to 15% with one

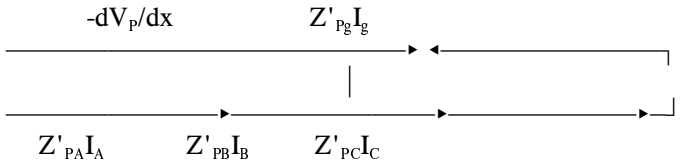

Fig. 4.16 - Induced voltage caused by currents $I_A = I_B = I_C$ and by I_g

steel ground wire, or 15 to 30% with one ACSR ground wire). The reduction effect of the ground wire on interference can be included in the calculations in two different ways:

(a) Obtain the mutual impedances from matrices in which ground wires have been eliminated and in which the parallel telephone lines has been retained as an additional conductor. Then the reduction effect of the ground wires is automatically contained in calculating the magnetically induced voltage from

$$-\frac{dV_P}{dx} = Z'_{PA-reduced}I_A + Z'_{PB-reduced}I_B + Z'_{PC-reduced}I_C \qquad (4.40a)$$

and, if needed, the electrostatically induced voltage for an insulated parallel telephone line from

$$0 = C'_{PA-reduced}V_A + C'_{PB-reduced}V_B + C'_{PC-reduced}V_C + C'_{PP-reduced}V_P \qquad (4.40b)$$

(b) Calculate the mutual impedances from P to the phases as well as to the ground wires (or obtain them from matrices in which the ground wires were retained), and recover the value of the ground wire currents with a "screening matrix" from the phase currents. By setting $V_g = 0$ in Eq. (4.27), the ground wire currents are obtained as

$$[I_g] = -[Z'_{g\,g}]^{-1}[Z_{gu}][I_u] \qquad (4.41)$$
$$[F_{screen}]$$

with "u" indicating ungrounded phase currents here. The screening matrix $[F_{screen}]$ is the transpose of the distribution factor matrix $[D_{12}]$ of Eq. (III.14) in Appendix III, and as indicated there, can easily be obtained as a by-product of the matrix reduction process. As an example, Fig. 4.17 shows the standing waves of the phase currents of the sixth harmonic of 60 Hz in the two poles A, B of the Pacific Intertie HVDC line, as well as the currents in the two ground wires recovered with Eq. (4.41) [11].

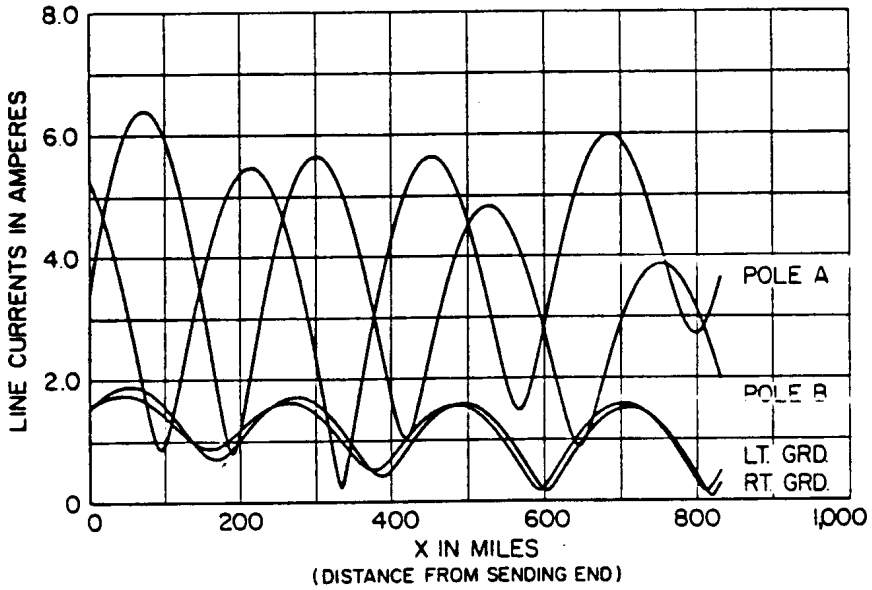

Fig. 4.17 - Currents of sixth harmonic in HVDC line [11]. © 1969 IEEE

4.1.3 Positive and Zero Sequence Parameters of Balanced[8] Lines

A "balanced" transmission line shall be defined as a line where all diagonal elements of $[Z'_{phase}]$ and $[C'_{phase}]$ are equal among themselves, and all off-diagonal elements are equal among themselves,

$$\begin{bmatrix} Z'_s & Z'_m & \cdots & Z'_m \\ Z'_m & Z'_s & \cdots & Z'_m \\ \cdot & \cdot & \cdot & \cdot \\ \cdot & \cdot & \cdot & \cdot \\ \cdot & \cdot & \cdot & \cdot \\ Z'_m & Z'_m & \cdots & Z'_s \end{bmatrix} \quad \begin{bmatrix} C'_s & C'_m & \cdots & C'_m \\ C'_m & C'_s & \cdots & C'_m \\ \cdot & \cdot & \cdot & \cdot \\ \cdot & \cdot & \cdot & \cdot \\ \cdot & \cdot & \cdot & \cdot \\ C'_m & C'_m & \cdots & C'_s \end{bmatrix} \tag{4.42}$$

[8]Also called "continuously transposed" in the EMTP Rule Book.

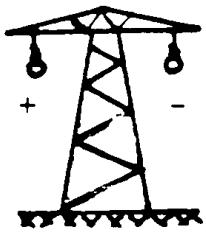

Fig. 4.18 - Bipolar dc line

The only line which is truly balanced is the symmetric bipolar dc line (Fig. 4.18), where $Z'_{11} = Z'_{22} = Z'_s$ and $Z'_{12} = Z'_m$. Single-circuit three-phase lines become more or less balanced if the line is transposed, as shown in Fig. 4.19, provided the length of the "barrel" (= 3 sections, or one cycle of the transposition scheme) is much less than the wavelength of the frequencies involved in the particular study. While the Westinghouse Reference Book [51, p. 777] mentions that a barrel may be 80 to 160 km in length on long lines, a German handbook [52, p. 555] recommends that one barrel be no longer than 80 km (at 50 Hz, or 67 km at 60 Hz) for lines with triangular conductor configuration, or 40 km (at 50 Hz, or 33 km at 60 Hz) for other conductor configurations. Whatever the length of the barrel, it is important to realize that while

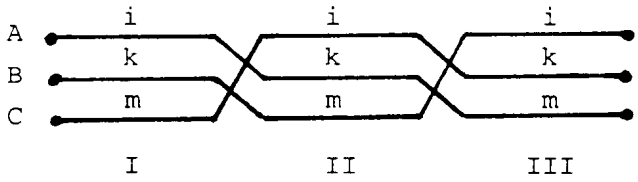

Fig. 4.19 - Transposition scheme for single three-phase circuit

a line may be reasonably balanced at power frequency, there may be enough unbalance at higher frequencies[9]. If the barrel length is much shorter than the wavelength, then series impedances can be averaged by themselves through the three sections, and shunt capacitances can be averaged by themselves, e.g., for the impedances of the line in Fig. 4.19,

$$\frac{1}{3}\left[\begin{bmatrix} Z'_{ii} & Z'_{ik} & Z'_{im} \\ Z'_{ki} & Z'_{kk} & Z'_{km} \\ Z'_{mi} & Z'_{mk} & Z'_{mm} \end{bmatrix} + \begin{bmatrix} Z'_{kk} & Z'_{km} & Z'_{ki} \\ Z'_{mk} & Z'_{mm} & Z'_{mi} \\ Z'_{ik} & Z'_{im} & Z'_{ii} \end{bmatrix} + \begin{bmatrix} Z'_{mm} & Z'_{mi} & Z'_{mk} \\ Z'_{im} & Z'_{ii} & Z'_{ik} \\ Z'_{km} & Z'_{ki} & Z'_{kk} \end{bmatrix}\right] = \begin{bmatrix} Z'_s & Z'_m & Z'_m \\ Z'_m & Z'_s & Z'_m \\ Z'_m & Z'_m & Z'_s \end{bmatrix}$$

with

[9]At the time of writing, studies at B.C. Hydro seem to indicate that transposed single-circuit lines with horizontal conductor configuration cannot be treated as balanced lines in switching surge studies.

$$Z'_s = \frac{1}{3}(Z'_{ii} + Z'_{kk} + Z'_{mm})$$
$$Z'_m = \frac{1}{3}(Z'_{ik} + Z'_{km} + Z'_{mi}) \tag{4.43}$$

The averaging process for the shunt capacitances is analogous.

4.1.3.1 Positive and Zero Sequence Parameters of Single-Circuit Three-Phase Lines

Balanced single-circuit three-phase lines can be studied much easier with symmetrical or α, β, 0-components because the three coupled equations in the phase domain,

$$-\left[\frac{dV_{phase}}{dx}\right] = \begin{bmatrix} Z'_s & Z'_m & Z'_m \\ Z'_m & Z'_s & Z'_m \\ Z'_m & Z'_m & Z'_s \end{bmatrix} [I_{phase}] \tag{4.44}$$

become three decoupled equations with symmetrical components,

$$\begin{aligned} -dV_{zero}/dx &= Z'_{zero} I_{zero} \\ -dV_{pos}/dx &= Z'_{pos} I_{pos} \\ -dV_{neg}/dx &= Z'_{pos} I_{neg} \end{aligned} \tag{4.45}$$

or with α, β, 0-components,

$$\begin{aligned} -dV_{zero}/dx &= Z'_{zero} I_{zero} \\ -dV_{\alpha}/dx &= Z'_{pos} I_{\alpha} \\ -dV_{\beta}/dx &= Z'_{pos} I_{\beta} \end{aligned} \tag{4.46}$$

Since transformation to symmetrical components involves complex coefficients, symmetrical components are not well suited for transient analysis where all variables are real, and are therefore only briefly discussed in Section 4.1.4. The impedances needed in both systems (4.45) and (4.46) are the same, however, namely Z'_{zero} and Z'_{pos}. The balanced distributed-parameter line models in the EMTP use transformations to α, β, 0-components, due to Edith Clarke [44],

$$[v_{phase}] = [T][v_{0\alpha\beta}] \qquad [v_{0\alpha\beta}] = [T]^{-1}[v_{phase}]$$

and

$$[i_{phase}] = [T][i_{0\alpha\beta}] \qquad [i_{0\alpha\beta}] = [T]^{-1}[i_{phase}] \tag{4.47}$$

where

$$[v_{0\alpha\beta}] = \begin{bmatrix} v_0 \\ v_\alpha \\ v_\beta \end{bmatrix}$$

with

$$[T] = \frac{1}{\sqrt{3}} \begin{bmatrix} 1 & \sqrt{2} & 0 \\ 1 & -\frac{1}{\sqrt{2}} & \frac{\sqrt{3}}{\sqrt{2}} \\ 1 & -\frac{1}{\sqrt{2}} & -\frac{\sqrt{3}}{\sqrt{2}} \end{bmatrix}$$

and

$$[T]^{-1} = \frac{1}{\sqrt{3}} \begin{bmatrix} 1 & 1 & 1 \\ \sqrt{2} & -\frac{1}{\sqrt{2}} & -\frac{1}{\sqrt{2}} \\ 0 & \frac{\sqrt{3}}{\sqrt{2}} & -\frac{\sqrt{3}}{\sqrt{2}} \end{bmatrix} \tag{4.48}$$

The columns in [T] and $[T]^{-1}$ are normalized; in that case [T] is orthogonal,

$$[T]^{-1} = [T]^t \tag{4.49}$$

Applying this transformation to Eq. (4.44) produces

$$-\begin{bmatrix} dV_0/dx \\ dV_\alpha/dx \\ dV_\beta/dx \end{bmatrix} = \begin{bmatrix} Z'_s+2Z'_m & 0 & 0 \\ 0 & Z'_s-Z'_m & 0 \\ 0 & 0 & Z'_s-Z'_m \end{bmatrix} \begin{bmatrix} I_0 \\ I_\alpha \\ I_\beta \end{bmatrix}$$

which is identical with Eq. (4.46), with

$$Z'_{zero} = Z'_s + 2Z'_m \tag{4.50a}$$

Eq. (4.50) and its inverse relationship is the same as discussed previously in Eq. (3.6) and (3.4). Going from the

$$Z'_{pos} = Z'_s - Z'_m \tag{4.50b}$$

three coupled equations in (4.44) to the three decoupled equations in (4.46) allows us to solve the line as if it consisted of three single-phase lines, which is much simpler than trying to solve the equations of a three-phase line.

The positive sequence inductance of overhead lines is practically constant, while the positive sequence resistance remains more or less constant until skin effect in the conductors becomes noticeable, as shown in Fig. 4.20. Zero sequence inductance and resistance are very much frequency-dependent, due to skin effects in the earth return.

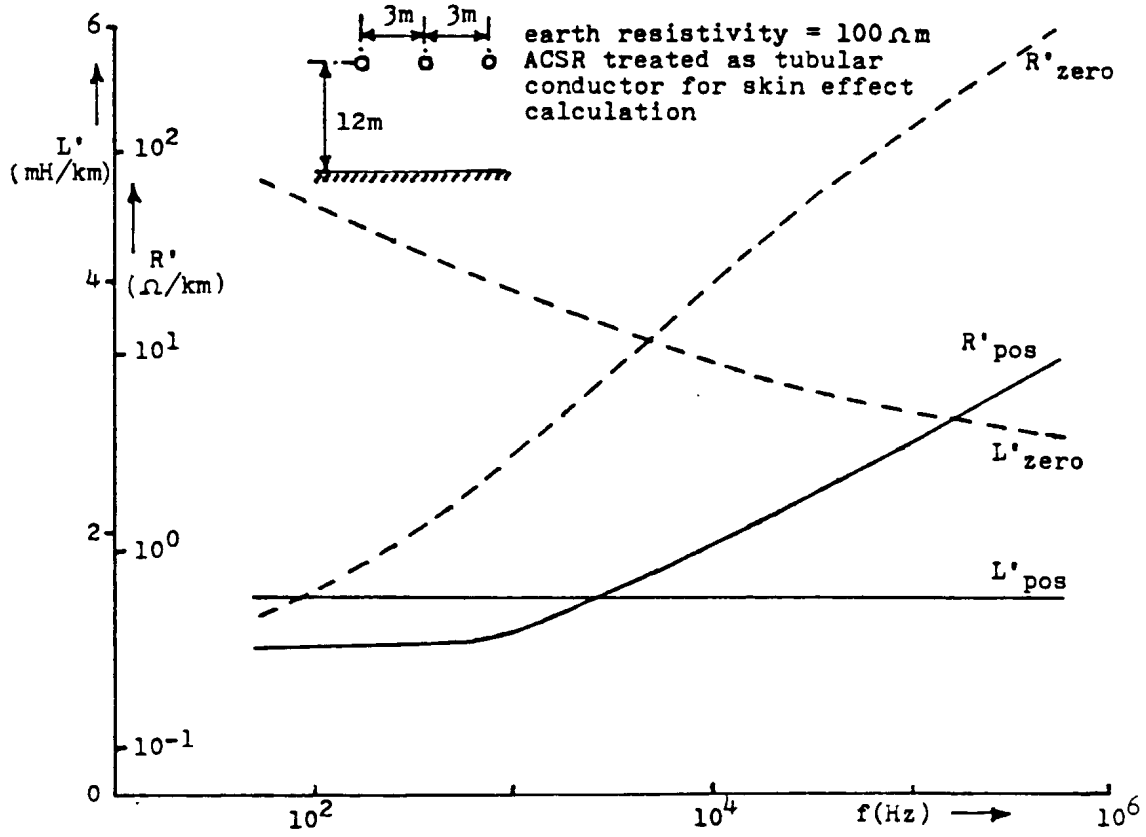

Fig. 4.20 - Positive and zero sequence resistance and inductance of a three-phase line

The shunt capacitance matrix of a balanced three-phase line becomes diagonal in α, β, 0-components as well, with

$$C'_{zero} = C'_s + 2C'_m \tag{4.51a}$$

$$C'_{pos} = C'_s - C'_m \tag{4.51b}$$

which is the inverse relationship of Eq. (3.13). The capacitances are constant over the frequency range of interest to power engineers.

Comparison with results from handbook formulas

The positive and zero sequence parameters obtained from the supporting routines LINE CONSTANTS and CABLE CONSTANTS may differ from those obtained with handbook formulas. Since some EMTP users may make comparisons, it may be worthwhile to explain the major differences for a specific example. Assume a typical 500 kV line with horizontal phase configuration, with phases 40 feet apart at an average height above ground of 50 feet. Each phase consists of a symmetrical bundle with 4 subconductors spaced 18 inches apart. Subconductor diameter = 0.9 inches, dc resistance = 0.1686 Ω/mile, GMR = 0.3672 inches. Throughout this comparison, the bundle conductors are represented as equivalent conductors with r_{equiv} = 7.80524 inches from Eq. (4.30) and GMR_{equiv} = 7.41838 inches from Eq. (4.29).

For positive sequence capacitance, most handbooks give the formula

$$C'_{pos} = \frac{2\pi\varepsilon_0}{\ln\frac{d_m}{r_{=}}} \tag{4.52}$$

with $d_m = \sqrt[3]{d_{AB}d_{AC}d_{BC}}$ (geometric mean distance among the three phases).
This produces a value approx. 4% lower than the more accurate value from Eq. (4.51) for the 500 kV line described above. The formula for zero sequence capacitance in [52] and [53],

$$C'_{zero} = \frac{2\pi\varepsilon_0}{\ln\frac{2h_m D_m^{\,2}}{r_{equiv} d_m^{\,2}}} \qquad (\textit{Siemens}) \tag{4.53}$$

with

$h_m = \sqrt[3]{h_A h_B h_C}$ (geometric mean height),

$D_m = \sqrt[3]{D_{AB}D_{AC}D_{BC}}$ (geometric mean distance between one phase and image of another phase),

can be derived by averaging the diagonal and off-diagonal elements in the $[P'_{phase}]$-matrix among themselves to account for transposition. Eq. (4.51) has this averaging process implied in the $[C'_{phase}]$-matrix. Both give practically the same answer, with results from Eq. (4.53) 0.23% lower than those from Eq. (4.51). In [51], Eq. (4.53) is further simplified by assuming $D_m \approx 2h_m$,

$$C'_{zero} = \frac{2\pi\varepsilon_0}{\ln\frac{(2h_m)^3}{r_{equiv} d_m^{\,2}}} \qquad (\textit{Westinghouse}) \tag{4.54}$$

which produces a value 4% higher than the value from Eq. (4.51). While Eq. (4.54) is theoretically less accurate, the value may actually be closer to measured values because the influence of towers, which is neglected in all

formulas, typically increases the calculated zero sequence capacitance by about 8 to 9% on 110 kV lines, about 6% on 220 and 380 kV lines, and about 4% on 700 kV lines [54, p. 218].

The formulas for zero and positive sequence impedances in most handbooks are based on the assumption that parameter a in Eq. (4.10) is so small that only the first term in the series of Eq. (4.11) must be retained. For normal phase spacings this is probably a reasonable assumption at power frequency 50 or 60 Hz. Then, after all diagonal and off-diagonal elements have been averaged out among themselves through transposition,

$$\Delta R'_s = \Delta R'_m \approx \frac{\omega\pi \cdot 10^{-4}}{2} \qquad in\ \Omega/km$$

and

$$\Delta X'_s \approx 2\omega \cdot 10^{-4}[0.6159315 - \ln(2h_m k\frac{\sqrt{f}}{\sqrt{\rho}})] \qquad in\ \Omega/km \tag{4.55}$$

$$\Delta X'_m \approx 2\omega \cdot 10^{-4}[0.6159315 - \ln(D_m k\frac{\sqrt{f}}{\sqrt{\rho}})] \qquad in\ \Omega/km$$

with

$$k = 4\pi \cdot \sqrt{5} \cdot 10^{-4}$$

This leads to the expression

$$Z'_{pos} = R'_{ac} + j2\omega \cdot 10^{-4} \ln\frac{d_m}{GMR_{equiv}} \qquad in\ \Omega/km \tag{4.56}$$

with R'_{ac} = ac resistance of equivalent phase conductor. It is interesting that the influence of ground resistivity and of conductor height, which is present in Z'_s and Z'_m, completely disappears here in taking the difference, $Z'_{pos} = Z'_s - Z'_m$. Eq. (4.56) is the formula found in most handbooks. Table 4.3 compares results from Eq. (4.50) with results from Eq. (4.56) for the 500 kV line described above with the following additional assumptions: Earth resistivity = 100 Ωm; skin effect within conductors ignored to limit differences to influence of earth return (that is, $R'_{ac} = R'_{dc}$ and GMR_{equiv} = constant).

Table 4.3 - Accurate and approximate positive sequence resistance and inductance

	ACCURATE R'_{pos} and L'_{pos} from Eq. (4.50)		APPROXIMATE R'_{pos} and L'_{pos} from Eq. (4.56)	
f (Hz)	R' (Ω/mile)	L' (mH/mile)	R' (Ω/mile)	L' (mH/mile)

10^{-6}	0.04215	1.417	0.04215	1.417
10	0.04215	1.416	0.04215	1.417
100	0.04229	1.416	0.04215	1.417
1 000	0.05003	1.416	0.04215	1.417
10 000	0.3528	1.413	0.04215	1.417
100 000	6.229	1.401	0.04215	1.417

Table 4.3 shows that L'_{pos} from Eq. (4.56) is quite accurate over a wide frequency range, whereas R'_{pos} becomes less accurate as the frequency increases (0.33% error at 100 Hz, but wrong by orders of magnitude at 100 kHz). The increase in R'_{pos} in the higher frequency range is caused by eddy currents in the earth, as indicated in Fig. 4.21 for a bipolar dc line. Ground wires also influence the positive sequence impedance, as mentioned in Section 4.1.2.5 (a). Both influences are ignored in Eq. (4.56), but automatically included in the method described here.

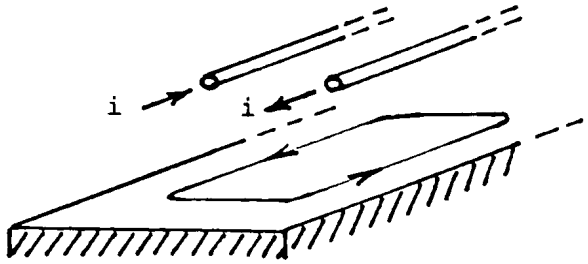

Fig. 4.21 - Eddy currents in earth

The zero sequence impedance obtained from Eq. (4.55) is

$$Z'_{zero} = \left(R'_{ac} + \frac{3\omega\pi\cdot 10^{-4}}{2}\right) + j6\omega\cdot 10^{-4}\ln\left(\frac{658.87\frac{\sqrt{\rho}}{\sqrt{f}}}{3\sqrt{GMR_{equiv}\cdot d_m^2}}\right) \quad in\ \Omega/km \tag{4.57}$$

with f in Hz, ρ in Ωm, and GMR_{equiv} and d_m in m. Eq. (4.57) is the same equation as in [51, 52, 53]. Table 4.4 compares the approximate results from Eq. (4.57) with the accurate results from Eq. (4.50). The inductance L'_{zero} is reasonably accurate over a wide frequency range (-0.75% error at 100 Hz, -33% error at 100 kHz), but the resistance R'_{zero} is less accurate (4.6% error at 100 Hz, 159% error at 100 kHz).

Table 4.4 - Accurate and approximate zero sequence resistance and inductance

	ACCURATE R'_{zero} and L'_{zero} from Eq. (4.50)		APPROXIMATE R'_{zero} and L'_{zero} from Eq. (4.57)	
f (Hz)	R' (Ω/mile)	L' (mH/mile)	R' (Ω/mile)	L' (mH/mile)

10^{-6}	0.04215	13.94	0.04215	13.94
10	0.08905	6.170	0.08980	6.158
100	0.4960	5.084	0.05187	5.046
1 000	4.169	4.052	4.807	3.934
10 000	32.12	3.164	47.69	2.823
100 000	184.0	2.568	476.6	1.711

4.1.3.2 Positive and Zero Sequence Parameters of Balanced M-Phase Lines

The EMTP can handle balanced distributed-parameter lines not only for the case of a three-phase line, but for any number of phases M. For this general case, the α, β, 0-transformation of Eq. (4.47) has been generalized to M phases, with the transformation matrix [55]

$$[T] = \begin{bmatrix} \frac{1}{\sqrt{M}} & \frac{1}{\sqrt{2}} & \frac{1}{\sqrt{6}} & \cdots & \frac{1}{\sqrt{J(J-1)}} & \cdots & \frac{1}{\sqrt{M(M-1)}} \\ \frac{1}{\sqrt{M}} & -\frac{1}{\sqrt{2}} & \frac{1}{\sqrt{6}} & \cdots & \frac{1}{\sqrt{J(J-1)}} & \cdots & \frac{1}{\sqrt{M(M-1)}} \\ \frac{1}{\sqrt{M}} & 0 & -\frac{2}{\sqrt{6}} & . & . & . & . \\ . & . & . & . & -\frac{(J-1)}{\sqrt{J(J-1)}} & . & . \\ . & . & . & . & 0 & . & . \\ . & . & . & . & . & . & . \\ \frac{1}{\sqrt{M}} & 0 & 0 & . & 0 & . & -\frac{(M-1)}{\sqrt{M(M-1)}} \end{bmatrix} \tag{4.58}$$

where again

$$[T]^{-1} = [T]^{t} \tag{4.59}$$

[T] of Eq. (4.48) is a special case of Eq. (4.58) for M = 3 if we assume that the phases are numbered 2, 3, 1 in Eq. (4.47) and if the α, β, 0-quantities are ordered 0, β, -α (sign reversal on α).

Applying this M-phase α, β, 0-transformation[10] to the matrices of M-phase balanced lines produces diagonal matrices of the form

[10]In the UBC EMTP, and in older versions of the BPA EMTP, Karrenbauer's transformation [57] is used instead, which produces the same diagonal matrices, but does not have the property of Eq. (4.59). This property is important because it makes the balanced line just a special case of the untransposed line discussed in Section 4.1.5.

$$\begin{bmatrix} Z'_{zero} & & & & \\ & Z'_{pos} & & & \\ & & Z'_{pos} & & \\ & & & \ddots & \\ & & & & Z'_{pos} \end{bmatrix}$$

with the first diagonal element being the zero sequence (ground mode) impedance, and the next M-1 diagonal elements being the positive sequence (aerial mode) impedance,

$$Z'_{zero} = Z'_s + (M-1)Z'_m \tag{4.60a}$$

$$Z'_{pos} = Z'_s - Z'_m \tag{4.60b}$$

and similarly for the capacitances,

$$C'_{zero} = C'_s + (M-1)C'_m \tag{4.61a}$$

$$C'_{pos} = C'_s - C'_m \tag{4.61b}$$

To refer to the two distinct diagonal elements as zero and positive sequence may be confusing, because the concept of sequence values has primarily been used for three-phase lines. "Ground mode" and "aerial mode" may be more appropriate. Confusion is most likely to arise for double-circuit three-phase lines, where each three-phase line has its own zero and positive sequence values defined by Eq. (4.50) and (4.51) with symmetrical components used for each three-phase circuit, while in the context of this section the double-circuit line is treated as a six-phase line with different zero and positive sequence values defined by Eq. (4.60) and (4.61). The fact that the terms zero and positive sequence are used for M ≠ 3 as well comes from the generalization of symmetrical components of Section 4.1.4 to M phases with the transformation matrix [56, p. 155]

$$[S_{M-phase}] = \begin{bmatrix} s_{11} & s_{12} & \cdots & s_{1M} \\ s_{21} & s_{22} & \cdots & s_{2M} \\ . & . & . & . \\ s_{M1} & s_{M2} & \cdots & s_{MM} \end{bmatrix} \tag{4.62a}$$

with

$$s_{ik} = \frac{1}{\sqrt{M}} \exp\{-j\frac{2\pi}{M}(i-1)(k-1)\} \tag{4.62b}$$

A special case of interest for symmetric bipolar dc lines[11] is M = 2. In this case [T] of Eq. (4.58) and [S] of Eq. (4.62a) are identical,

$$[T_{2-phase}] = \frac{1}{\sqrt{2}}\begin{bmatrix} 1 & 1 \\ 1 & -1 \end{bmatrix} \tag{4.63}$$

4.1.3.3 Two Identical Three-Phase Lines with Zero Sequence Coupling Only

Just as a transposed single-circuit three-phase line can usually be approximated as a balanced line, so two identical and parallel three-phase lines can often be approximated as "almost balanced" lines with an impedance matrix of the form

$$\begin{bmatrix} Z'_s & Z'_m & Z'_m & Z'_p & Z'_p & Z'_p \\ Z'_m & Z'_s & Z'_m & Z'_p & Z'_p & Z'_p \\ Z'_m & Z'_m & Z'_s & Z'_p & Z'_p & Z'_p \\ Z'_p & Z'_p & Z'_p & Z'_s & Z'_m & Z'_m \\ Z'_p & Z'_p & Z'_p & Z'_m & Z'_s & Z'_m \\ Z'_p & Z'_p & Z'_p & Z'_m & Z'_m & Z'_s \end{bmatrix} \tag{4.64}$$

The transposition scheme of Fig. 4.22 would produce such a matrix form, which implies that the two circuits are only coupled in zero sequence, but not in positive or negative sequence. Such a complicated transposition scheme is seldom, if ever, used, but the writer suspects that positive and negative sequence couplings in the more common double-circuit transposition scheme of Fig. 4.23 is often so weak that the model discussed here may be a useful approximation for the case of Fig. 4.23 as well.

---

[11] To be consistent, lines with M = 1 and M = 2 are called "single-phase" and "two-phase" lines, respectively, in this manual. This differs from the IEEE Standards [76, p. 647], in which circuits with one phase conductor and one neutral conductor (which could be replaced by ground return), as well as circuits with two phase conductors and one neutral conductor (or ground return) are both called single-phase circuits for historical reasons. For M ≥ 3, the definition in the IEEE Standards is the same as in this manual.

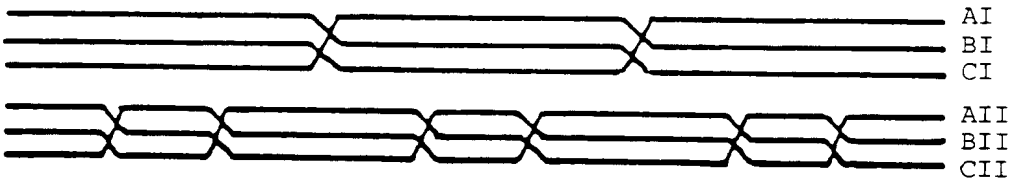

Fig. 4.22 - Double-circuit transposition scheme with zero sequence coupling only

The matrix of Eq. (4.64) is diagonalized by modifying the transformation matrix of Eq. (4.58) to

$$[T] = \frac{1}{\sqrt{6}} \begin{bmatrix} 1 & 1 & \sqrt{3} & 1 & 0 & 0 \\ 1 & 1 & -\sqrt{3} & 1 & 0 & 0 \\ 1 & 1 & 0 & -2 & 0 & 0 \\ 1 & -1 & 0 & 0 & \sqrt{3} & 1 \\ 1 & -1 & 0 & 0 & -\sqrt{3} & 1 \\ 1 & -1 & 0 & 0 & 0 & -2 \end{bmatrix} \tag{4.65}$$

with $[T]^{-1} = [T]^t$ again, which produces the diagonal matrix

$$\begin{bmatrix} Z'_G & & & & & \\ & Z'_{IL} & & & & \\ & & Z'_L & & & \\ & & & Z'_L & & \\ & & & & Z'_L & \\ & & & & & Z'_L \end{bmatrix} \tag{4.66}$$

If each circuit has three-phase sequence parameters Z'_{zero}, Z'_{pos}, and if the three-phase zero sequence coupling between the two circuits is $Z'_{zero\text{-}coupling}$, then the ground mode G, inter-line mode IL and line mode L values required by the EMTP are found from

$$\begin{aligned} Z'_G &= Z'_{zero} + Z'_{zero-coupling} \\ Z'_{IL} &= Z'_{zero} - Z'_{zero-coupling} \\ Z'_L &= Z'_{pos} \end{aligned} \tag{4.67}$$

with identical equations for the capacitances.

If the two three-phase circuits are not identical, then the transformation matrix of Eq. (4.65) can no longer be used; instead, [T] depends on the particular tower configuration.

4.1.4 Symmetrical Components

Symmetrical components are not used as such in the EMTP, except that the parameters of balanced lines after transformation to M-phase α, β, 0-components are the same as the parameters of symmetrical components, namely zero and positive sequence values. The supporting routine LINE CONSTANTS does have output options for more detailed symmetrical component information, however, which may warrant some explanations.

In addition to zero and positive sequence values, LINE CONSTANTS also prints full symmetrical component matrices. Its diagonal elements are the familiar zero and positive sequence values of the line; they are correct for the untransposed line as well as for a line which has been balanced through proper transpositions. The off-diagonal elements are only meaningful for the untransposed case, because they would become zero for the balanced line. For the untransposed case, these off-diagonal elements are used to define unbalance factors [47, p. 93]. The full symmetrical component matrices are no longer symmetric, unless the columns for positive and negative sequence are exchanged [27]. This exchange is made in the output of the supporting routine LINE CONSTANTS with rows listed in order "zero, pos, neg,..." and columns in order "zero, neg, pos,...". With this trick, matrices can be printed in triangular form (elements in and below the diagonal), as is done with the matrices for individual and equivalent phase conductors.

Symmetrical components for two-phase lines are calculated with the transformation matrix of Eq. (4.63), while those of three-phase lines are calculated with

$$[v_{phase}] = [S][v_{symm}] \qquad \textit{and} \quad [v_{symm}] = [S]^{-1}[v_{phase}] \tag{4.68a}$$

identical for currents,

$$\textit{where} \qquad [v_{symm}] = \begin{bmatrix} v_{zero} \\ v_{pos} \\ v_{neg} \end{bmatrix}$$

$$[S] = \frac{1}{\sqrt{3}} \begin{bmatrix} 1 & 1 & 1 \\ 1 & a^2 & a \\ 1 & a & a^2 \end{bmatrix}$$

$$[S]^{-1} = \frac{1}{\sqrt{3}} \begin{bmatrix} 1 & 1 & 1 \\ 1 & a & a^2 \\ 1 & a^2 & a \end{bmatrix} \tag{4.68b}$$

and $a = e^{j120^\circ}$.

The columns in these matrices are normalized[12]; in that form, [S] is unitary,

$$[S]^{-1} = [S^{\bigstar}]^t \tag{4.69}$$

[12]The electric utility industry usually uses unnormalized transformation, in which the factor for the [S]-matrix is 1 instead of $1 / \sqrt{3}$, and for the $[S]^{-1}$-matrix 1/3 instead of $1 / \sqrt{3}$. The symmetrical component impedances are identical in both cases, but the sequence currents and voltages differ by a factor of $\sqrt{3}$.

where "*" indicates conjugate complex and "t" transposition.

For M ≥ 3, the supporting routine LINE CONSTANTS assumes three-phase lines in parallel. Examples:

M = 6: Two three-phase lines in parallel

M = 9: Three-phase lines in parallel

M = 8: Two three-phase lines in parallel, with equivalent phase conductors no. 7 and 8 ignored in the transformation to symmetrical components.

The matrices are then transformed to three-phase symmetrical components and not to M-phase symmetrical components of Eq. (4.62). For example for M = 6 (double-circuit three-phase line),

$$[Z'_{symm}] = \begin{bmatrix} [S]^{-1} & 0 \\ 0 & [S]^{-1} \end{bmatrix} [Z'_{phase}] \begin{bmatrix} [S] & 0 \\ 0 & [S] \end{bmatrix} \tag{4.70}$$

with [S] defined by Eq. (4.68), Eq. (4.70) produces the three-phase symmetrical component values required in Eq. (4.67).

Balancing of double-circuit three-phase lines through transpositions never completely diagonalizes the respective symmetrical component matrices. The best that can be achieved is with the seldom-used transposition scheme of Fig. 4.22, which leads to

$$[Z'_{symm}] = \begin{bmatrix} Z'_{zero-I} & 0 & 0 & Z_{zero-coupling} & 0 & 0 \\ 0 & Z'_{pos-I} & 0 & 0 & 0 & 0 \\ 0 & 0 & Z'_{pos-I} & 0 & 0 & 0 \\ Z_{zero-coupling} & 0 & 0 & Z'_{zero-II} & 0 & 0 \\ 0 & 0 & 0 & 0 & Z'_{pos-II} & 0 \\ 0 & 0 & 0 & 0 & 0 & Z'_{pos-II} \end{bmatrix} \tag{4.71}$$

If both circuits are identical, then $Z'_{zero-I} = Z'_{zero-II} = Z'_{zero}$, and $Z'_{pos-I} = Z'_{pos-II} = Z'_{pos}$; in that case, the transformation matrix of Eq. (4.65) can be used for diagonalization. The more common transposition scheme of Fig. 4.23 produces positive and zero sequence coupling between the two

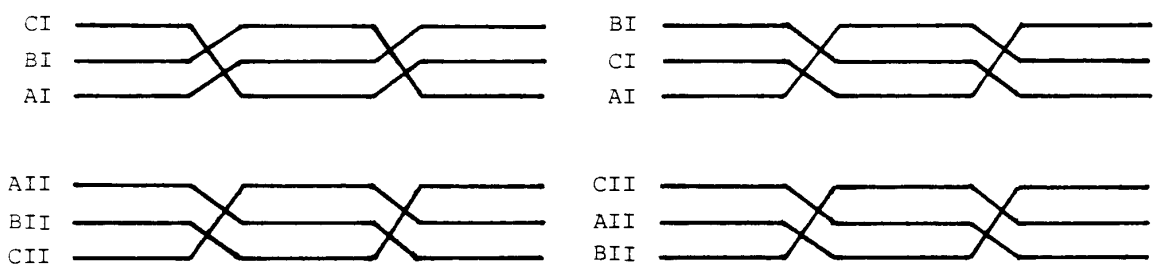

(a) barrels rolled in opposite direction

(b) barrels rolled in same direction

Fig. 4.23 - Double-circuit transposition scheme

circuits as well, with the nonzero pattern of the matrix in Eq. (4.71) changing to

$$\begin{bmatrix} X & 0 & 0 & X & 0 & 0 \\ 0 & X & 0 & 0 & X & 0 \\ 0 & 0 & X & 0 & 0 & X \\ \overline{X} & \overline{0} & \overline{0} & \overline{X} & \overline{0} & \overline{0} \\ 0 & X & 0 & 0 & X & 0 \\ 0 & 0 & X & 0 & 0 & X \end{bmatrix}$$

where "X" indicates nonzero terms. Re-assigning the phases in Fig. 4.23(b) to CI, BI, AI, AII, BII, CII from top to bottom would change the matrix further to cross-couplings between positive sequence of one circuit and negative sequence of the other circuit, and vice versa,

$$\begin{bmatrix} X & 0 & 0 & X & 0 & 0 \\ 0 & X & 0 & 0 & 0 & X \\ 0 & 0 & X & 0 & X & 0 \\ \overline{X} & \overline{0} & \overline{0} & \overline{X} & \overline{0} & \overline{0} \\ 0 & 0 & X & 0 & X & 0 \\ 0 & X & 0 & 0 & 0 & X \end{bmatrix}.$$

4.1.5 Modal Parameters

From the discussions of Section 4.1.3 it should have become obvious that the solution of M-phase transmission line equations becomes simpler if the M coupled equations can be transformed to M decoupled equations. These decoupled equations can then be solved as if they were single-phase equations. For balanced lines, this transformation is achieved with Eq. (4.58).

Many lines are untransposed, however, or each section of a transposition barrel may no longer be short compared with the wave length of the highest frequencies occurring in a particular study, in which case each section must be represented as an untransposed line. Fortunately, the matrices of untransposed lines can be diagonalized as well, with transformations to "modal" parameters derived from eigenvalue/eigenvector theory. The transformation matrices for untransposed lines are no longer known a priori, however, and must be calculated for each particular pair of parameter matrices $[Z'_{phase}]$ and $[Y'_{phase}]$.

To explain the theory, let us start again from the two systems of equations (4.31) and (4.32),

$$-\left[\frac{dV_{phase}}{dx}\right] = [Z'_{phase}]\,[I_{phase}] \tag{4.72a}$$

and

$$-\left[\frac{dI_{phase}}{dx}\right] = [Y'_{phase}][V_{phase}] \tag{4.72b}$$

with $[Y'_{phase}] = j\omega[C'_{phase}]$ if shunt conductances are ignored, as is customarily done. By differentiating the first equation with respect to x, and replacing the current derivative with the second equation, a second-order differential equation for voltages only is obtained,

$$\left[\frac{d^2V_{phase}}{dx^2}\right] = [Z'_{phase}]\,[Y'_{phase}]\,[V_{phase}] \tag{4.73a}$$

Similarly, a second-order differential equation for currents only can be obtained,

$$\left[\frac{d^2I_{phase}}{dx^2}\right] = [Y'_{phase}]\,[Z'_{phase}]\,[I_{phase}] \tag{4.73b}$$

where the matrix products are now in reverse order from that in Eq. (4.73a), and therefore different. Only for balanced matrices, and for the lossless high-frequency approximations discussed in Section 4.1.5.2, would the matrix products in Eq. (4.73a) and (4.73b) be identical.

With eigenvalue theory, it becomes possible to transform the two coupled equations (4.73) from phase quantities to "modal" quantities in such a way that the equations become decoupled, or in terms of matrix algebra, that the associated matrices become diagonal, e.g., for the voltages,

$$\left[\frac{d^2V_{mode}}{dx^2}\right] = [\Lambda]\,[V_{mode}] \tag{4.74}$$

with $[\Lambda]$ being a diagonal matrix. To get from Eq. (4.73a) to (4.74), the phase voltages must be transformed to mode voltages, with

$$[V_{phase}] = [T_v]\,[V_{mode}] \tag{4.75a}$$

and

$$[V_{mode}] = [T_v]^{-1}\,[V_{phase}] \tag{4.75b}$$

Then Eq. (4.73a) becomes

$$\left[\frac{d^2V_{mode}}{dx^2}\right] = [T_v]^{-1}\,[Z'_{phase}]\,[Y'_{phase}]\,[T_v]\,[V_{mode}] \tag{4.76a}$$

which, when compared with Eq. (4.74), shows us that

$$[\Lambda] = [T_v]^{-1} [Z'_{phase}] [Y'_{phase}] [T_v] \tag{4.76b}$$

To find the matrix $[T_v]$ which diagonalizes $[Z'_{phase}][Y'_{phase}]$ is the eigenvalue/eigenvector problem. The diagonal elements of $[\Lambda]$ are the eigenvalues of the matrix product $[Z'_{phase}][Y'_{phase}]$, and $[T_v]$ is the matrix of eigenvectors or modal matrix of that matrix product. There are many methods for finding eigenvalues and eigenvectors. The most reliable method for finding the eigenvalues seems to be the QR-transformation due to Francis [3], while the most efficient method for the eigenvector calculation seems to be the inverse iteration scheme due to Wilkinson [4, 5]. In the supporting routines LINE CONSTANTS and CABLE CONSTANTS, the "EISPACK"-subroutines [67] are used, in which the eigenvalues and eigenvectors of a complex upper Hessenberg matrix are found by the modified LR-method due to Rutishauser. This method is a predecessor of the QR-method, and where applicable, as in the case of positive definite matrices, is more efficient than the QR-method [68]. To transform the original complex matrix to upper Hessenberg form, stabilized elementary similarity transformations are used. For a given eigenvalue λ_k, the corresponding eigenvector $[t_{vk}]$ (= k-th column of $[T_v]$) is found by solving the system of linear equations

$$\{[Z'_{phase}] [Y'_{phase}] - \lambda_k [U]\} [t_{vk}] = 0 \tag{4.77}$$

with [U] = unit or identity matrix. Eq. (4.77) shows that the eigenvectors are not uniquely defined in the sense that they can be multiplied with any nonzero (complex) constant and still remain proper eigenvectors[13], in contrast to the eigenvalues which are always uniquely defined.

Floating-point overflow may occur in eigenvalue/eigenvector subroutines if the matrix is not properly scaled. Unless the subroutine does the scaling automatically, $[Z'_{phase}][Y'_{phase}]$ should be scaled before the subroutine call, by dividing each element by $-(\omega^2\varepsilon_0\mu_0)$, as suggested by Galloway, Shorrows and Wedepohl [39]. This division brings the matrix product close to unit matrix, because $[Z'_{phase}][Y'_{phase}]$ is a diagonal matrix with elements $-\omega^2\varepsilon_0\mu_0$ if resistances, internal reactances and Carson's correction terms are ignored in Eq. (4.7) and (4.8), as explained in Section 4.1.5.2. The eigenvalues from this scaled matrix must of course be multiplied with $-\omega^2\varepsilon_0\mu_0$ to obtain the eigenvalues of the original matrix. In [39] it is also suggested to subtract 1.0 from the diagonal elements after the division; the eigenvalues of this modified matrix would then be the p.u. deviations from the eigenvalues of the lossless high-frequency approximation of Section 4.1.5.2, and would be much more separated from each other than the unmodified eigenvalues which lie close together. Using subroutines based on [67] gave identical results with and without this subtraction of 1.0, however.

In general, a different transformation must be used for the currents,

$$[I_{phase}] = [T_i] [I_{mode}] \tag{4.78a}$$

---

[13]This is important if matrices $[T_v]$ obtained from different programs are compared. The ambiguity can be removed in a number of ways, e.g., by agreeing that the elements in the first row should always be 1.0, or by normalizing the columns to a Euclidean vector length of 1.0, that is, by requiring $t_{v1}t_{v1}^* + t_{v2}t_{v2}^* + \ldots = 1.0$, with t* = conjugate complex of t. In the latter case, there is still ambiguity in the sense that each column could be multiplied with a rotation constant $e^{j\alpha}$ and still have vector length = 1.0.

and

$$[I_{mode}] = [T_i]^{-1} [I_{phase}] \tag{4.78b}$$

because the matrix products in Eq. (4.73a) and (4.73b) have different eigenvectors, though their eigenvalues are identical. Therefore, Eq. (4.73b) is transformed to

$$\left[\frac{d^2 I_{mode}}{dx^2}\right] = [\Lambda] [I_{mode}] \tag{4.79}$$

with the same diagonal matrix as in Eq. (4.74). While $[T_i]$ is different from $[T_v]$, both are fortunately related to each other [58],

$$[T_i] = [T_v^t]^{-1} \tag{4.80}$$

where "t" indicates transposition. It is therefore sufficient to calculate only one of them.

Modal analysis is a powerful tool for studying power line carrier problems [59-61] and radio noise interference [62, 63]. Its use in the EMTP is discussed in Section 4.1.5.3. It is interesting to note that the modes in single-circuit three-phase lines are almost identical with the α, β, 0-components of Section 4.1.3.1 [58]. Whether the matrix products in Eq. (4.73) can always be diagonalized was first questioned by Pelissier in 1969 [64]. Brandao Faria and Borges da Silva have shown in 1985 [65] that cases can indeed be constructed where the matrix product cannot be diagonalized. It is unlikely that such situations will often occur in practice, because extremely small changes in the parameters (e.g., in the 8th significant digit) seem to be enough to make it diagonalizable again. Paul [66] has shown that diagonalization can be guaranteed under simplifying assumptions, e.g., by neglecting conductor resistances.

The physical meaning of modes can be deduced from the transformation matrices $[T_v]$ and $[T_i]$. Assume, for example, that column 2 of $[T_i]$ has entries of (-0.6, 1.0, -0.4). From Eq. (4.78a) we would then know that mode-2 current flows into phase B in one way, with 60% returning in phase A and 40% returning in phase C.

4.1.5.1 Line Equations in Modal Domain

With the decoupled equations of (4.74) and (4.79) in modal quantities, each mode can be analyzed as if it were a single-phase line. Comparing the modal equation

$$\frac{d^2 V_{mode-k}}{dx^2} = \lambda_k V_{mode-k}$$

with the well-known equation of a single-phase line,

$$\frac{d^2 V}{dx^2} = \gamma^2 V$$

with the propagation constant γ defined in Eq. (1.15), shows that the modal propagation constant γ_{mode-k} is the square

root of the eigenvalue,

$$\gamma_{mode-k} = \alpha_k + j\beta_k = \sqrt{\gamma_k} \tag{4.81}$$

with

α_k = attenuation constant of mode k (e.g., in Np/km),

β_k = phase constant of mode k (e.g., in rad/km).

The phase velocity of mode k is

$$phase\ velocity = \frac{\omega}{\beta_k} \tag{4.82a}$$

and the wavelength is

$$wave\ length = \frac{2\pi}{\beta_k} \tag{4.82b}$$

While the modal propagation constant is always uniquely defined, the modal series impedance and shunt admittance as well as the modal characteristic impedance are not, because of the ambiguity in the eigenvectors. Therefore, modal impedances and admittances only make sense if they are specified together with the eigenvectors used in their calculation. To find them, transform Eq. (4.72a) to modal quantities

$$-\left[\frac{dV_{mode}}{dx}\right] = [T_v]^{-1}\,[Z'_{phase}]\,[T_i]\,[I_{mode}] \tag{4.83}$$

The triple matrix product in Eq. (4.83) is diagonal, and the modal series impedances are the diagonal elements of this matrix

$$[Z'_{mode}] = [T_v]^{-1}\,[Z'_{phase}]\,[T_i] \tag{4.84a}$$

or with Eq. (4.80),

$$[Z'_{mode}] = [T_i^t]\,[Z'_{phase}]\,[T_i] \tag{4.84b}$$

Similarly, Eq. (4.72b) can be transformed to modal quantities, and the modal shunt admittances are then the diagonal elements of the matrix

$$[Y'_{mode}] = [T_i]^{-1}\,[Y'_{phase}]\,[T_v] \tag{4.85a}$$

or with Eq. (4.80),

$$[Y'_{mode}] = [T_v^t]\,[Y'_{phase}]\,[T_v] \tag{4.85b}$$

The proof that both $[Z'_{mode}]$ and $[Y'_{mode}]$ are diagonal is given by Wedepohl [58]. Finally, the modal characteristic impedance can be found from the scalar equation

$$Z_{char-mode-k} = \frac{\sqrt{Z'_{mode-k}}}{\sqrt{Y'_{mode-k}}} \tag{4.86a}$$

or from the simpler equation

$$Z_{char-mode-k} = \frac{\gamma_{mode-k}}{Y'_{mode-k}} \tag{4.86b}$$

A good way to obtain the modal parameters may be as follows: First, obtain the eigenvalues λ_k and the eigenvector matrix $[T_v]$ of the matrix product $[Z'_{phase}][Y'_{phase}]$. Then find $[Y'_{mode}]$ from Eq. (4.85b), and the modal series impedance from the scalar equation

$$Z'_{mode-k} = \frac{\lambda_k}{Y'_{mode-k}} \tag{4.86c}$$

The modal characteristic impedance can then be calculated from Eq. (4.86a), or from Eq. (4.86b) if the propagation constant from Eq. (4.81) is needed as well. If $[T_i]$ is needed, too, it can be found efficiently from Eq. (4.85a)

$$[T_i] = [Y'_{phase}]\,[T_v]\,[Y'_{mode}]^{-1} \tag{4.85c}$$

because the product of the first two matrices is available anyhow when $[Y'_{mode}]$ is found, and the post-multiplication with $[Y'_{mode}]^{-1}$ is simply a multiplication of each column with a constant (suggested by Luis Marti). Eq. (4.85c) also establishes the link to an alternative formula for $[T_i]$ mentioned in [57],

$$[T_i] = [Y'_{phase}]\,[T_v]\,[D]$$

with [D] being an arbitrary diagonal matrix. Setting $[D] = [Y'_{mode}]^{-1}$ leads us to the desirable condition $[T_i] = [T_v^t]^{-1}$ of Eq. (4.80). If the unit matrix were used for [D], all modal matrices in Eq. (4.84) and (4.85) would still be diagonal, but with the strange-looking result that all modal shunt admittances become 1.0 and that the modal series impedances become λ_k. Eq. (4.80) would, of course, no longer be fulfilled. For a lossless line, the modal series impedance would then become a negative resistance, and the modal shunt admittance would become a shunt conductance with a value of 1.0 S. As long as the case is solved in the frequency domain, the answers would still be correct, but it would obviously be wrong to associate such modal parameters with

$$-\frac{\partial v}{\partial x} = R'i \qquad and \qquad -\frac{\partial i}{\partial x} = G'v$$

(with R' negative and G' = 1.0) in the time domain.

4.1.5.2 Lossless High-Frequency Approximation

In lightning surge studies, many simplifying assumptions are made. For example, the waveshape and amplitude of the current source representing the lightning stroke is obviously not well known. Similarly, flashover criteria in the form of volt-time characteristics or integral formulas [8] are only approximate. In view of all these uncertainties, the use of highly sophisticated line models is not always justified. Experts in the field of lightning surge studies normally use a simple line model in which all wave speeds are equal to the speed of light, with a surge impedance matrix $[Z_{surge}]$ in phase quantities, where

$$Z_{ii-surge} = 60 \ln(2h_i/r_i) \tag{4.87a}$$

$$Z_{ik-surge} = 60 \ln(D_{ik}/d_{ik}) \tag{4.87b}$$

$$\textit{all wave speeds} = \textit{speed of light} \tag{4.87c}$$

with r_i being the radius of the conductor, or the radius of the equivalent conductor from Eq. (4.30) in case of a bundle conductor.[14]

Typically, each span between towers is represented separately as a line, and only a few spans are normally modelled (3 for shielded lines, or 18 for unshielded lines in [8]). For such short distances, losses in series resistances and differences in modal travel times are negligible. The effect of corona is sometimes included, however, by modifying the simple model of Eq. (4.87) [8].

It is possible to develop a special line model based on Eq. (4.87) for the EMTP, in which all calculations are done in phase quantities. But as shown here, the simple model of Eq. (4.87) can also be solved with modal parameters as a special case of the untransposed line. The simple model follows from Eq. (4.72) by making two assumptions for a "lossless high-frequency approximation":

1. Conductor resistances and ground return resistances are ignored.
2. The frequencies contained in the lightning surges are so high that all currents flow on the surface of the conductors, and on the surface of the earth.

Then the elements of $[Z'_{phase}]$ become

$$Z'_{ii} = j\omega\frac{\mu_0}{2\pi}\ln(2h_i/r_i) \ , \quad Z'_{ik} = j\omega\frac{\mu_0}{2\pi}\ln(D_{ik}/d_{ik}) \tag{4.88}$$

while $[Y']$ is obtained by inverting the potential coefficient matrix,

$$[Y'] = j\omega[P']^{-1} \tag{4.89}$$

with the elements of $[P']$ being the same as in Eq. (4.88) if the factor $j\omega\mu_0/(2\pi)$ is replaced by $1/(2\pi\varepsilon_0)$. Then both matrix

[14]Ground wires are usually retained as phase conductors in such studies. If they are eliminated, the method of Section 4.1.2.1 must be used on $[Z_{surge}]$.

products in Eq. (4.73) become diagonal matrices with all elements being

$$\lambda_k = -\omega^2\varepsilon_0\mu_0, \quad k=1,\ldots M \tag{4.90}$$

These values are automatically obtained from the supporting routines LINE CONSTANTS and CABLE CONSTANTS as the eigenvalues of the matrix products in Eq. (4.73), by simply using the above two assumptions in the input data (all conductor resistances = 0, GMR/r = 1.0, no Carson correction terms). The calculation of the eigenvector matrix $[T_v]$ or $[T_i]$ needed for the untransposed line model of Section 4.2 breaks down, however, because the matrix products in Eq. (4.73) are already diagonal. To obtain $[T_v]$, let us first assume equal, but nonzero conductor resistances R'. Then the eigenvectors $[t_{vk}]$ are defined by

$$(-\omega^2\varepsilon_0\mu_0[U] + j\omega R'[P']^{-1})\,[t_{vk}] = \lambda_k[t_{vk}] \tag{4.91}$$

with the expression in parentheses being the matrix product $[Z'_{phase}][Y'_{phase}]$, and [U] = unit matrix. Eq. (4.91) can be rewritten as

$$[P']^{-1}\,[t_{vk}] = \lambda_{k-modified}\,[t_{vk}] \tag{4.92}$$

with modified eigenvalues

$$j\omega R'\lambda_{k-modified} = \lambda_k + \omega^2\varepsilon_0\mu_0 \tag{4.93}$$

Eq. (4.92) is valid for any value of R', including zero. It therefore follows that $[T_v]$ is obtained as the eigenvectors of $[P']^{-1}$, or alternatively as the eigenvectors of [P'] since the eigenvectors of a matrix are equal to the eigenvectors of its inverse. The eigenvalues of $[P]^{-1}$ are not needed because they are already known from Eq. (4.90), but they could also be obtained from Eq. (4.93) by setting R' = 0.

For this simple mode, $[T_v]$ is a real, orthogonal matrix,

$$[T_v]\,[T_v]^t = [U] \tag{4.94}$$

and therefore,

$$[T_i] = [T_v] \tag{4.95}$$

D.E. Hedman has solved this case of the lossless high-frequency approximation more than 15 years ago [45]. He recommended that the eigenvectors be calculated from the surge impedance matrix of Eq. (4.87), which is the same as calculating them from [P'] since both matrices differ only by a constant factor.

One can either modify the line constants supporting routines to find the eigenvectors from [P'] for the lossless high-frequency approximation, as was done in UBC's version, or use the same trick employed in Eq. (4.91) in an unmodified program: Set all conductor resistances equal to some nonzero value R', set GMR/r = 1, and ask for zero Carson correction terms. If the eigenvectors are found from [P'], then it is advisable to scale this matrix first by multiplying all elements with $2\pi\varepsilon_0$.

The lossless high-frequency approximation produces eigenvectors which differ from those of the lossy case

at very high frequencies [61]. This is unimportant for lightning surge studies, but important for power line carrier problems.

Example: For a distribution line with one ground wire (Fig. 4.24) the lossless high-frequency approximation produces the following modal surge impedances and transformation matrix,

mode	$Z_{surge\text{-}mode}$ (Ω)
1	993.44
2	209.67
3	360.70
4	310.62

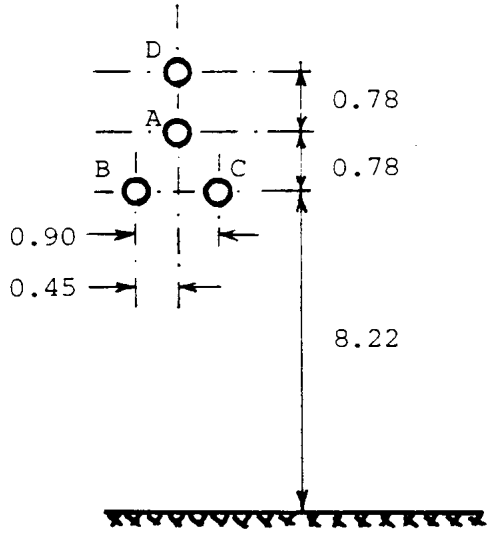

Fig. 4.24 - Position of phase conductors A, B, C and ground wire D (average height, all dimensions in m). Conductor diameter = 10.1092 mm

0.52996 0.82860 −0.18(
0.49080 −0.21322 0.462
0.49080 −0.21322 0.462
0.48721 −0.47170 −0.73

Converted to phase quantities, the surge impedance matrix becomes $[T_v][Z_{surge\text{-}mode}][T_v]^t$, or

$$[Z_{surge\text{-}phase}] = \begin{bmatrix} 490.33 & & & \\ 176.95 & 484.89 & \textit{symmetric} & \\ 176.95 & 174.27 & 484.89 & \\ 190.74 & 144.26 & 144.26 & 495.31 \end{bmatrix} \ \Omega$$

The elements from Eq. (4.87) are slightly larger, by a factor of 300,000/299,792, because the supporting routine LINE CONSTANTS uses 299,792 km/s for the speed of light, versus 300,000 km/s implied in Eq. (4.87).

Representation in EMTP then would be by means of a 4-phase, constant-parameter, lossless line. The following branch cards are for the first of 4 such cascaded sections:

```
-11A   2A        993.44 .3E-6     2   4
-11B   2B        993.44 .3E-6     2   4
-11C   2C        993.44 .3E-6     2   4
-11D   2D        993.44 .3E-6     2   4
```

The modelling of long lines as coupled shunt resistances [R] = [$Z_{surge-phase}$] has already been discussed in Section 3.1.3. In the example above, such a shunt resistance matrix could be used to represent the rest of the line after the 4 spans from the substation. Simply using the 4 x 4 matrix would be unrealistic with respect to the ground wire, however, because it would imply that the ground wire is ungrounded on the rest of the line. More realistic, though not totally accurate, would be a 3 x 3 matrix obtained from [Z'_{phase}] and [Y'_{phase}] in which the ground wire has been eliminated. This model implies zero potential everywhere on the ground wire, in contrast to the four spans where the potential will more or less oscillate around zero because of reflections up and down the towers.

Comparison with More Accurate Models: For EMTP users who are reluctant to use the simple model described in this section, a few comments are in order. First, let us compare exact values with the approximate values. If we use constant parameters and choose 400 kHz as a reasonable frequency for lightning surge studies, then we obtain the results of table 4.5 for the test example above, assuming T/D = 0.333 for skin effect correction and internal inductance calculation with the tubular conductor formula, R'_{dc} = 0.53609 Ω/km, and ρ = 100 Ωm.

Table 4.5 - Exact line parameters at 400 kHz

mode	$Z_{surge-mode}$ (Ω)	wave velocity (m/s)	R' (Ω/km)
1	1027.6-j33.9	285.35	597.4
2	292.0-j0.5	299.32	7.9
3	361.9-j0.5	299.37	8.2
4	311.1-j0.5	299.32	8.0

The differences are less than 0.5% in surge impedance and wave speed for the aerial modes 2 to 4, and not more than 5% for the ground return mode 1. These are small differences, considering all the other approximations which are made in lightning surge studies. If series resistances are included by lumping them in 3 places, totally erroneous results may be obtained if the user forgets to check whether $R/4 \leq Z_{surge}$ in the ground return mode. For the very short line length of 90 m in this example, this condition would still be fulfilled here.

Using constant parameters at a particular frequency is of course an approximation as well, and some users may therefore prefer frequency-dependent models. For very short line lengths, such as 90 m in the example, most frequency-dependent models are probably unreliable, however. It may therefore be more sensible to use the simple model

described here, for which answers are reliable, rather than sophisticated models with possibly unreliable answers.

A somewhat better lossless line model for lightning surge studies than the preceding one has been suggested by V. Larsen [92]. To obtain this better model, the line parameters are first calculated in the usual way, at a certain frequency which is typical for lightning surges (e.g., at 400 kHz). The resistances are then set to zero when the matrix product $[Z'_{phase}][Y'_{phase}]$ is formed, before the modal parameters are computed. With this approach, $[T_i]$ will always be real. Table 4.6 shows the modal parameters of this better lossless model. They differ very little from those in Table 4.5.

Table 4.6 - Approximate modal parameters at 400 kHz with R=0

mode	$Z_{surge\text{-}mode}$ (Ω)	wave velocity (m/s)
1	1026.3	285.50
2	292.0	299.32
3	362.0	299.37
4	311.1	299.32

In particular, the wave velocity of the ground return mode 1 is now much closer to the exact value of Table 4.5. The transformation matrix which goes with the modal parameters of Table 4.6 is

$$[T_i] = \begin{bmatrix} 0.40795 & 0.84115 & -0.22316 & 0 \\ 0.55628 & -0.18448 & 0.44910 & -0.70711 \\ 0.55628 & -0.18448 & 0.44910 & 0.70711 \\ 0.46335 & -0.47371 & -0.73947 & 0 \end{bmatrix}$$

In this case $[T_v]$ is no longer to $[T_i]$; Eq. (4.80) must be used instead.

4.1.5.3 Approximate Transformation Matrices for Transient Solutions

The transformation matrices $[T_v]$ and $[T_i]$ are theoretically complex, and frequency-dependent as well. With a frequency-dependent transformation matrix, modes are only defined at the frequency at which the transformation matrix was calculated. Then the concept of converting a polyphase line into decoupled single-phase lines (in the modal domain) cannot be used over the entire frequency range. Since the solution methods for transients are much simpler if the modal composition is the same for all frequencies, or in other words, if the transformation matrices are constant with real coefficients, it is worthwhile to check whether such approximate transformation matrices can be used without producing too much error. Fortunately, this is indeed possible for overhead lines [66, 78].

Guidelines for choosing approximate (real and constant) transformation matrices have not yet been worked out at the time when these notes are being written. The frequency-dependent line model of J. Marti discussed in Section 4.2.2.6 needs such a real and constant transformation matrix, and wrong answers would be obtained if a complex transformation matrix were used instead. Since a real and constant transformation matrix is always an approximation,

its use will always produce errors, even if they are small and acceptable. The errors may be small in one particular frequency region, and larger in other regions, depending on how the approximation is chosen.

One choice for an approximate transformation matrix would be the one used in the lossless approximations discussed in Section 4.1.5.2. This may be the best choice for lightning surge studies.

For switching surge studies and similar types of studies, the preferred approach at this time seems to be to calculate $[T_v]$ at a particular frequency (e.g., at 1 kHz), and then to ignore the imaginary part of it. In this approach, $[T_v]$ should be predominantly real before the imaginary part is discarded. One cannot rely on this when the subroutine returns the eigenvectors, since an eigenvector multiplied with e^{j50° or any other constant would still be a proper eigenvector. Therefore, the columns of $[T_v]$ should be normalized in such a way that its components lie close to the real axis. One such normalization procedure was discussed by V. Brandwajn [79]. The writer prefers a different approach, which works as follows:

1. Ignore shunt conductances, as is customarily done. Then $[Y'_{phase}]$ is purely imaginary. Use Eq. (4.85) to find the diagonal elements of the modal shunt admittance matrix $Y'_{mode\text{-}k\text{-}preliminary}$.
2. In general, these "preliminary" modal shunt admittances will not be purely imaginary, but $j\omega C'_{mode\text{-}k}e^{-j\alpha k}$ instead. Then normalize $[T_v]$ by multiplying each column with $e^{j\alpha k/2}$. With this normalized transformation matrix, the modal shunt admittances will become $j\omega C'_{mode\text{-}k}$, or purely imaginary as in the phase domain.
3. To obtain the approximate (real and constant) transformation matrix, discard the imaginary part of the normalized matrix from step 2.
4. Use the approximate matrix $[T_{v\text{-}approx.}]$ from step 3 to find modal series impedances and modal shunt admittances from Eq. (4.84) and (4.85) over the frequency range of interest. If $[T_i]$ is needed, use

$$[T_{i-approx.}] = [T^t_{v-approx.}]^{-1} \tag{4.96}$$

5. If the line model requires nonzero shunt conductances, add them as modal parameters. Usually, only conductances from phase to ground are used (with phase-to-phase values being zero); in that case, the modal conductances are the same as the phase-to-ground conductances if the latter are equal for all phases.

An interesting method for finding approximate (real and constant) transformation matrices has been suggested by Paul [66]. By ignoring conductor resistances, and by assuming that the Carson correction terms $\Delta R'_{ii} + j\Delta X'_{ii}$ in Eq. (4.7) and $\Delta R'_{ik} + j\Delta X'_{ik}$ in Eq. (4.8) are all equal (all elements in the matrix of correction terms have one and the same value), the approximate transformation matrix $[T_{i\text{-}approx.}]$ is obtained as the eigenvectors of the matrix product

$$[C'_{phase}]\begin{bmatrix} 111\ldots1 \\ \ldots\ldots \\ 111\ldots1 \end{bmatrix}$$

with all elements of the second matrix being 1. To find $[T_{v\text{-}approx.}]$, Eq. (4.96) would have to be used. Wasley and

Selvavinayagamoorthy [93] find the approximate transformation matrices by simply taking the magnitudes of the complex elements, with an appropriate sign reflecting the values of their arguments. They compared results using these approximate matrices with the exact results (using complex, frequency-dependent matrices), and report that fairly high accuracy can be obtained if the approximate matrix is computed at a low frequency, even for the case of double-circuit lines.

If the M-phase line is assumed to be balanced (Section 4.1.3.2), then the transformation matrix is always real and constant, and known a priori with Eq. (4.58) and Eq. (4.59). Two identical and balanced three-phase lines with zero sequence coupling only have the real and constant transformation matrix of Eq. (4.65).

4.2 Line Models in the EMTP

The preceding Section 4.1 concentrated on the line parameters per unit length. These are now used to develop line models for liens of a specific length.

For steady-state solutions, lines can be modelled with reasonable accuracy as nominal π-circuits, or rigorously as equivalent π-circuits. For transient solutions, the methods become more complicated, as one proceeds from the simple case of a single-phase lossless line with constant parameters to the more realistic case of a lossy polyphase line with frequency-dependent parameters.

4.2.1 AC Steady-State Solutions

Lines can be represented rigorously in the steady-state solution with exact equivalent π-circuits. Less accurate representations are sometimes used, however, to match the model to the one used in the transient simulation (e.g., lumping R in three places, rather than distributing it evenly along the line, or using approximate real transformation matrices instead of exact complex matrices). For lines of moderate "electrical" length (typically $\leq$ 100 km at 60 Hz), nominal π-circuits are often accurate enough, and are probably the best models to use for steady-state solutions at power frequency. If the steady-state solution is followed by a transient simulation, or if steady-state solutions are requested over a wide frequency range, then the nominal π-circuit must either be replaced by a cascade connection of shorter nominal π-circuits, or by an exact equivalent π-circuit derived from the distributed parameters.

4.2.1.1 Nominal M-Phase π-Circuit

For the nominal M-phase π-circuit of Fig. 3.10, the series impedance matrix and the two equal shunt susceptance matrices are obtained from the per unit length matrices by simply multiplying them with the line length, as shown in Eq. (4.35) and (4.36). The equations for the coupled lumped elements of this M-phase π-circuit have already been discussed at length in Section 3, and shall not be repeated here.

Nominal π-circuits are fairly accurate if the line is electrically short. This is practically always the case if complicated transposition schemes are studied at power frequency (60 Hz or 50 Hz). Fig. 4.25 shows a typical example, with three circuits on the same right-of-way. In this case, each of the five transposition sections (1-2, 2-3, 3-4, 4-5, 5-6) would be represented as a nominal 9-phase π-circuit. While a nominal π-circuit would already be reasonably accurate

for the total line length of 95 km, nominal π-circuits are certainly accurate for each transposition section, since the longest section is only 35 km long. A comparison between measurements on the de-energized line L3 and computer results is shown in table 4.7 [80]. The coupling in this case is predominantly capacitive.

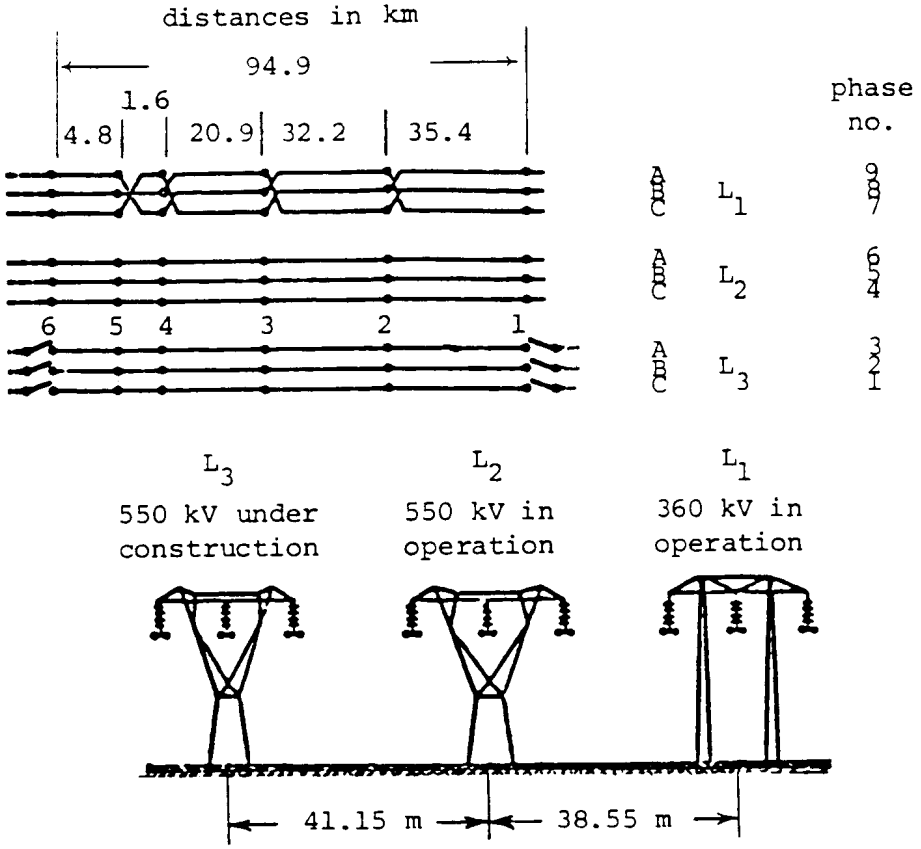

Fig. 4.25 - Transposition scheme for three adjacent circuits

Table 4.7 - Comparison between measurements and EMTP results (voltages on energized line L1 = 372 kV and on L2 = 535 kV)

	phase	measurement	EMTP results
Induced voltages on de-energized line L3 if open at both ends	A	30 kV	27.5 kV
	B	15 kV	13.8 kV
	C	10 kV	7.8 kV
Grounding currents if de-energized line L3 is grounded at right end	A	11 A	10.5 A
	B	5 A	3.2 A
	C	1 A	1.5 A

Because nominal π-circuits are so useful for studying complicated transposition schemes, a "CASCADED PI" option was added to the BPA EMTP. With this option, the entire cascade connection is converted to one single π-circuit, which is an exact equivalent for the cascade connection. This is done by adding one "component" at a time, as shown in Fig. 4.26. The "component" may either be an M-phase π-circuit, or other types of network elements such as

shunt reactors or series capacitors. Whenever component k is added, the nodal admittance matrix

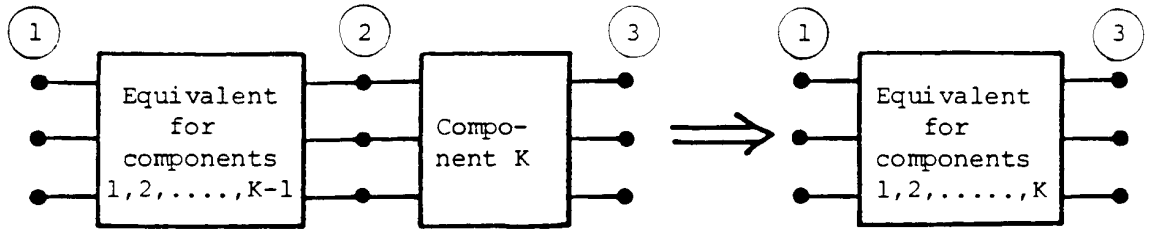

Fig. 4.26 - Schematic illustration of cascading operation for K-th component

for nodes 1, 2, 3 is reduced by eliminating the inner nodes 2, to form the new admittance matrix of the equivalent for the cascaded components 1, 2, ... K. This option keeps the computational effort in the steady-state solution as low as possible by not having to use nodal equations for the inner nodes of the cascade connection, at the expense of extra computational effort for the cascading procedure.

4.2.1.2 Equivalent π-Circuit for Single-Phase Lines

Lines defined with distributed parameters at input time are always converted to equivalent π-circuits for the steady-state solution.

For lines with frequency-dependent parameters, the exact equivalent π-circuit discussed in Section 1 is used, with Eq. (1.14) and (1.15). The same exact equivalent π-circuit is used for distortionless and lossless line models with constant parameters.

In many applications, line models with constant parameters are accurate enough. For example, positive sequence resistances and inductances are fairly constant up to approximately 1 kHz, as shown in Fig. 4.20. But even with constant parameters, the solution for transients becomes very complicated (except for the unrealistic assumption of distortionless propagation). Fortunately, experience showed that reasonable accuracy can be obtained if L' and C' are distributed and if

$$R = R'\ell \tag{4.97}$$

is lumped in a few places as long as $R << Z_{surge}$. In the EMTP, R/2 is lumped in the middle and R/4 at both ends of an otherwise lossless line, as shown in Fig. 4.27, and as further discussed in Section 4.2.2.5. For this transient representation, the EMTP uses the same assumption[15] in the

[15]The EMTP should probably be changed to by-pass this option if only steady-state solutions are requested, either at one frequency or over a range of frequencies.

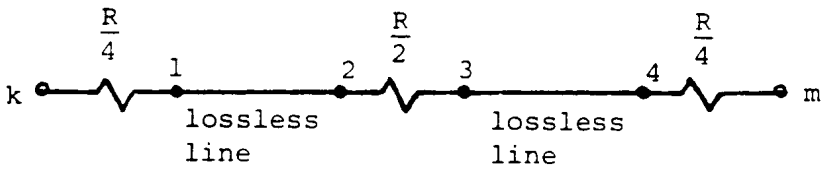

Fig. 4.27 - Line representation with lumped resistances

steady-state solution, to avoid any discrepancies between ac steady-state initialization and subsequent transient simulation, even though experiments have shown that the differences are extremely small at power frequency. By using equivalent π-circuits for each lossless, half-length section in Fig. 4.27, and by eliminating the "inner" nodes 1, 2, 3, 4, an equivalent π-circuit (Fig. 1.2) was obtained by R.M. Hasibar with

$$Z_{series} = R\cos^2\omega\tau - \left(0.5 + 0.03125\frac{R^2}{Z^2}\right) R \sin^2\omega\tau + j \sin\omega\tau\cos\omega\tau \cdot (0.375\frac{R^2}{Z} + 2Z)$$

$$\frac{1}{2}Y_{shunt} = \frac{(-2 - 0.125\frac{R^2}{Z^2})\sin^2\omega\tau + j\frac{R}{Z}\sin\omega\tau\cos\omega\tau}{Z_{series}} \qquad (4.98)$$

where

$$\tau = length\ \sqrt{L'C'}$$

$$Z = \sqrt{\frac{L'}{C'}}$$

$$R = length \cdot R' \qquad (4.99)$$

4.2.1.3 Equivalent M-Phase π-Circuit

To obtain an equivalent M-phase π-circuit, the phase quantities are first transformed to modal quantities with Eq. (4.84) and (4.85) for untransposed lines, or with Eq. (4.58) and (4.59) for balanced lines. For identical balanced three-phase lines with zero sequence coupling only, Eq. (4.65) is used. For each mode, an equivalent single-phase π-circuit is then found in the same way as for single-phase lines; that is, either as an exact equivalent π-circuit with Eq. (1.14) and (1.15), or with Eq. (4.98) and (4.99) for the case of lumping R in three places. These single-phase modal π-circuits each has a series admittance $Y_{series\text{-}mode}$ and two equal shunt admittances 1/2 $Y_{shunt\text{-}mode}$. By assembling these admittances as diagonal matrices, the admittance matrices of the M-phase π-circuit in phase quantities are obtained from

$$[Y_{series}] = [T_i]\,[Y_{series-mode}]\,[T_i]^t \qquad (4.100)$$

and

$$\frac{1}{2}[Y_{shunt}] = \frac{1}{2}[T_i]\,[Y_{shunt-mode}]\,[T_i]^t \qquad (4.101)$$

While it is always possible to obtain the exact equivalent M-phase π-circuit at any frequency in this way, approximations are sometimes used to match the representation for the steady-state solution to the one used in the transient solution. One such approximation is the lumping of resistances as shown in Fig. 4.27. Another approximation is the use of real and constant transformation matrices in Eq. (4.100) and (4.101), as discussed in Section 4.1.5.3.

4.2.2 Transient Solutions

Historically, the first line models in the EMTP were cascade connections of π-circuits, partly to prove that computers could match switching surge study results obtained on transient network analyzers (TNA's) at that time. On TNA's, balanced three-phase lines are usually represented with decoupled 4-conductor π-circuits, as shown in Fig. 4.28. This representation can easily be derived from Eq. (4.44) by rewriting it as

$$-\frac{dV_A}{dx} = (Z'_s - Z'_m)I_A + Z'_m(I_A + I_B + I_C) \qquad (4.102)$$

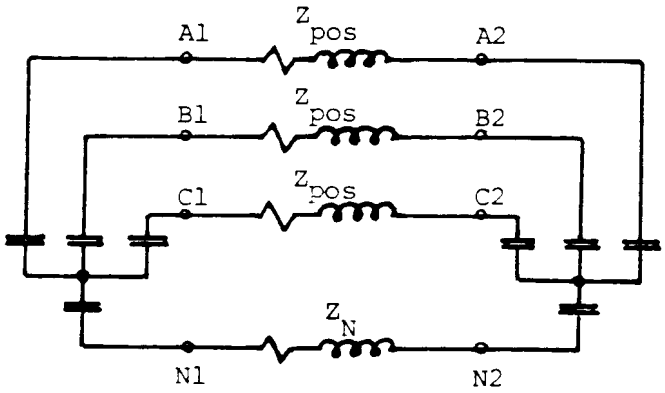

Fig. 4.28 - Four-conductor π-circuit used on TNA's

for phase A, and similar for phases B and C. The first term in Eq. (4.102) is $Z'_{pos}I_A$ (or branch A1-A2 in Fig. 4.28), while the second term is the common voltage drop caused by the earth and ground wire return current $I_A + I_B + I_C$ (branch N1-N2 in Fig. 4.28). Note, however, that Fig. 4.28 is only valid if the sum of the currents flowing out through a line returns through the earth and ground wires of that same line. For that reason, the neutral nodes N2, N3, ... must be kept floating, and only N1 at the sending end is grounded. Voltages with respect to ground at location i are obtained by measuring between the phase and node N_i. In meshed networks with different R/X-ratios, this assumption is probably not true. For this reason, and to be able to handle balanced as well as untransposed lines with any number of phases, M-phase π-circuits were modelled directly with M x M matrices, as discussed in Section 4.1.2.4. Voltages to ground are then simply the node voltages. Comparisons between these M-phase π-circuits, and with the four-conductor π-circuits of Fig. 4.28 confirmed that the results are identical.

The need for travelling wave solutions first arose in connection with rather simple lightning arrester studies, where lossless single-phase line models seemed to be adequate. Section 1 briefly discusses the solution method used in the EMTP for such lines. This method was already known in the 1920's and 1930's and strongly advocated by Bergeron [81]; it is therefore often called Bergeron's method. In the mathematical literature, it is known as the method of characteristics, supposedly first described by Riemann.

It soon became apparent that travelling wave solutions were much faster and better suited for computers than cascaded π-circuits. To make the travelling wave solutions useful for switching surge studies, two changes were needed from the simple single-phase lossless line: First, losses had to be included, which could be done with reasonable accuracy by simply lumping R in three places. Secondly, the method had to be extended to M-phase lines, which was achieved by transforming phase quantities to modal quantities. Originally, this was limited to balanced lines with built-in transformation matrices, then extended to double-circuit lines, and finally generalized to untransposed lines. Fig. 4.29 compared EMTP results with results obtained on TNA's, using the built-in transformation matrix for balanced three-phase lines and simply lumping R in three places.

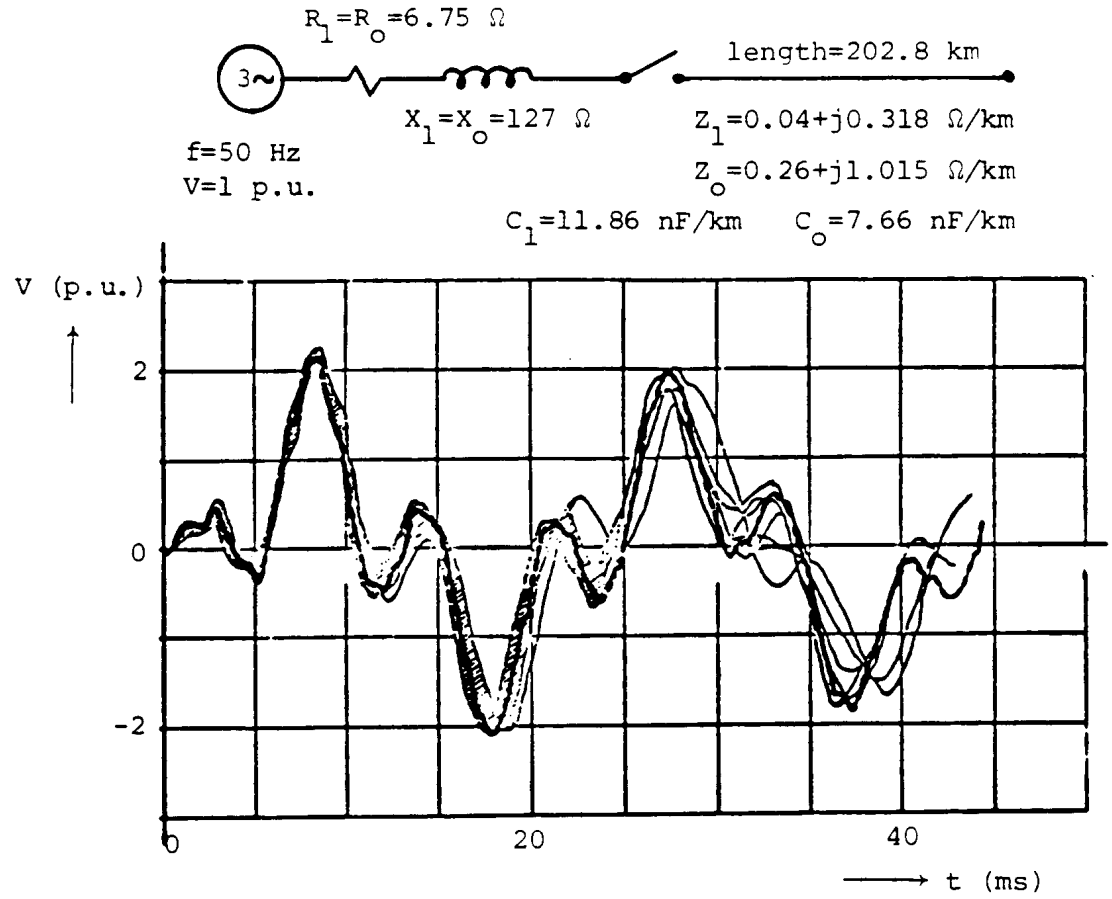

Fig. 4.29 - Energization of a three phase line. Computer simulation results (dotted line) superimposed on 8 transient

network analyzer results for receiving end voltage in phase B. Breaker contacts close at 3.05 ms in phase A, 8,05 ms in phase B, and 5.55 ms in phase C (t=0 when source voltage of phase A goes through zero from negative to positive) [82]. Reprinted by permission of CIGRE

While travelling wave solutions with constant distributed L', C' and constant lumped R produced reasonable accurate answers in many cases, as shown in Fig. 4.29, there were also cases where the frequency dependence, especially of the zero sequence impedance, could not be ignored. Choosing constant line parameters at the dominant resonance frequency sometimes improved the results. Eventually, frequency-dependent line models were developed by Budner [83], by Meyer and Dommel [84] based on work of Snelson [85], by Semlyen [86], and by Ametani [87]. A careful re-evaluation of frequency-dependence by J. Marti [88] led to a fairly reliable solution method, which seems to become the preferred option as these notes are being written. J. Marti's method will therefore be discussed in more detail.

4.2.2.1 Nominal π-Circuits

Nominal π-circuits are generally not the best choice for transient solutions, because travelling wave solutions are faster and usually more accurate. Cascade connections of nominal π-circuits may be useful for untransposed lines, however, because one does not have to make the approximations for the transformation matrix discussed in Section 4.1.5.3. On the other hand, one cannot represent frequency-dependent line parameters and one has to accept the spurious oscillations caused by the lumpiness. Fig. 4.30 shows these oscillations for the simple case of a single-phase line being represented with 8 and 32 cascaded nominal π-circuits. The exact solution with distributed parameters is shown for comparison purposes as well. The proper choice of the number of π-circuits for one line is discussed in [89], as well as techniques for damping the spurious oscillations with damping resistances in parallel with the series R-L branches of the π-circuit of Fig. 4.28.

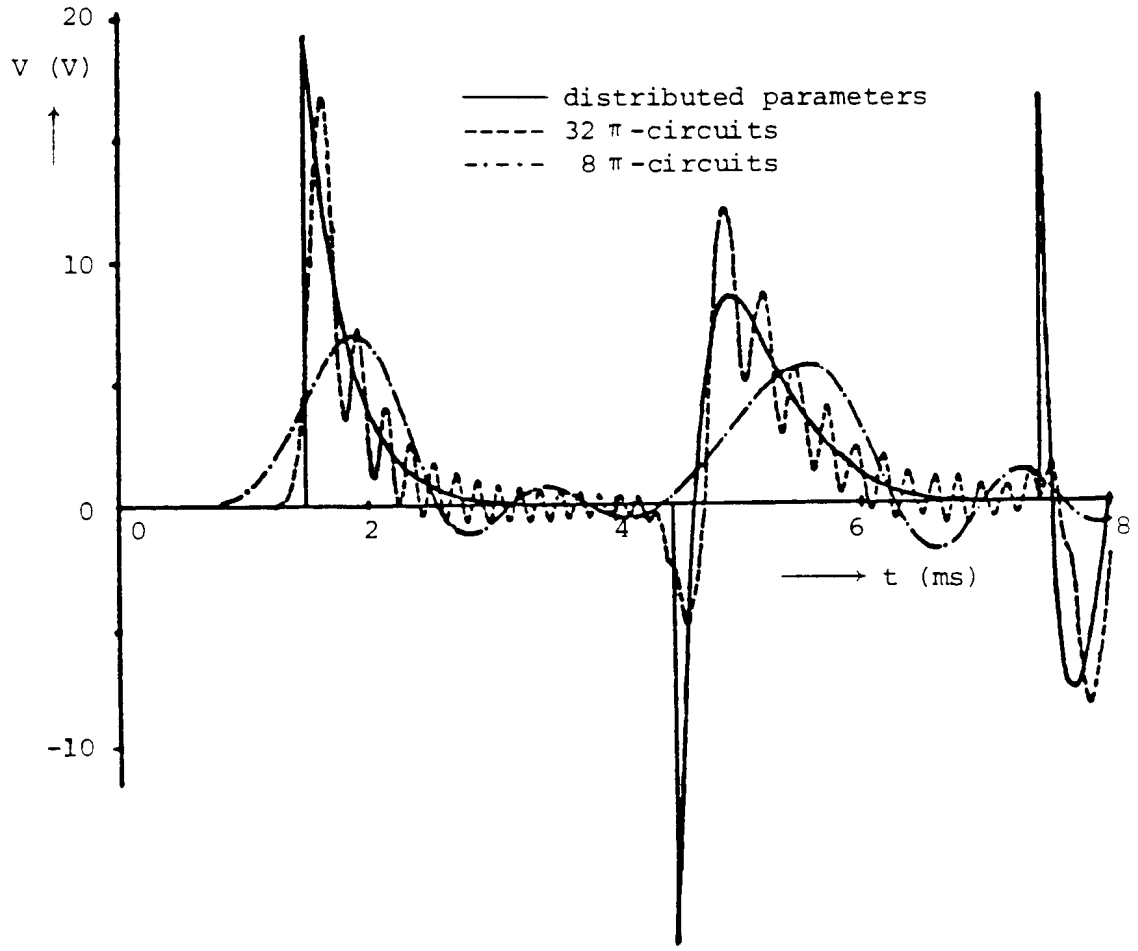

Fig. 4.30 - Voltage at receiving end of a single phase line if a dc voltage of 10 V is connected to the sending end at t=0 (line data: R=0.0376 Ω/mile, L=1.52 mH/mile, C=14.3 nF/mile, length-320 miles; receiving end terminated with shunt inductance of 100 mH)

The solution methods for nominal π-circuits have already been discussed in Section 3.4. With M-phase nominal π-circuits, untransposed lines (or sections of a line) are as simple to represent as balanced lines. In the former case, one simply uses the matrices of the untransposed line, whereas in the latter case one would use matrices with averaged equal diagonal and averaged equal off-diagonal elements.

4.2.2.2 Single-Phase Lossless Line with Constant L' and C'

The solution method for the single-phase case has already been explained in Section 1. The storage scheme for the history terms is the same as the one discussed in the next Section 4.2.2.3 for M-phase lossless lines, except that each single-phase line occupies only one section in the table, rather than M section for M modes. Similarly, the initialization of the history terms for cases starting from linear ac steady-state initial conditions is the same as in Eq. (4.108).

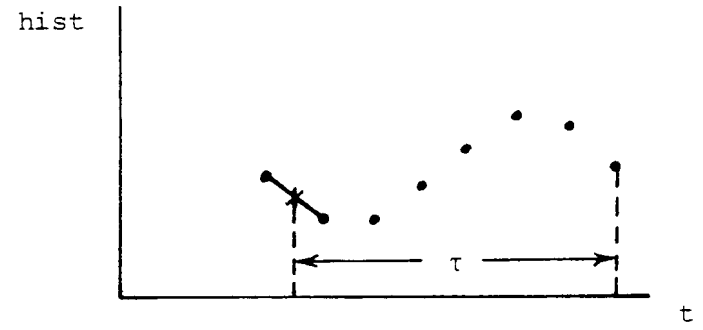

Fig. 4.31 - Linear interpolation

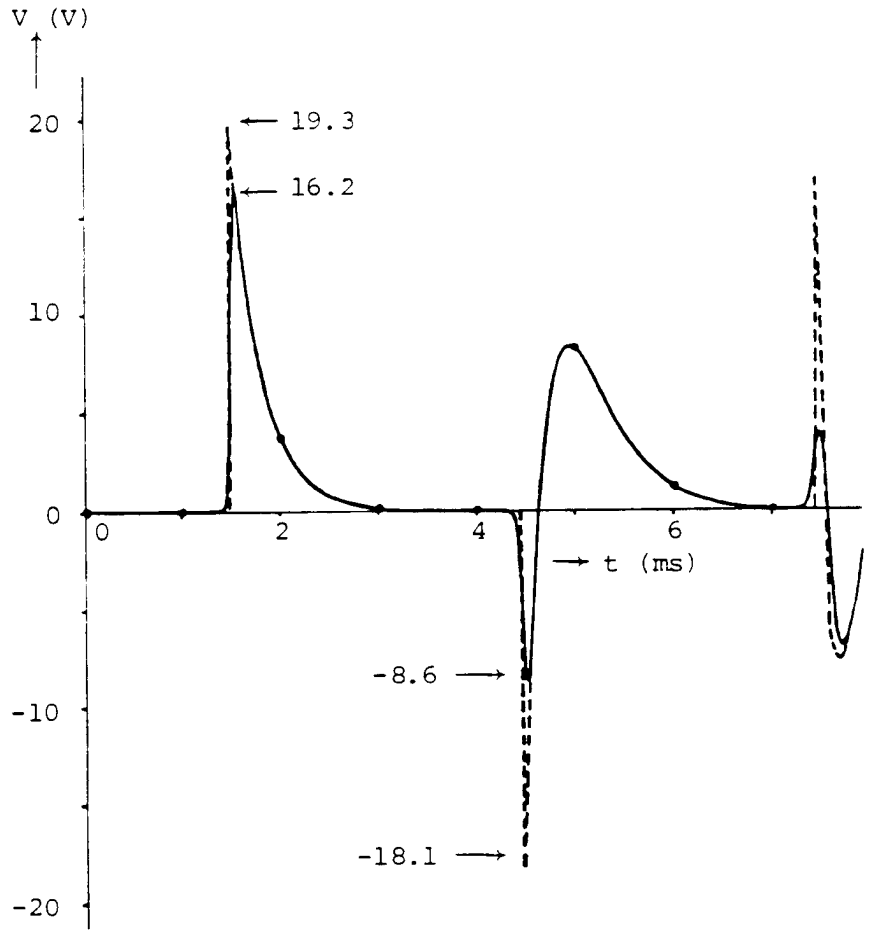

Fig. 4.32 - Effect of linear interpolation on sharp peaks. Dotted line: Δt = 9.324…μs to make τ integer multiple of Δt. Solid line: Δt = 10 μs (τ not integer multiple of Δt)

The solution is exact as long as the travel time τ is an integer multiple of the step size Δt. If this is not the case, then linear interpolation is used in the EMTP, as indicated in Fig. 4.31. Linear interpolation is believed to be a reasonable approximation for most cases, since the curves are usually smooth rather than discontinuous. If discontinuities or very sharp peaks do exist, then rounding τ to the nearest integer multiple of Δt may be more sensible than interpolation, however. There is no option for this rounding procedure in the EMTP, but the user can easily accomplish this through changes in the input data. Fig. 4.32 compares results for the case of Fig. 4.30 with sharp peaks with and without linear interpolation. The line was actually not lossless in this case, but the losses were represented in a simple way by subdividing the line into 64 lossless sections and lumping resistances in between and at both ends. The interpolation errors are more severe if lines are split up into many sections, as was done here. If the line were only split up into two lossless sections, with R lumped in between and at both ends, then the errors in the peaks would be less (the first peak would be 18.8, and the second peak would be -15.4).

The accumulation of interpolation errors on a line broken up into many sections, with τ of each section not being an integer multiple of Δt, can easily be explained. Assume that a triangular pulse is switched onto a long, lossless line, which is long enough so that no reflections come back from the remote end during the time span of the study (Fig. 4.33). Let us look at how this pulse becomes distorted through interpolation as it travels down the line if

(a) the line is broken up into short sections of travel time 1.5 Δt each, and

(b) the line from the sending end to the measuring point is represented as one section ($\tau = k \cdot 1.5\ \Delta t$, with k = 1, 2, 3,...).

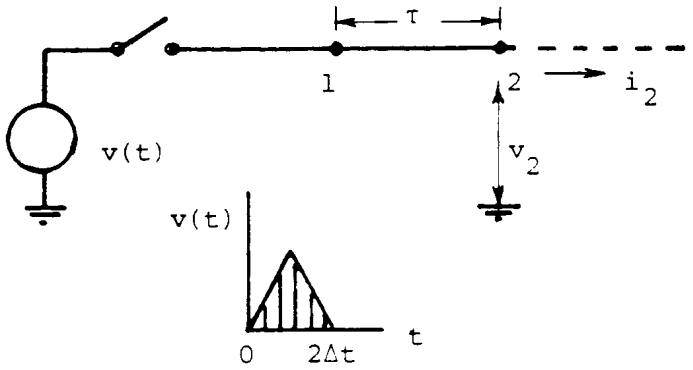

Fig. 4.33 - Single-phase lossless line energized with triangular pulse

At any point on the line, the current will be

$$i = \frac{1}{Z} v$$

and between points 1 and 2 separated by τ (Fig. 4.33),

$$v2(t + \tau) = v1(t)$$

This last equation was used in Fig. 4.34, together with linear interpolation, to find the shape of the pulse as it travels

down the line. The pulse loses its amplitude and becomes wider and wider if it is broken up into sections of travel time 1.5 Δt each. On the other hand, the pulse shape never becomes as badly distorted if the line is represented as one single section.

What are the practical consequences of this interpolation error? Table 4.8 compares peak overvoltages from a BPA switching surge study on a 1200 kV three-phase line[16], 133 miles long. Each section was split up into two lossless half-sections, with R lumped in the middle and

Table 4.8 - Interpolation errors in switching surge study with $\Delta t = 50$ µs

Run	Line model	Peak overvoltages (MV)		
		phase A	phase B	phase C
1	single section	1.311	1.191	1.496
2	7 sections	1.276	1.136	1.457
3	single section with τ rounded	1.342	1.167	1.489

at both ends, as explained in Section 4.2.2.4. Run no. 1 shows the results of the normal line representation as one section. Run no. 2 with subdivision into 7 sections produces differences of 2.6 to 4.7%. In run no. 3 the zero and positive sequence travel times $\tau_0 = 664.93$ µs and $\tau_1 = 445.74$ µs were rounded to 650 and 450 µs, respectively, to make them integer multiples of $\Delta t = 50$ µs. These changes could be interpreted as a decrease in both L'_0 and C'_0 of 2.25%, and as an increase in both L'_1 and C'_1 of 0.96%, with the surge impedances remaining unchanged. Since line parameters are probably no more accurate than ±5% at best anyhow, these implied changes are quite acceptable. With rounding, a slightly modified case is then solved without interpolation errors. Whether an option for rounding τ to the nearest integer multiple of Δt should be added to the EMTP is debatable. In general, rounding may imply much larger changes in L', C' than in this case, and if implemented, warning messages with the magnitude of these implied changes should be added as well. In Table 4.8, runs no. 3 to 1 differ by no more than 2.3%, and the interpolation error is therefore acceptable if the line is represented as one section. Breaking the line up into very many sections may produce unacceptable interpolation errors, however.

If the user is interested in a "voltage profile" along the line, then a better alternative to subdivisions into sections would be a post-processor "profile program" which would calculate

[16]The problem of interpolation errors is basically the same for single-phase and M-phase lines; therefore, a three-phase case is presented here for which data was already available. Choosing a step size Δt which makes the travel time τ an integer multiple of Δt is more difficult for three-phase lines, however, because there are two travel times for the positive and zero sequence mode on balanced lines (or three travel times for the 3 modes on untransposed lines).

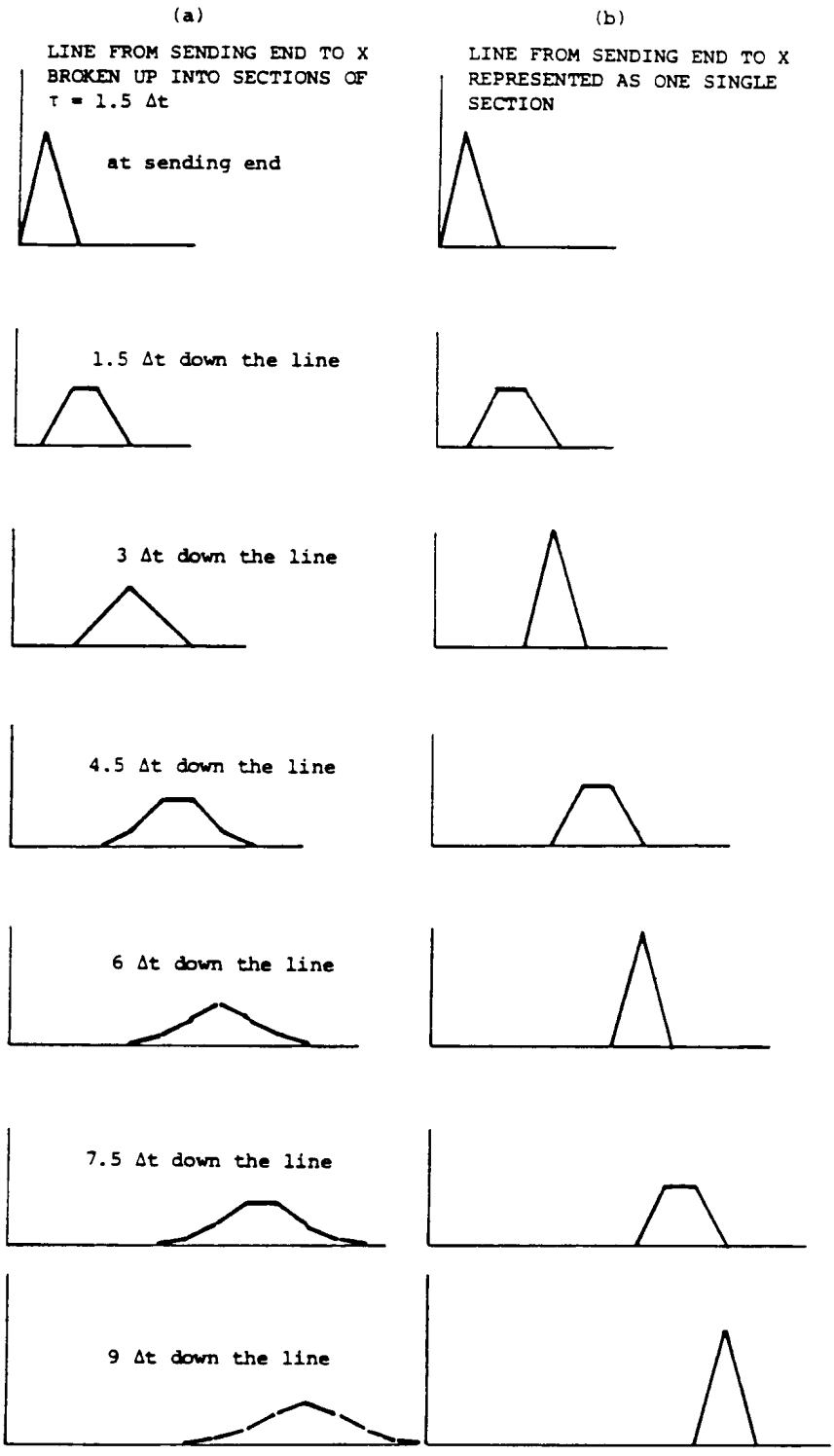

Fig. 4.34 - Pulse at incremental distances down the line

voltages and currents at intermediate points along the line from the results at both ends of the line. Such a program is easy to write for lossless and distortionless lines. Luis Marti developed such a profile algorithm for the more complicated frequency-dependent line models, which he merged into the time step loop of the EMTP [90]. This was used to produce moves of travelling waves by displaying the voltage profile at numerous points along the line at time intervals of Δt.

Fig. 4.34(a) suggests a digital filtering effect from the interpolation which is similar to that of the trapezoidal rule described in Section 2.2.1. To explain this effect, Eq. (1.6) must first be transformed from the time domain

$$\frac{1}{Z} v_k(t) - i_{km}(t) = \frac{1}{Z} v_m(t-\tau) + i_{mk}(t-\tau)$$

into the frequency domain,

$$I = \frac{1}{Z} V_k - I_{km} = \left(\frac{1}{Z} V_m + I_{mk} \right) \cdot e^{-j\omega\tau} \tag{4.103}$$

For simplicity, let us assume that voltage and current phasors V_m and I_{mk} at node m are known, and that we want to find $I = V_k/Z - I_{km}$ at node k. Without interpolation errors, Eq. (4.103) provides the answer. If interpolation is used, and if for the sake of simplicity we assume that the interpolated value lies in the middle of an interval Δt, then Eq. (4.103) becomes

$$I_{interpolated} = \left(\frac{1}{Z} V_m + I_{mk} \right) \cdot \frac{1}{2} \cdot \left(e^{-j\omega(\tau + \frac{\Delta t}{2})} + e^{-j\omega(\tau - \frac{\Delta t}{2})} \right) \tag{4.104}$$

Therefore, the ratio of the interpolated to the exact value becomes

$$\frac{I_{interpolated}}{I_{exact}} = \cos\left(\omega \frac{\Delta t}{2} \right) \tag{4.105}$$

which is indeed somewhat similar to Fig. 2.10 for the error produced by the trapezoidal rule.

Single-phase lossless line models can obviously only approximate the complicated phenomena on real lines. Nonetheless, they are useful in a number of applications, for example

(a) in simple studies where one wants to gain insight into the basic phenomena,

(b) in lightning surge studies, and

(c) as a basis for more sophisticated models discussed later.

For lightning surge studies, single-phase lossless line models have been used for a long time. They are probably accurate enough in many cases because of the following reasons:

(1) Only the phase being struck by lightning must be analyzed, because the voltages induced in the other phases will be much lower.

(2) Assumptions about the lightning stroke are by necessity very crude, and very refined line models are therefore not warranted.

(3) The risk of insulation failure in substations is highest for backflashovers at a distance of approx. 2 km or less. Insulation co-ordination studies are therefore usually made for nearby strokes. In that case, the modal waves of an M-phase line "stay together," because differences in wave velocity and distortion among the M waves are still small over such short distances. They can then easily be combined into one resultant wave on the struck phase. There seems to be some uncertainty, however, about the value of the surge impedance which should be used in such simplified single-phase representations. It appears that the "self surge impedance" $Z_{ii\text{-}surge}$ of Eq. (4.87a) should be used. For nearby strokes it is also permissible to ignore the series resistance. Attenuation caused by corona may be more important than that caused by conductor losses. At the time of writing these notes, corona is still difficult to model, and it may therefore be best to ignore losses altogether to be on the safe side.

4.2.2.3 M-Phase Lossless Line with Constant L' and C'

Additional explanations are needed for extending the method of Section 1 from single-phase lines to M-phase lines. In principle, the equations are first written down in the modal domain, where the coupled M-phase line appears as if it consisted of M single-phase lines. Since the solution for single-phase lines is already known, this is straightforward. For solving the line equations together with the rest of the network, which is always defined in phase quantities, these modal equations must then be transformed to phase quantities, as schematically indicated in Fig. 4.35.

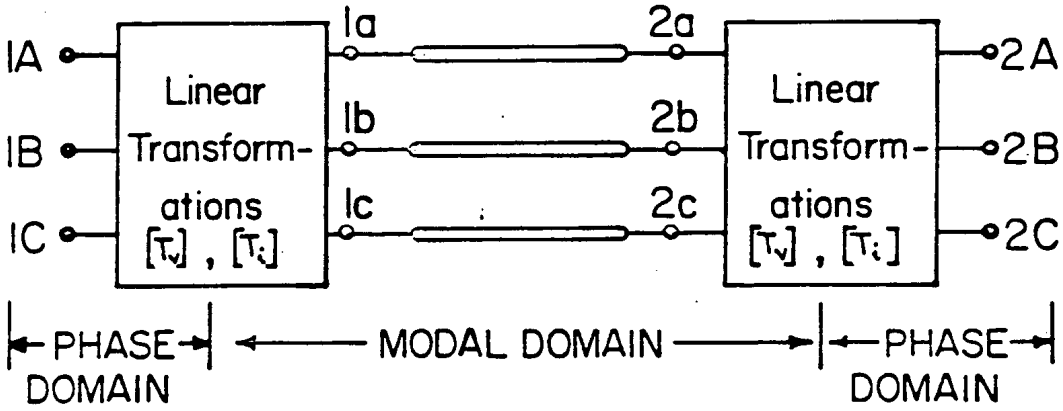

Fig. 4.35 - Transformation between phase and modal domain on a three-phase line

For simplicity, let us assume that the line has 3 phases. Then, with the notations from Fig. 4.35, each mode is described by an equation of the form of Eq. (1.6), or

$$i_{1a\text{-}2a}(t) = \frac{1}{Z_a} v_{1a}(t) + hist_{1a\text{-}2a}(t-\tau_a)$$

$$i_{1b\text{-}2b}(t) = \frac{1}{Z_b} v_{1b}(t) + hist_{1b\text{-}2b}(t-\tau_b) \qquad (4.106)$$

$$i_{1c-2c}(t) = \frac{1}{Z_c} v_{1c}(t) + hist_{1c-2c}(t-\tau_c)$$

where each history term hist was computed and stored earlier. For mode a, this history term would be

$$hist_{1a-2a}(t-\tau_a) = -\frac{1}{Z_a} v_{2a}(t-\tau_a) - i_{2a-1a}(t-\tau_a) \qquad (4.107)$$

and analogous for modes b and c. These history terms are calculated for both ends of the line as soon as the solution has been obtained at instant t, and entered into a table for use at a later time step. As indicated in Fig. 4.36, the history terms of a three-phase line would occupy 3 sections of the history tables for modes a, b, c, and the length of each section would be $\tau_{increased}/\Delta t$, with $\tau_{increased}$ being the travel time of the particular mode increased to the nearest integer multiple of Δt[17]. Since the modal travel times τ_a, τ_b, τ_c differ from each other, the 3 sections in this table are generally of different length. This is also the reason for storing history terms as modal values, because one has to go back different travel times for each mode in picking up history terms. For the solution at time t, the history terms of Eq. (4.106) are obtained by using linear interpolation on the top two entries of each mode section.

[17]A single-phase line would simply occupy one section, whereas a six-phase line would occupy six sections in this table.

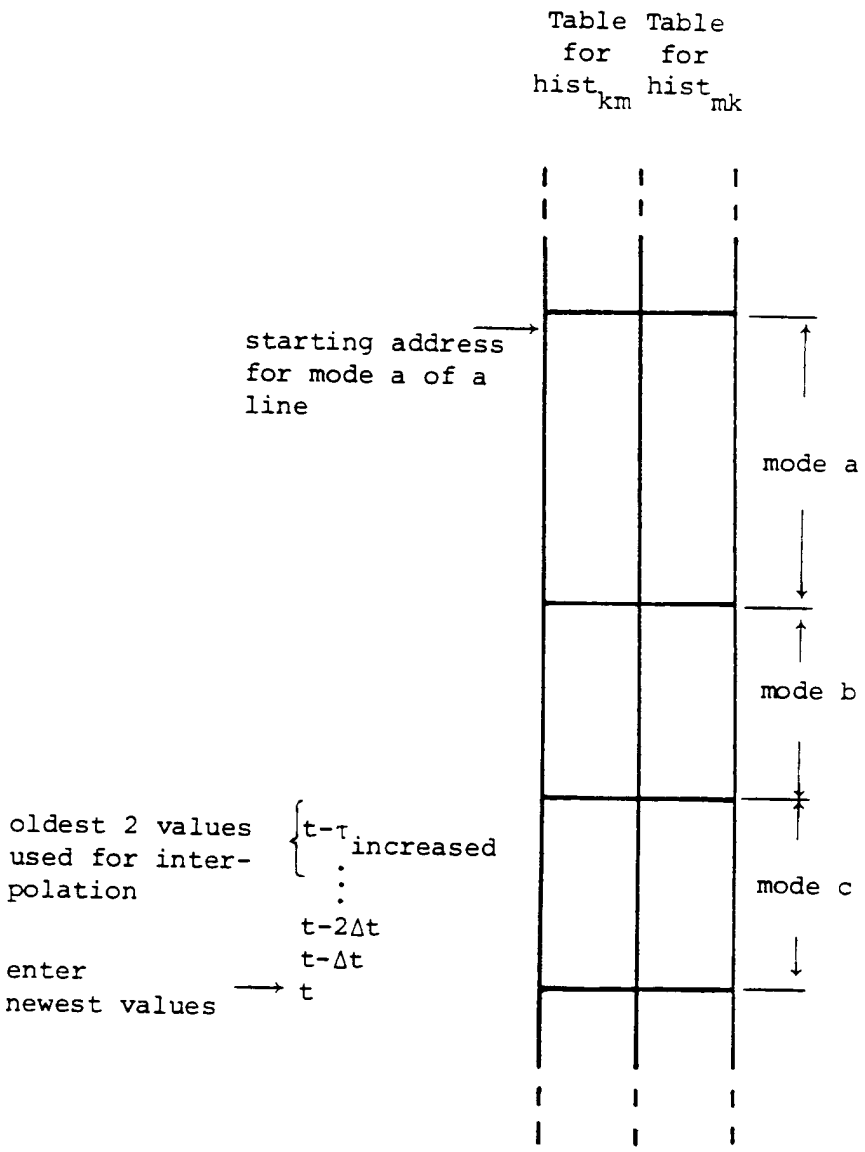

Fig. 4.36 - Table for history terms of transmission lines

After the solution in each time step, the entries in the tables of Fig. 4.36 must be shifted upwards by one location, thereby throwing away the values at the oldest point at $t-\tau_{increased}$. This is then followed by entering the newly calculated history terms hist(t) at the newest point t. Instead of physically shifting values, the EMTP moves the pointer for the starting address of each section down by 1 location. When this pointer reaches the end of the table, it then goes back again to the beginning of the table ("wrap-around table") [91].

The initial values for the history terms must be known for t = 0, $-\Delta t$, $-2\Delta t$, ... $-\tau_{increased}$. The necessity for knowing them beyond t = 0 comes from the fact that only terminal conditions are recorded. If the conditions were also given along the line at travel time increments of Δt, then the initial values at t = 0 would suffice. For zero initial conditions, the history table is simply preset to zero. For linear ac steady-state conditions (at one frequency ω), the history terms are first computed as phasors (peak, not rms),

$$HIST_{km} = -\frac{1}{Z} V_m - I_{mk} \tag{4.108a}$$

where V_m and I_{mk} are the voltage and current phasors at line end m (analogous for $HIST_{mk}$). With HIST = $|HIST| \cdot e^{j\alpha}$, the instantaneous history terms are then

$$hist_{km}(t) = |HIST_{km}| \cdot \cos(\omega t + \alpha) \ , \quad with \ t = 0, \ -\Delta t, \ -2\Delta t, \ \ldots \tag{4.108b}$$

Eq. (4.108) is used for single-phase lines as well as for M-phase lines, except that mode rather than phase quantities must be used in the latter case.

Eq. (4.106) are interfaced with the rest of the network by transforming them from modal to phase quantities with Eq. (4.78a),

$$\left[i_{1-2}^{phase}\right] = \left[Y_{surge}\right]\left[v_1^{phase}\right] + \left[hist_{1-2}^{phase}\right] \tag{4.109a}$$

with the surge admittance matrix in phase quantities,

$$\left[Y_{surge}\right] = \left[T_i\right]\begin{bmatrix} Z_a^{-1} & 0 & 0 \\ 0 & Z_b^{-1} & 0 \\ 0 & 0 & Z_c^{-1} \end{bmatrix}\left[T_i\right]^t \tag{4.109b}$$

and the history terms in phase quantities,

$$\left[hist_{1-2}^{phase}\right] = \left[T_i\right]\begin{bmatrix} hist_{1a-2a} \\ hist_{1b-2b} \\ hist_{1c-2c} \end{bmatrix} \tag{4.109c}$$

For a lossless line with constant L' and C', the transformation matrix $[T_i]$ will always be real, as explained in the last paragraph of Section 4.1.5.2. It is found as the eigenvector matrix of the product [C'][L'] for each particular tower configuration, where [L'] and [C'] are the per unit length series inductance and shunt capacitance matrices of the line. For balanced lines, $[T_i]$ is known a priori from Eq. (4.58), and for identical balanced three-phase lines with zero sequence coupling only it is known a priori from Eq. (4.65).

The inclusion of Eq. (4.109) into the system of nodal equations (1.8a) for the entire network is quite straightforward. Assume that for the example of Fig. 4.35, rows and columns for nodes 1A, 1B, 1C follow each other, as do those for nodes 2A, 2B, 2C (Fig. 4.37). Then the 3 x 3 matrix $[Y_{surge}]$ enters into two 3 x 3 blocks on the diagonal, as indicated in Fig. 4.37, while the history terms $[hist_{1-2}{}^{phase}] = [hist_{1A-2A}, hist_{1B-2B}, hist_{1C-2C}]$ of Eq. (4.109c) enter into rows 1A, 1B, 1C, on the right-hand side with negative signs. Analogous history terms for terminal 2 enter into rows 2A, 2B,

2C on the right-hand side. While [Y_{surge}] is entered into [G] only once outside the time-step loop, the history terms must be added to the right-hand side in each time step.

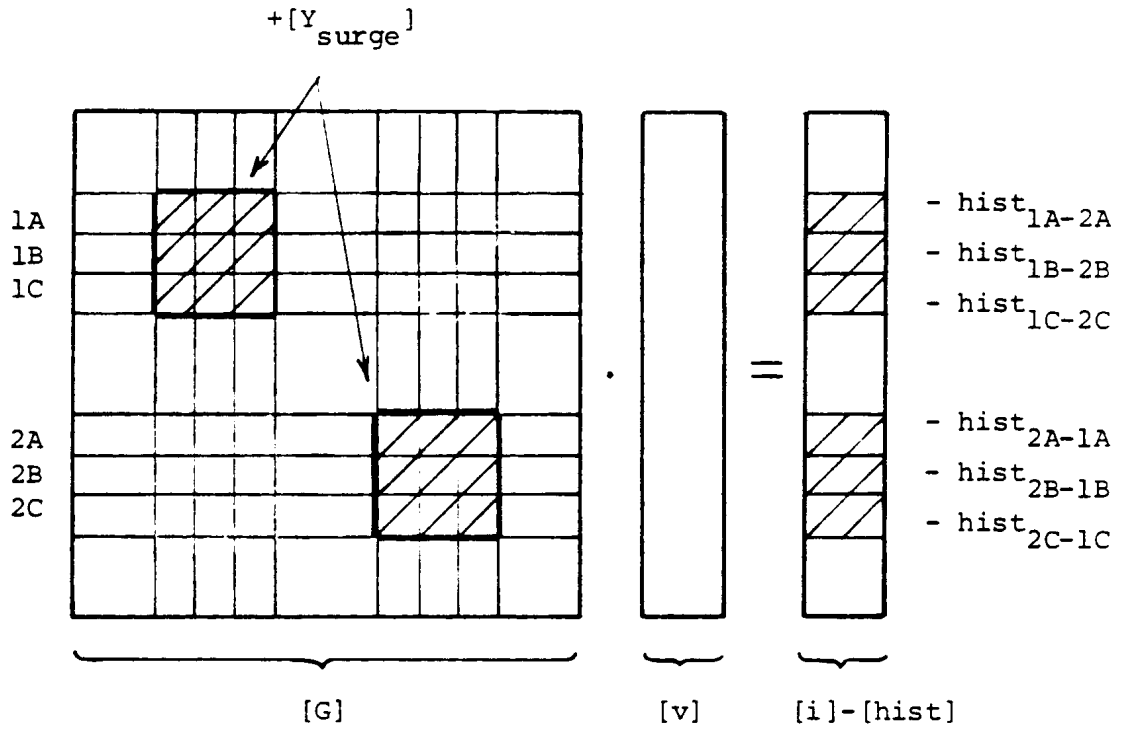

Fig. 4.37 - Entries for a three-phase line into system of equations

M-phase lossless line models are useful, among other things, for

(a) simple studies where one wants to investigate basic phenomena,

(b) in lightning surge studies, where single-phase models are no longer adequate, and

(c) as a basis for more sophisticated models discussed later.

Lightning surge studies cannot always be done with single-phase models. For simulating backflashovers on lines with ground wires, for example, the ground wire and at least the struck phase must be modelled ("2-phase line"). Since it is not always known which phase will be struck by the backflashover, it is probably best to model all three phases in such a situation ("4-phase line"). An example for such a study is discussed in Section 4.1.5.2, with 4-phase lossless line models representing the distribution line, and single-phase lossless line models representing the towers. Not included in the data listing are switches (or some other elements) for the simulation of potential flashovers from the tower top (nodes D) to phases A, B, C.

4.2.2.4 Single and M-Phase Distortionless Lines with Constant Parameters

Distortionless line models are seldom used, because wave propagation on power transmission lines is far from distortionless. They have been implemented in the EMTP, nonetheless, simply because it takes only a minor modification to change the lossless line equation into the distortionless line equation.

A single-phase transmission line, or a mode of an M-phase line, is distortionless if

$$\frac{R'}{L'} = \frac{G'}{C'} \tag{4.110}$$

Losses are incurred in the series resistance R' as well as in the shunt conductance G'. The real shunt conductance of an overhead line is very small (close to zero), however. If its value must be artificially increased to make the line distortionless, with a resulting increase in shunt losses, then it is best to compensate for that by reducing the series resistance losses. The EMTP does this automatically by regarding the input value R'_{INPUT} as an indicator for the total losses, and uses only half of it for R',

$$\frac{R'}{L'} = \frac{G'}{C'} = \frac{1}{2}\frac{R'_{INPUT}}{L'} \tag{4.111}$$

With this formula, the ac steady-state results are practically identical for the line being modelled as distortionless or with R lumped in 3 places; the transient response differs mainly in the initial rate of rise. From Eq. (4.111), the attenuation constant α becomes

$$\alpha = \frac{R'_{INPUT}}{2}\sqrt{\frac{C'}{L'}} \tag{4.112}$$

The factor 1/2 can also be justified by using an approximate expression for the attenuation constant for lines with low attenuation and low distortion [48, p. 257],

$$\alpha = \frac{R'_{INPUT}}{2}\sqrt{\frac{C'}{L'}} + \frac{G'_{INPUT}}{2}\sqrt{\frac{L'}{C'}} \tag{4.113}$$

which is reasonably accurate if $R' << \omega L'$ and $G' << \omega C'$. This condition is fulfilled on overhead lines, except at very low frequencies. Eq. (4.112) is then obtained by dropping the term with G'_{INPUT} and by ignoring the fact that the waves are not only attenuated but distorted as well.

If a user wants to represent a truly distortionless line where G' is indeed nonzero, then the factor 1/2 should of course not be used. The factor 1/2 is built into the EMTP, however, and the user must therefore specify R'_{INPUT} twice as large as the true series resistance in this case.

With α known, an attenuation factor $e^{-\alpha\ell}$ is calculated (ℓ = length of line). The lossless line of Eq. (1.6) is then changed into a distortionless line by simply multiplying the history term of Eq. (1.6b) with this attenuation factor,

$$hist_{km}(t-\tau) = \left[-\frac{1}{Z}v_m(t-\tau) - i_{mk}(t-\tau)\right]\cdot e^{-\alpha\ell} \tag{4.114}$$

The surge impedance remains the same, namely $\sqrt{L'/C'}$.

For M-phase lines, any of the M modes can be specified as distortionless. Mixing is allowed (e.g., mode 1 could be modelled with lumped resistances, and modes 2 and 3 as distortionless).

Better results are usually obtained with the lumped resistance model described next, even though lumping of resistances in a few places is obviously an approximation, whereas the distortionless line is solved exactly if the travel time is an integer multiple of Δt.

4.2.2.5 Single and M-Phase Lines with Lumped Resistances

Experience has shown that a lossy line with series resistance R' and negligible shunt conductance can be modelled with reasonable accuracy as one or more sections of lossless lines with lumped resistances in between. The simplest such approach is one lossless line with two lumped resistances R/2 at both ends. The equation for this model is easily derived from the cascade connection of R/2 - lossless line - R/2, and leads to a form which is identical with that of Eq. (1.6),

$$i_{km}(t) = \frac{1}{Z_{modified}} v_k(t) + hist_{km}(t-\tau) \tag{4.115}$$

except that the values for the surge impedance and history terms are slightly modified. With Z, R and τ calculated from Eq. (4.99),

$$Z_{modified} = Z + \frac{R}{2}$$

and

$$hist_{km}(t-\tau) = -\frac{1}{Z_{modified}}\left[v_m(t-\tau) + (Z-\frac{R}{2}) i_{mk}(t-\tau)\right]$$

This model with R/2 at both ends is not used in the EMTP. Instead, the EMTP goes one step further and lumps resistances in 3 places, namely R/4 at both ends and R/2 in the middle, as shown in Fig. 4.27. This approach was taken because the form of the equation still remains the same as in Eq. (4.115), except that

$$Z_{modified} = Z + \frac{R}{4} \tag{4.116}$$

now. The history term becomes more complicated[18], and contains conditions from both ends of the line at $t - \tau$,

$$hist_{km}(t-\tau) = -\frac{Z}{Z^2_{modified}}\left[v_m(t-\tau) + (Z-\frac{R}{4}) i_{mk}(t-\tau)\right]$$

[18]The equation at the bottom of p. 391, left column, in [50] contains an error. I_k and I_m should not be computed from Eq. (7b); instead, use $I_k = -(1/Z)\, e_k(t - \tau) - hi_{k,m}(t - \tau)$ with the notation of [50], where Z is $Z_{modified}$ of Eq. (4.116). For I_m, exchange subscripts k and m.

$$-\frac{R/4}{Z^2_{modified}}\left[v_k(t-\tau) + (Z-\frac{R}{4})i_{km}(t-\tau)\right] \qquad (4.117)$$

Users who want to lump resistances in more than 3 places can do so with the built-in three-resistance model, by simply subdividing the line into shorter segments in the input data. For example, 32 segments would produce lumped resistances in 65 places. Interestingly enough, the results do not change much if the number of lumped resistances is increased as long as R << Z. For example, results in Fig. 4.30 for the distributed-parameter case were practically identical for lumped resistances in 3, 65, or 301 places. Fig. 4.29 shows as well that TNA results are closely matched with R lumped in 3 places only.

One word of caution is in order, however. The lumped resistance model gives reasonable answers only if R/4 << Z, and should therefore not be used if the resistance is high. High resistances do appear in lightning surge studies if the parameters are calculated at a high frequency, e.g., at 400 kHz in Table 4.5, where R' = 597.4 Ω/km in the zero sequence mode. Lumping R in 3 places would still be reasonable in the case discussed there where each tower span of 90 m is modelled as one line, since 13.4 Ω is still reasonably small compared with Z = 1028 Ω. If it were used to model a longer line, say 90 km, then R/4 = 13,400 Ω, which would produce totally erroneous results[19]. In such a situation it might be best to ignore R altogether, or to use the frequency-dependent option if higher accuracy is required.

For M-phase lines, any of the M modes can be specified with lumped resistances. Mixing is allowed (e.g., mode 1 could be modelled with lumped resistances, and modes 2, ... M as distortionless). The lumped resistances do not appear explicitly as branches, but are built into Eq. (4.115) (4.116) and (4.117) for each mode. Should a user want to add them explicitly as branches, e.g., for testing purposes, then they would have to be specified as M x M - matrices [R] in phase quantities, which could easily be done with the M-phase nominal π-circuit input option by setting L = 0 and C = 0. All modes would have to use the lumped resistance model in this set-up, that is, mixing of models would not be allowed in it.

4.2.2.6 Single and M-Phase Lines with Frequency-Dependent Parameters

The two important parameters for wave propagation are the characteristic impedance

$$Z_c = \sqrt{\frac{R' + j\omega L'}{G' + j\omega C'}} \qquad (4.118)$$

and the propagation constant

$$\gamma = \sqrt{(R' + j\omega L')(G' + j\omega C')} \qquad (4.119)$$

Both parameters are functions of frequency, even for constant distributed parameters R', L', G', C' (except for lossless and distortionless lines). The line model with frequency-dependent parameters can handle this case of constant

[19]The UBC version of the EMTP stops with an error message if R/4 > Z. It would be advisable to add a warning message as well as soon as R/4 gets fairly large (e.g. > 0.05 * Z).

distributed parameters[20], even though it has primarily been developed for frequency-dependent series impedance parameters R'(ω) and L'(ω). This frequency-dependence of the resistance and inductance is most pronounced in the zero sequence mode, as seen in Fig. 4.20. Frequency-dependent line models are therefore important for types of transients which contain appreciable zero sequence voltages and currents. One such type is the single line-to-ground fault.

To develop a line model with frequency-dependent parameters which fits nicely into the EMTP, it is best to use an approach which retains the basic idea behind Bergeron's method. Let us therefore look at what the expression v + Zi used by Bergeron looks like now, as one travels down the line. Since the parameters are given as functions of frequency, this expression must first be derived in the frequency domain. At any frequency, the exact ac steady-state solution is described by the equivalent π-circuit of Eq. (1.13), or in an input-output relationship form more convenient here,

$$\begin{bmatrix} V_k \\ I_{km} \end{bmatrix} = \begin{bmatrix} \cosh(\gamma\ell) & Z_c \sinh(\gamma\ell) \\ \frac{1}{Z}\sinh(\gamma\ell) & \cosh(\gamma\ell) \end{bmatrix} \begin{bmatrix} V_m \\ -I_{mk} \end{bmatrix} \tag{4.120}$$

which can be found in any textbook on transmission lines. Assume that we want to travel with the wave from node m to node k. Then the expression $V + Z_c I$ is obtained by subtracting Z_c times the second row from the first row in Eq. (4.120),

$$V_k - Z_c I_{km} = (V_m + Z_c I_{mk}) \cdot e^{-\gamma\ell} \tag{4.121a}$$

or rewritten as

$$I_{km} = V_k/Z_c - (V_m/Z_c + I_{mk}) \cdot e^{-\gamma\ell} \tag{4.121b}$$

with a negative sign on I_{km} since its direction is opposite to the travel direction. Eq. (4.121) is very similar to Bergeron's method; the expression $V + Z_c I$ encountered when leaving node m, after having been multiplied with a propagation factor $e^{-\gamma\ell}$, the same when arriving at node k. This is very similar to Bergeron's equation for the distortionless line, except that the factor is $e^{-\alpha\ell}$ there, and that Eq. (4.121) is in the frequency domain here rather than in the time domain.

Before proceeding further, it may be worthwhile to look at the relationship between the equations in the frequency and time domain for the simple case of a lossless line. In that case,

$$Z_c = \sqrt{\frac{L'}{C'}}, \quad \gamma = j\omega\sqrt{L'C'}, \quad \textit{and} \quad e^{-\gamma\ell} \approx e^{-j\omega\tau}$$

Anybody familiar with Fourier transformation methods for transforming an equation from the frequency into the time domain will recall that a phase sift of $e^{-j\omega\tau}$ in the frequency domain will become a time delay τ in the time domain. Furthermore, Z_c is now just a constant (independent of frequency), and Eq. (4.121) therefore transforms to

[20]This case differs from the line with lumped resistances inasmuch as the resistance becomes truly distributed now.

$$v_k(t) - Z_c i_{km}(t) = v_m(t-\tau) + Z_c i_{mk}(t-\tau)$$

which is indeed Bergeron's equation (1.6).

For the general lossy case, the propagation factor

$$A(\omega) = e^{-\gamma \ell} = e^{-\alpha \ell} \cdot e^{-j\beta \ell}$$

with $\gamma = \alpha + j\beta$, contains an attenuation factor $e^{-\alpha \ell}$ as well as a phase shift $e^{-j\beta \ell}$, which are both functions of frequency. To explain its physical meaning, let us connect a voltage source V_{source} to the sending end m through a source impedance which is equal to $Z_c(\omega)$, to avoid reflections in m (Fig. 4.38). In that case, $V_m + Z_c I_{mk} = V_{source}$. Furthermore, let us assume that the receiving end k is open. Then from Eq. (4.121),

$$V_k = V_{source} \cdot A(\omega) \tag{4.122}$$

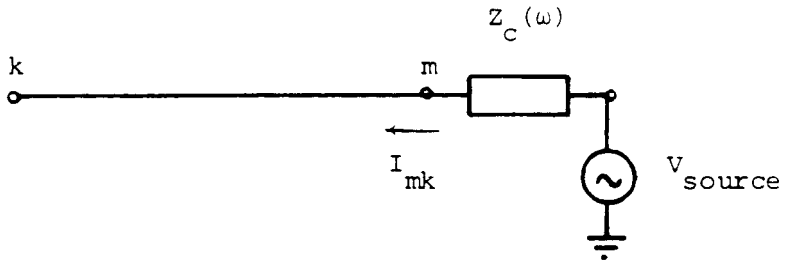

Fig. 4.38 - Voltage source connected to end m through matching impedance

that is, the propagation factor is the ratio (receiving end voltage) / (source voltage) of an open-ended line if the line is fed through a matching impedance $Z_c(\omega)$ to avoid reflections at the sending end[21]. If $V_{source} = 1.0$ at all frequencies from dc to infinity, then its time domain transform $v_{source}(t)$ would be a unit impulse (infinitely high spike which is infinitely narrow with an area of 1.0), and the integral of $v_{source}(t)$ would be a unit step. Setting $V_{source} = 1.0$ in Eq. (4.122) shows that $A(\omega)$ transformed to the time domain must be the impulse which arrives at the other end k, if the source is a unit impulse. This response to the unit impulse,

$$a(t) = \textit{inverse Fourier transform of } \{A(\omega)\} \tag{4.123}$$

will be attenuated (no longer infinitely high), and distorted (no longer infinitely narrow). Fig. 4.39 shows these responses for a typical 500 kV line of 100 miles length. They were obtained

[21]One could also connect a matching impedance $Z_c(\omega)$ from node k to ground to avoid reflections at the receiving end as well. In that case, the left-hand side of Eq. (4.122) becomes $2V_k$ rather than V_k. Note that the ratio $e^{-\gamma \ell}$ starts from 1.0 and becomes less than 1.0 as the line length (or frequency) is increased. This is in contrast to the open-circuit response $V_k/V_m = 1.0/\cosh(\gamma \ell)$ more familiar to power engineers, which increases with length or frequency (Ferranti rise).

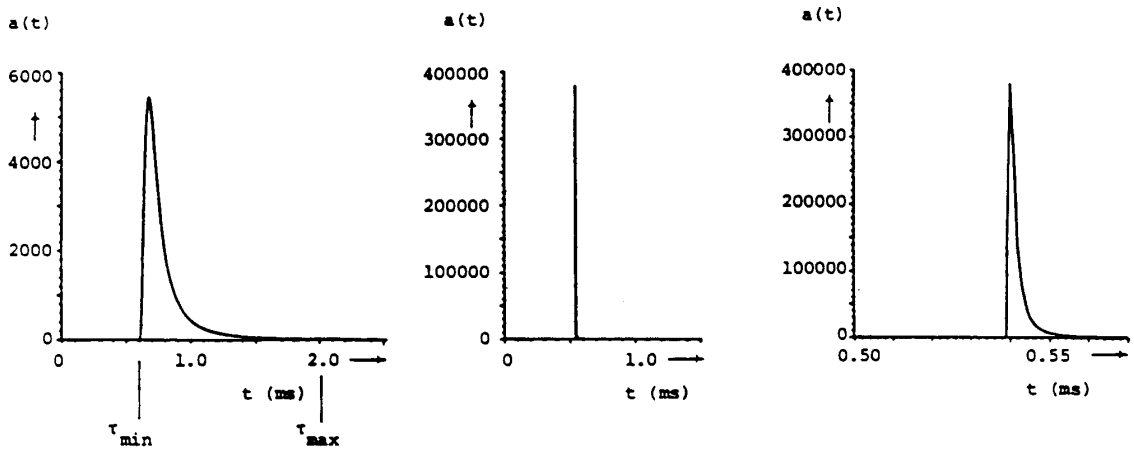

(a) zero sequence mode

(b) positive sequence mode with same scale as (a)

(c) positive sequence mode with expanded scale

Fig. 4.39 - Receiving end response $v_k(t) = a(t)$ for the network of Fig. 4.38 if $v_{source}(t)$ = unit impulse [94]. Reprinted by permission of J. Marti

from the inverse Fourier transformation of $A(\omega) = \exp(-\gamma\ell)$ calculated by the LINE CONSTANTS supporting routine at a sufficient number of points in the frequency domain. The amplitude of the propagation factors $A(\omega)$ for the case of Fig. 4.39 is shown in Fig. 4.40.

The unit impulse response of a lossless line would be a unit impulse at $t = \tau$ with an area of 1.0. In Bergeron's method, this implies picking up the history term $v_m/Z + i_{mk}$ at $t - \tau$ with a weight of 1.0. In the more general case here, history terms must now be picked up at more than one point, and weighted with the "weighting function" a(t). For the example of Fig. 4.39(a),

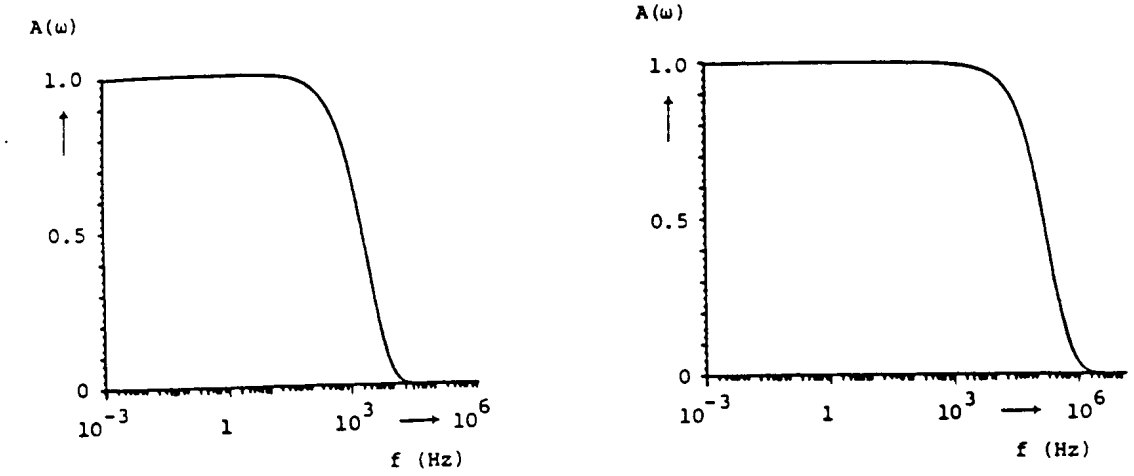

(a) zero sequence mode

(b) positive sequence mode

Fig. 4.40 - Propagation factor $A(\omega)$ for the line of Fig. 4.39 [94]. Reprinted by permission of J. Marti

history terms must be picked up starting at τ_{min} = 0.6 ms back in time, to approx. τ_{max} = 2.0 ms back in time. The value τ_{min} is the travel time of the fastest waves, while τ_{max} is the travel time of the slowest waves. Each terms has its own weight, with the highest weight of approx. 5400 around τ = 0.7 ms back in time. Mathematically, this weighting of history at the other end of the line is done with the convolution integral

$$hist_{propagation} = -\int_{\tau_{min}}^{\tau_{max}} i_{m-total}(t-u)a(u)du \qquad (4.124)$$

which can either be evaluated point by point, or more efficiently with recursive convolution as discussed later. The expression $i_{m\text{-}total}$ in Eq. (4.124) is the sum of the line current i_{mk} and of a current which would flow through the characteristic impedance if the voltage v_m were applied to it (expression $I_{mk} + V_m/Z_c$ in the frequency domain).

With propagation of the conditions from m to k being taken care of through Eq. (4.124), the only unresolved issue is the representation of the term V_k/Z_c in Eq. (4.121b). For the same 500 kV line used in Fig. 4.39, the magnitude and angle of the characteristic impedance Z_c are shown in Fig. 4.41. If the shunt conductance per unit length G' were ignored, as is usually done, Z_c would become infinite at ω = 0. This complicates the mathematics somewhat, and since G' is not completely zero anyhow, it was therefore decided to use a nonzero value, with a default option of 0.03 µs/km. As originally suggested by E. Groschupf [96] and further developed by J. Marti [94], such a frequency-dependent impedance can be approximated with a Foster-I R-C

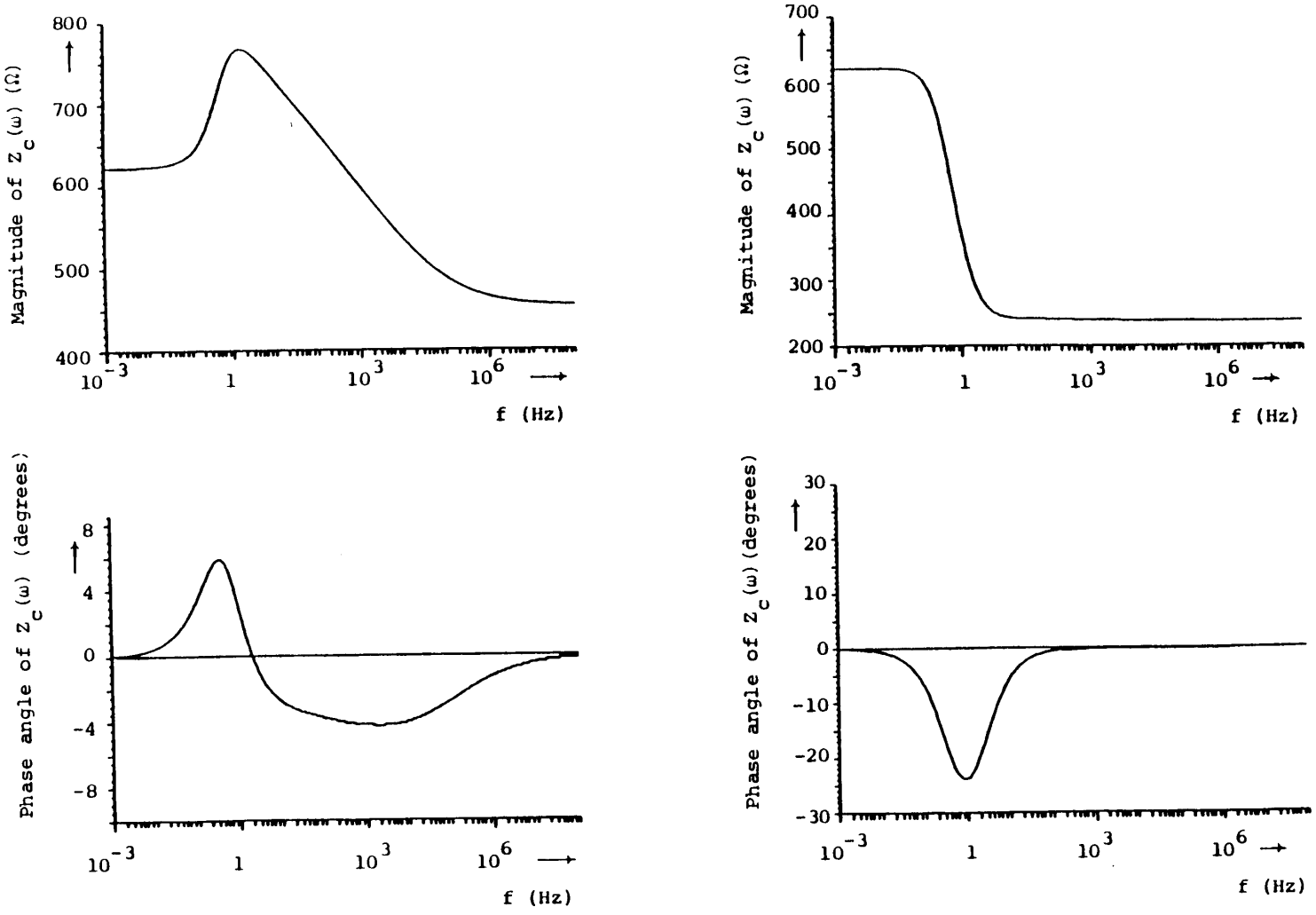

(a) zero sequence mode

(b) positive sequence mode

Fig. 4.41 - Characteristic impedance $Z_c(\omega)$ for the line of Fig. 4.39 [94]. Reprinted by permission of J. Marti

network. Then the line seen from node k becomes a simple R-C network in parallel with a current source $hist_{propagation}$ (Fig. 4.42(a)). One can then apply the trapezoidal rule of integration to the capacitances, or use any other method of implicit integration. This transforms each R-C block into a current source in parallel with an equivalent resistance. Summing these for all R-C blocks produces one voltage source in series with one equivalent resistance, or one current source in parallel with one equivalent resistance (Fig. 4.42(b)). In the solution of the entire network with Eq. (1.8), the frequency-dependent line is then simply represented again as a constant resistance R_{equiv} to ground, in parallel with a current source $hist_{RC} + hist_{propagation}$, which has exactly the same form as the equivalent circuit for the lossless line.

To represent the line in the form of Fig. 4.42 in the EMTP, it is necessary to convert the line parameters into a weighting function a(t) and into an R-C network which approximates the characteristic impedance. To do this, Z_c and γ are first calculated with the support routine LINE CONSTANTS, from dc to such a high frequency where both $A(\omega) = \exp(-\gamma\ell)$ becomes negligibly small and $Z_c(\omega)$ becomes practically constant. J. Marti [94] has shown that it is best to approximate $A(\omega)$ and $Z_c(\omega)$ by rational functions directly in the frequency domain. The weighting function a(t) can then be written down explicitly as a sum of exponentials, without any need for numerical inverse Fourier transformation. Similarly, the rational function approximation of $Z_c(\omega)$ produces directly the values of R and C in the R-C network in Fig. 4.42.

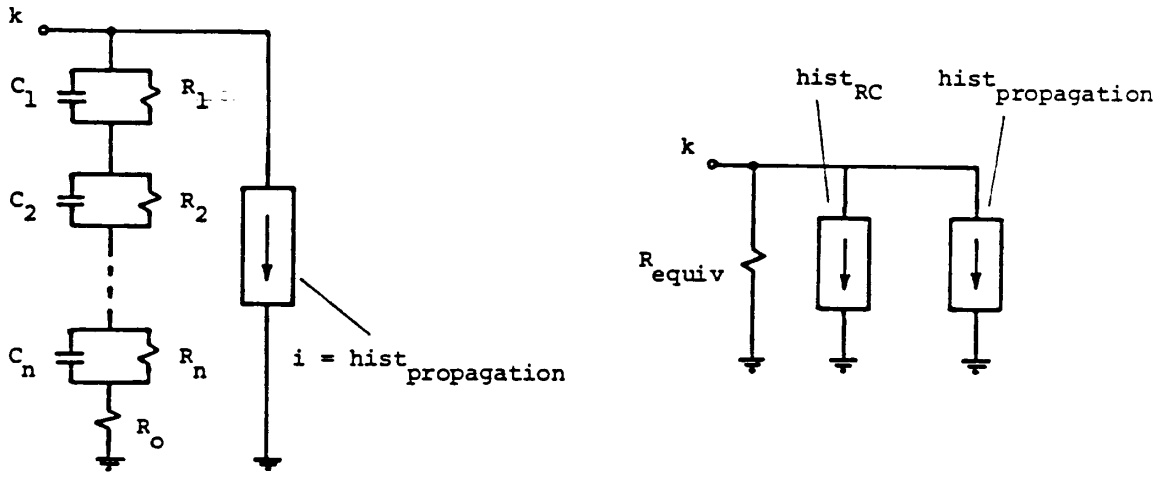

(a) with R-C network

(b) with equivalent resistance after applying implicit integration

Fig. 4.42 - Frequency-dependent line representation seen from line end k

The rational function which approximates A(ω) has the form

$$A_{approx}(s) = e^{-s\tau_{min}} k \frac{(s+z_1)(s+z_2)\ldots(s+z_n)}{(s+p_1)(s+p_2)\ldots(s+p_m)} \tag{4.125}$$

with s = jω and n < m. The subscript "approx" indicates that Eq. (4.125) is strictly speaking only an approximation to the given function A(ω), even though the approximation is very good. The factor $e^{-j\omega\tau min}$ is included to take care of the fact that a(t) in Fig. 4.39 is zero up to $t = \tau_{min}$; this avoids fitting exponentials through the portion $0 \le t \le \tau_{min}$ where the values are zero anyhow (remember that a time shift $-\tau$ in the time domain is a phase shift $e^{-j\omega\tau}$ in the frequency domain). All poles p_i and zeros z_i in Eq. (4.125) are negative, real and simple (multiplicity one). With n < m, the rational function part of Eq. (4.125) can be expanded into partial fractions,

$$k \frac{(s+z_1)(s+z_2)\ldots(s+z_n)}{(s+p_1)(s+p_2)\ldots(s+p_m)} = \frac{k_1}{s+p_1} + \frac{k_2}{s+p_2} \ldots + \frac{k_m}{s+p_m} \tag{4.126}$$

The corresponding time-domain form of Eq. (4.15) then becomes

$$a_{approx}(t) = \left[k_1 e^{-p_1(t-\tau_{min})} + k_2 e^{-p_2(t-\tau_{min})} \ldots + k_m e^{-p_m(t-\tau_{min})}\right] \quad for\ t \ge \tau_{min}$$

$$= 0 \qquad for\ t < \tau_{min} \tag{4.127}$$

This weighting function $a_{approx}(t)$ is used to calculate the history term $hist_{propagation}$ of Eq. (4.124) in each time step. Because of its form as a sum of exponentials, the integral can be found with recursive convolution much more efficiently

than with a point-by-point integration. If we look at the contribution of one exponential term $k_i e^{-pi(t-\tau min)}$,

$$s_i(t) = \int_{\tau_{min}}^{\infty} i(t-u) k_i e^{-p_i(t-\tau_{min})} du \tag{4.128}$$

then $s_i(t)$ can be directly obtained from the value $s_i(t - \Delta t)$ known from the preceding time step, with only 3 multiplications and 3 additions,

$$s_i(t) = c_1 \cdot s_i(t-\Delta t) + c_2 \cdot i(t-\tau_{min}) + c_3 \cdot i(t-\tau_{min}-\Delta t) \tag{4.129}$$

as explained in Appendix V, with c_1, c_2, c_3 being constants which depend on the particular type of interpolation used for i.

The characteristic impedance $Z_c(\omega)$ is approximated by a rational function of the form [94]

$$Z_{c-approx}(s) = k \frac{(s+z_1)(s+z_2)\ldots(s+z_n)}{(s+p_1)(s+p_2)\ldots(s+p_n)} \tag{4.130}$$

with $s = j\omega$. All poles and zeros are again real, negative and simple, but the number of poles is equal to the number of zeros now. This can be expressed as

$$Z_{c-approx}(s) = k_0 + \frac{k_1}{s+p_1} + \frac{k_2}{s+p_2} \ldots \frac{k_n}{s+p_n} \tag{4.131}$$

which corresponds to the R-C network of Fig. 4.42, with

$$R_0 = k_0$$

$$R_i = \frac{k_i}{p_i}, \quad C_i = \frac{1}{k_i}, \quad i=1,\ldots n \tag{4.132}$$

Rather than applying the trapezoidal rule to the capacitances in Fig. 4.42, J. Marti chose to use implicit integration with Eq. (I.3) of Appendix I[22], with linear interpolation on i. For each R-c block

$$i = \frac{v_i}{R_i} + C_i \frac{dv_i}{dt}$$

which has the exact solution

$$v_i(t) = e^{-\alpha_i \Delta t} \cdot v_i(t-\Delta t) + \frac{1}{C_i} \int_{t-\Delta t}^{t} e^{-\alpha_i (t-u)} i(u) du \tag{4.133}$$

[22]This method is identical to the recursive convolution of Appendix V applied to Eq. (4.131). Whether recursive convolution is better than the trapezoidal rule is still unclear.

with $\alpha_i = 1/(R_i C_i)$. By using linear interpolation on i, the solution takes the form of

$$v_i(t) = R_{equiv-i} \cdot i(t) + e_i(t-\Delta t) \tag{4.134}$$

with $e_i(t - \Delta t)$ being known values of the preceding time step (formula omitted for simplicity), or after summing up over all R-C blocks and R_0,

$$v(t) = R_{equiv} \cdot i(t) + e(t-\Delta t) \tag{4.135a}$$

with

$$R_{equiv} = R_0 + \sum_{i=1}^{n} R_{equiv-i} \quad and \quad e = \sum_{i=1}^{n} e_i \tag{4.135b}$$

which can be rewritten as

$$i(t) = \frac{1}{R_{equiv}} v(t) + hist_{RC} \tag{4.136}$$

The equivalent resistance R_{equiv} enters into matrix [G] of Eq. (1.8), whereas the sum of the history terms $hist_{RC} + hist_{propagation}$ enters into the right hand side.

The key to the success of this approach is the quality of the rational function approximations for $A(\omega)$ and $Z_c(\omega)$. J. Marti uses Bode's procedure for approximating the magnitudes of the functions. Since the rational functions have no zeros in the right-hand side of the complex plane, the corresponding phase functions are uniquely determined from the magnitude functions (the rational functions are minimum phase-shift approximations in this case) [94]. To illustrate Bode's procedure, assume that the magnitude of the characteristic impedance in decibels is plotted as a function of the logarithm of the frequency, as shown in Fig. 4.43 [94]. The basic principle is to approximate the given curve by straight-line segments which are either horizontal or have a slope which is a multiple of 20 decibels/decade. The points where the slopes change define the poles and zeros of the rational function. By taking the logarithm on both sides of Eq. (4.130), and multiplying by 20 to follow the convention of working with decibels, we obtain

$$\begin{aligned} 20\log|Z_{c-approx}(s)| &= 20\log k + 20\log|s+z_1| \ldots + 20\log|s+z_n| \\ &- 20\log|s+p_1| \cdots - 20\log|s+p_n| \end{aligned} \tag{4.137}$$

For $s = j\omega$, each one of the terms in this expression has a straight-line asymptotic behavior with respect to ω. For instance, $20 \log |j\omega + z_1|$ becomes $20 \log z_1$ for $\omega << z_1$, which is constant, and $20 \log \omega$ for $\omega >> z_i$, which is a straight line with a slope of 20 db/decade. The approximation to Eq. (4.137) is constructed step by step: Each time a zero corner (at $\omega = z_i$) is added, the slope of the asymptotic curve is increased by 20 db, or decreased by 20 db each time a pole corner (at $\omega = p_i$) is added. The straight-line segments in Fig. 4.43 are only asymptotic traces; the actual function becomes a smooth curve without sharp corners. Since the entire curve is traced from dc to the

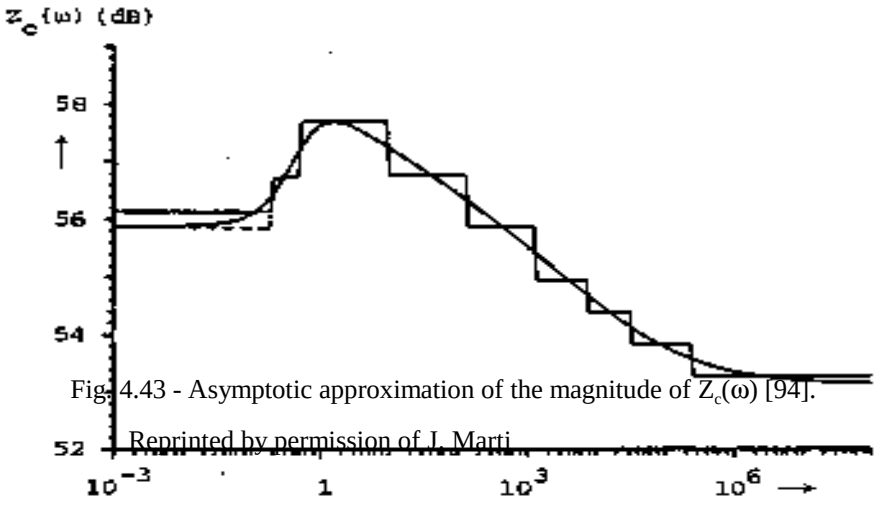

Fig. 4.43 - Asymptotic approximation of the magnitude of $Z_c(\omega)$ [94].
Reprinted by permission of J. Marti.

highest frequency at which the approximated function becomes practically constant, the entire frequency range is approximated quite closely, with the number of poles and zeros not determined a priori. J. Marti improves the accuracy further by shifting the location of the poles and zeros about their first positions. Fig. 4.44 shows the magnitude and phase errors of the approximation of $A(\omega)$, and Fig. 4.45 shows the errors for the approximation of $Z_c(\omega)$ for the line used in Fig. 4.39.

L. Marti has recently shown [95] that very good results can be obtained by using lower-order approximations with typically 5 poles and zeros rather than the 15 poles and zeros used in Fig. 4.44 and 4.45. Furthermore, he shows that positive and zero sequence parameters at power frequency (50 or 60 Hz) can be used to infer what the tower geometry of the line was, and use this geometry in turn to generate frequency-dependent parameters. With this approach, simple input data (60 Hz parameters) can be used to generate a frequency-dependent line model internally which is fairly accurate.

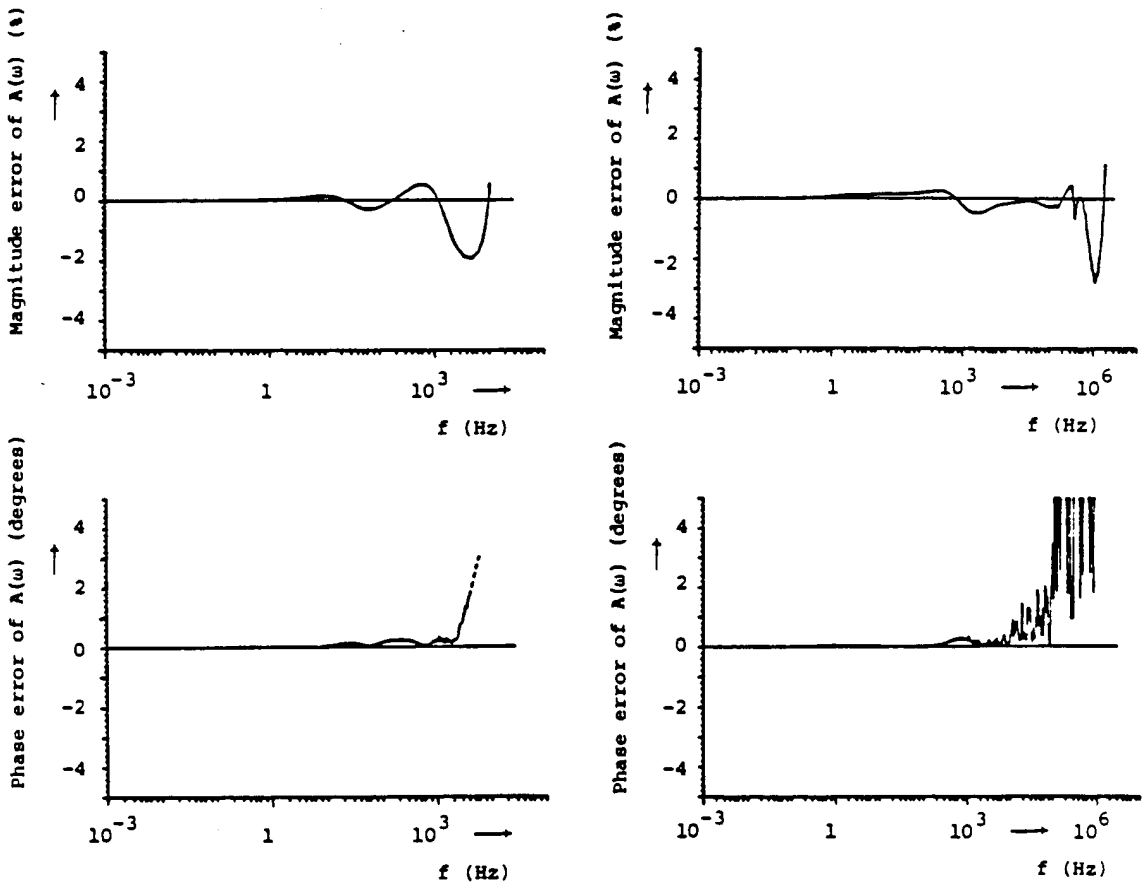

(a) zero sequence mode (15 zeros and 20 poles)

(b) positive sequence mode (13 zeros and 17 poles)

Fig. 4.44 - Errors in approximation of A(ω) for line of Fig. 4.39 [94]. Reprinted by permission of J. Marti

For M-phase lines, any of the M modes can be specified as frequency-dependent, or with lumped resistances, or as distortionless. Mixing is allowed. A word of caution is in order here, however: At the time of writing these notes, the frequency-dependent line model works only reliably for balanced lines. For untransposed lines, approximate real and constant transformation matrices must be used, as explained in Section 4.1.5.3, which seems to produce reasonably

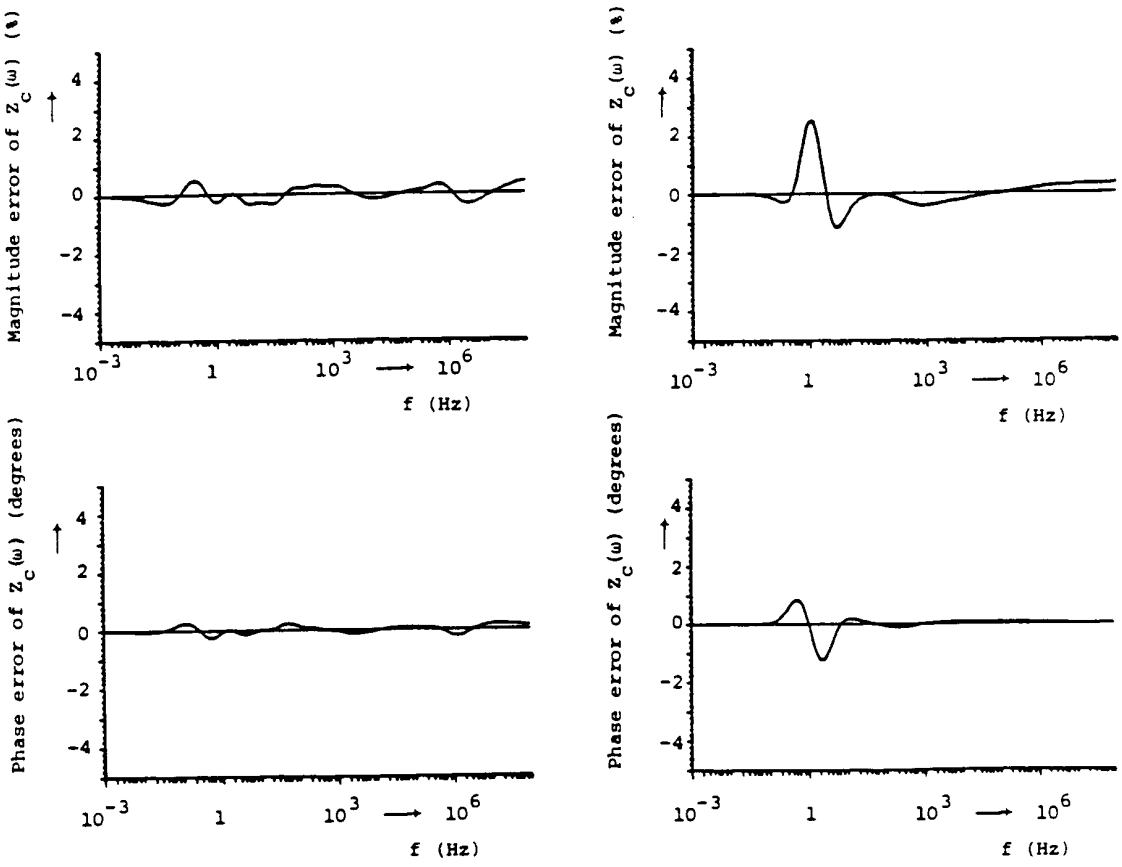

(a) zero sequence mode (15 zeros and poles)

(b) positive sequence mode (16 zeros and poles)

Fig. 4.45 - Errors in approximation of $Z_c(\omega)$ for line for Fig. 4.39 [94]. Reprinted by permission of J. Marti

accurate results for single-circuit lines, but not for double-circuit lines. Research by L. Marti into frequency-dependent transformation matrices in connection with models for underground cables will hopefully improve this unsatisfactory state of affairs.

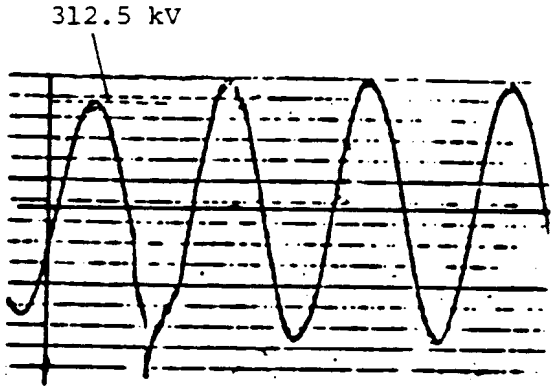
312.5 kV

(a)

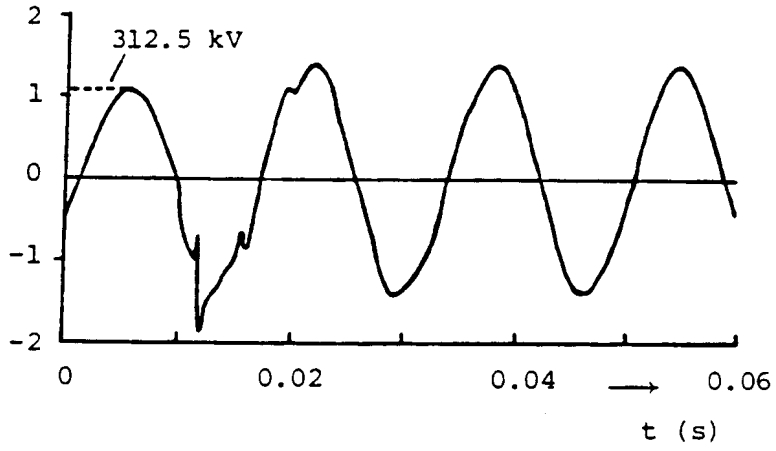
2
1
0
-1
-2
312.5 kV
0
0.02
0.04
0.06
t (s)

(b)

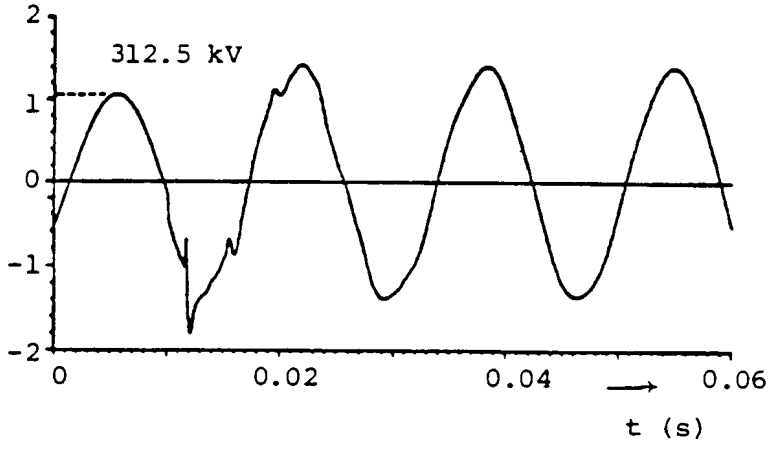
2
1
0
-1
-2
312.5 kV
0
0.02
0.04
0.06
t (s)

(c)

Fig. 4.46 - Comparison between voltages at phase b for [94]:
(a) Field test oscillograph
(b) BPA's frequency-dependence simulation
(c) New model simulation
Reprinted by permission of J. Marti

Field test results for a single-line-to-ground fault from Bonneville Power Administration have been sued by various authors to demonstrate the accuracy of frequency-dependent line models [84]. Fig. 4.46 compares the field test results with simulation results from an older method which used two weighting functions a_1 and a_2 [84], and from the newer method described here. The peak overvoltage in the field test was 1.60 p.u., compared with 1.77 p.u. in the older method and 1.71 p.u. in the newer method. Constant 60 Hz parameters would have produced an answer of 2.11 p.u.